ELSEVIER

Biochimica et Biophysica Acta 1187 (1994) 1–65

BBA Biochimica et Biophysica Acta

Review

# Energy transfer and trapping in photosynthesis

Rienk van Grondelle [a,*], Jan P. Dekker [a], Tomas Gillbro [b], Villy Sundstrom [b]

[a] *Department of Physics and Astronomy, Institute for Molecular Biological Sciences, Vrije Universiteit, De Boelelaan 1081, 1081 HV Amsterdam, The Netherlands,*

[b] *Department of Physical Chemistry, University of Umeå, Umeå, Sweden*

Received 16 March 1994

*Key words:* Energy transfer; Excitation energy transfer; Photosynthesis; Light harvesting; Carotenoid; Ultrafast laser spectroscopy; Polarized light spectroscopy; (Bacteria)

## Contents



Abbreviations: Ant, antenna; APC, allophycocyanin; (B)Chl, (bacterio)chlorophyll; (B)Pheo, (bacterio)pheophytin; Car, carotenoid; CD, circular dichroism; C-PC, C-phycocyanin; DAS, decay-associated spectrum; FMO, Fenna-Matthews-Olson BChl *a* complex; LD, linear dichroism; LHC, light-harvesting complex; PEC, phycoerythrocyanin; PS, Photosystem; RC, reaction center.

* Corresponding author. Fax: +31 20 4447899.


*SSDI* 0005-2728(94)00055-A

## 1. Introduction

Key processes in photosynthesis are the absorption of solar energy by antenna pigments and the efficient transfer of excitation energy to photochemical reaction centers, where the energy is trapped in the form of a stable charge separation. This sequence of fine-tuned photophysical and photochemical reactions, which occurs with a remarkably high quantum yield of 90% or higher, allows photosynthetic organisms to use solar light effectively and at relatively low costs. Since the products of photosynthesis form the basis of the food chain, all life on earth depends on the success of these primary photosynthetic reactions. In addition, if one ever wants to mimic the natural process of light-harvesting in an artificial system, the key physical, chemical and biological elements of the process should be fully understood.

Photosynthetic organisms have provided us with a wealth of biological materials which are well capable to

absorb light in a specific spectral window of the solar emission. These materials are all organized in photosynthetic light-harvesting complexes in such a way that they are able to participate in ultrafast excitation energy transfer to the photochemical reaction center. Research on energy transfer in photosynthesis covers studies in a wide range of disciplines, including biology, chemistry, genetics of pigments and pigment-protein complexes, the three-dimensional structure of these pigment-protein complexes, the elementary physics of densely packed pigments in a protein environment, the ultrafast femto- and picosecond energy transfer and electron transfer, the regulation of the light-harvesting processes, etc.

The early concepts of the remarkable features of light-harvesting have been developed between 1950 and 1970. Purified biochemical preparations of pigment-protein complexes have since then become available for a large number of photosynthetic organisms. A large amount of the elementary spectroscopic, structural and mechanistic properties of the light-harvesting processes were reviewed in [1]. Since 1985 we have seen four major developments in this field:

(1) The refined purification of a number of crucial components of the photosynthetic process in native, undenatured and highly active forms, amongst which the Photosystem II reaction center [2], the Photosystem I reaction center [3], several of the plant light-harvesting complexes [4], a subunit of the core antenna of photosynthetic purple bacteria [5], the green bacterial reaction center [6,7], the reaction center complex of the recently discovered heliobacteria [8,9], etc.
(2) The advent of pico- and femtosecond laser spectroscopy, which allowed (in particular by using low-intensity lasers) the study of the elementary dynamics of energy transfer and electron transfer (see for reviews Refs. [10–15]).
(3) The crystallization and, in some cases, the resolution of the structure of a variety of pigment-protein complexes, amongst which the purple bacterial photosynthetic reaction center [16,17], the LHC-II light-harvesting complex from green plants [18,19], the cyanobacterial PS I core [20] and phycobiliproteins of various cyanobacteria [21,22].
(4) The development of molecular genetics for photosynthetic bacteria and cyanobacteria, which allowed the introduction of selected structural alterations (see, for example, Refs. [23–25]).

The current review discusses the recent developments in photosynthetic excitation energy transfer with major emphasis on the advances in the areas mentioned above. For reviews that discuss the early history of energy transfer we refer to Refs. [26–29]. Between 1985 and today several excellent reviews have appeared that discuss the structural organization of plant [3,4,30,31] and bacterial [32,33] photosynthetic systems or overview the ultrafast kinetic experiments in plant and bacterial antennae [11,14,15,34,35].

## 2. Theoretical aspects of excitation energy transfer

### 2.1. Introduction

In the 1985 version of this review [1], an overview was presented of the elementary theory underlying the processes of excitation transfer and excitation trapping. Most of the pertinent theory will not be repeated here and interested readers are referred to the 1985 review and references cited therein. Throughout this review it will be assumed that the dominant mechanism for excitation energy transfer is the Förster mechanism described in detail and discussed extensively in Refs. [1,28,36–39]. For the description of the physics of energy transfer in larger systems in the presence of traps, which relates to the excitation dynamics of a photosynthetic unit or in photosynthetic domains (collections of photosynthetic units), we refer to Refs. [1,27,28,40–44].

Between 1980 and 1990 it was realized that excitation energy transfer between individual (bacterio)-chlorophyll sites could occur on a subpicosecond timescale. For example, from excitation annihilation experiments in simple purple bacterial systems, Bakker et al. [45] estimated on the basis of a straightforward energy transfer model that the lifetime of single excited BChl *a* site in the domain was between 0.1 and 0.2 ps. Similarly, from time-resolved measurements on PS I cores, Owens et al. [46] estimated a 0.2 ps lifetime for a single excited Chl *a* site in the core antenna of PS I. Since the advent of femtosecond lasers and their application in photosynthetic energy transfer research, several subpicosecond energy transfer processes have been time-resolved. For the bacterial reaction center, Breton and co-workers [47] have shown that energy transfer from the BPheo and the accessory BChl *a* molecules to the special pair (with center-to-center distances in the 1–2 nm range) occurs within 100 fs. Very similar time constants have been observed for energy transfer between the chlorophylls and pheophytins in the PS II reaction center [48]. For the LHCII complex of green plants the rate of energy transfer from Chl *b* to Chl *a* was shown to occur with a time-constant of about 0.5 ps [49–51], although additional slower components were also observed. In the PS I core antenna the single step energy transfer rate, as reflected by the time-resolved depolarization of the fluorescence, occurs on a timescale of 200 fs [52], in agreement with the earlier estimate. For a variety of phycobiliproteins, energy transfer processes on a subpicosecond timescale have been observed [53–55]. For the LH2 (B800–850) com-

plex of *Rb. sphaeroides* the B800 → B850 transfer takes place on a timescale of 0.7 ps at room temperature [56,57]; between 77 K and 1 K the rate is constant (2.2 ps) and only a factor of 3 slower compared to that obtained at 293 K [58,57].

The physical theory of excitation energy transfer and trapping in photosynthesis has to account for these ultrafast ($\leq 0.1$–$1.0$ ps) single-step hopping times and their temperature dependence. It is, however, highly possible that the Förster theory is no longer sufficient to explain these ultrafast rates. A more complex theory is required to correctly describe the competition between vibrational relaxation and energy transfer and to correctly account for special effects arising from the coherent excitation of sets of vibrational or electronic levels and the decay of coherence [59]. For instance, in the decay of the excited special pair of bacterial RC's specific oscillations are observed in the stimulated emission and transient absorption [60]; very similar phenomena were recently observed for the LH1 and LH2 light-harvesting antenna complexes of *Rb. sphaeroides* [61] and chlorosomes of *Cf. aurantiacus* [62]. Recently, a theory was presented by Gülen and Knox [63] concerning the complex time-resolved depolarization that may be observed upon the coherent excitation of an excitonically coupled dimer with a short laser pulse. In this review we will not further consider these special effects; for discussions we refer to Refs. [60,64].

It is well known that many photosynthetic systems are heterogeneous in their pigment-protein composition, giving rise to multiple absorption bands in the visible, red (plants, algae) and near-infrared (photosynthetic purple bacteria, green bacteria) parts of the spectrum. The various bands in the spectrum can be correlated with the occurrence of specific pools of pigment-protein complexes, which tend to be organized in such a way that the pigments absorbing at relatively high energy are found at the periphery of the antenna, whereas those absorbing at lower energy are generally found closer to the reaction centers. Good examples of such funnel systems are the phycobilisome/PS II antenna of cyanobacteria, the LH2/LH1 antenna of *Rb. sphaeroides*, and the chlorosome/BChl *a* antenna of green photosynthetic bacteria. In general, the excitation transfer between these (sometimes large) pools of pigments involves many transfer steps among chemically identical pigments, and the time necessary for the equilibration of the excitation density is of a few tens of picoseconds at the most. For instance, in green photosynthetic bacteria energy transfer from the chlorosome, containing at least a few thousand BChl *c* molecules, to the membrane occurs at the amazing speed of 10–20 ps [65,66]. Similarly, the excitation equilibration time between LHC-II and the PS II-core antenna in green plants is about 10 ps [67,68].

Trapping of excitation energy by the photochemical reaction center involves excitation of the primary electron donor by one of the neighboring antenna pigments, followed by a rapid charge separation. In this process there are three important aspects to consider: (i) the rate of energy transfer from the antenna to the primary donor is not necessarily identical to the rate of energy transfer in the antenna; (ii) the probability for charge separation upon excitation of the primary donor is not necessarily identical to one (the excitation may escape from the reaction center through back transfer to the surrounding antenna pigments); (iii) the initial charge separated state is not necessarily deep in free energy relative to the antenna excited state. This implies that, even after charge separation has occurred, the state [Antenna + P]* is equilibrated with the state $[P^+I^-]$ (in which I is the initial electron acceptor) and that a significant fraction of the equilibrium may occur in the state [Antenna + P]*. This is particularly notable for photosynthetic systems with a large number of (almost isoenergetic) antenna pigments per RC, such as the PS II antenna. This point was extensively discussed in the previous version of this review [1], and later elaborated upon by Holzwarth and co-workers in the so-called exciton-radical pair equilibrium model [69].

### 2.2. Excitonic interactions

#### 2.2.1. Excitonic interactions in a dimer

In this section we will recapitulate the basic principles of exciton theory with the specific aim to illustrate how in a pigment protein complex excitonic interactions and disorder (inhomogeneous broadening) contribute to the final spectral properties of a dimer. The resulting expressions will be used to calculate the spectral properties of the B820 light-harvesting 1 (LH-1) subunit of photosynthetic purple bacteria.

When two pigment molecules, 1 and 2, are sufficiently close in space, their electron clouds will interact and, as a consequence, the spectral and dynamic properties of this pair of molecules will be modified. In the case of strong coupling, in which the coupling strength $V_{12}$ exceeds the width of the individual transitions of 1 and/or 2, the combined spectrum of D and A is modified such that two new absorption bands appear due to transitions from the unperturbed ground state to weighted combinations of the locally excited states $\phi_1^1\phi_2^0$ and $\phi_1^0\phi_2^1$, where $\phi_i^j$ reflects the $j^{\text{th}}$ excited state of molecule $i$.

For a dimer, the relevant Hamiltonian that must be diagonalized is given by:

$$H = \begin{bmatrix} E_1 & V_{12} \\ V_{12} & E_2 \end{bmatrix} \quad (1)$$

in which $E_1$ and $E_2$ represent the excited state energies of the original molecules and $V_{12}$ is coupling, which for dipole-dipole interactions is given by:

$$V_{12} = \frac{\mu_1\mu_2}{R_{12}^3} - \frac{3(\mu_1 R_{12})(\mu_2 R_{12})}{R_{12}^5}. \quad (2)$$

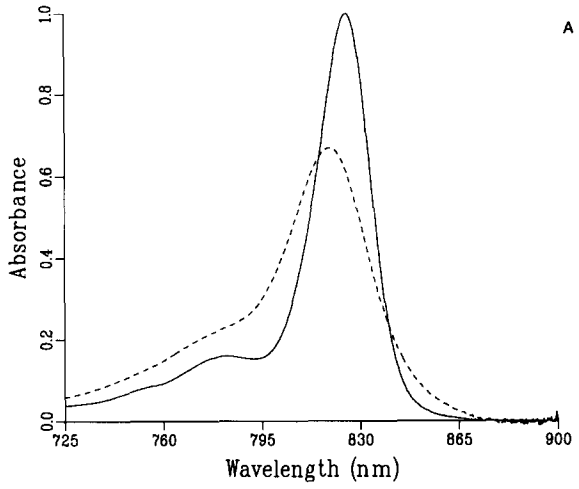


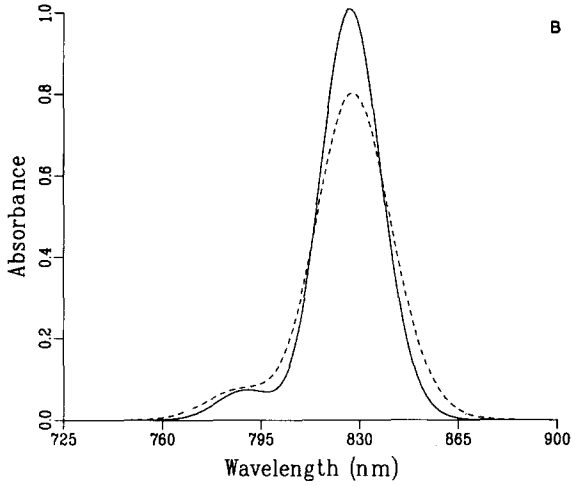


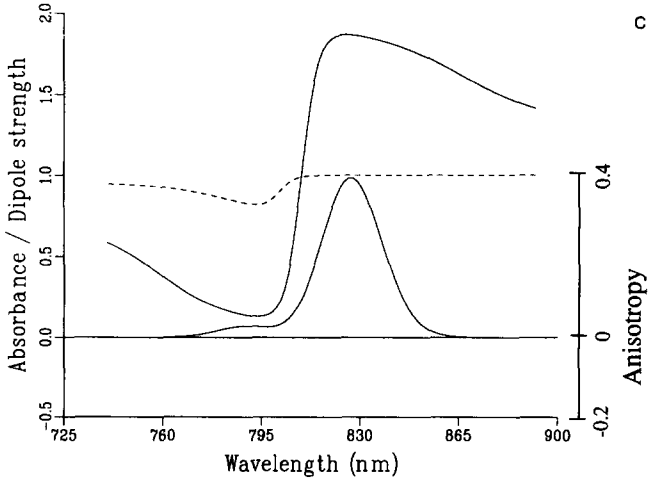


In Eq. 2 $\mu_i$ is the transition dipole molecule of molecule $i$, corresponding to the transition of $\phi_i^1 \leftarrow \phi_i^0$,$R_{12}$ is the vector connecting the molecules 1 and 2 and $R_{12} = |R_{12}|$. The new wavefunctions $\Psi_\pm$ are given by:

$$\Psi_\pm = \sin\alpha\phi_1^1\phi_2^0 + \cos\alpha\phi_1^0\phi_2^1 \quad (3)$$

where $\alpha$ is found from the solution of Eq. (1) and is given by:

$$\tan\alpha = \frac{(E_2 - E_1) \pm \sqrt{(E_2 - E_1)^2 + 4V_{12}^2}}{2V_{12}} \quad (4)$$

For $V_{12} \gg |E_2 - E_1|$ the new wavefunctions are the true in-phase and out-of-phase linear combinations at the two locally excited states. In such a case (a head-to-tail or head-to-head dimer) the major allowed transition is the low-energy exciton component and the high energy component is almost completely forbidden. It is hardly relevant to discuss energy transfer between the partners of the dimer; the excitation oscillates between the two partners at a frequency $2V_{12}/h$ and is only instantaneously localized. For $V_{12} \ll |E_2 - E_1|$ the situation is rather different. In fact, as may be seen from Eqs. (3) and (4) the new wavefunctions are almost identical to the localized excited states, with only small admixtures of the other.

For a dimer in which the monomer absorption frequencies show a certain width (given by $\sigma_{inh}$) all possible combinations of $E_1$ and $E_2$ occur. Consequently, selecting the monomers randomly from the inhomogeneous distribution, we may have simultaneously strongly coupled and weakly coupled dimers contributing to the spectrum. Based on these ideas, we have recently attempted to fit the absorption spectrum of the B820-subunit [70,71] of the LH1-core antenna of photosynthetic purple bacteria (a protein-bound dimer of BChl *a* [72,73]), using Eqs. (1–4). The width of the inhomogeneous distribution of site energies was obtained from the triplet-minus-singlet spectrum of the dimer. The spectrum shown in Fig. 1B was calculated for a head-to-tail dimer (the angle between the

Fig. 1. (A) Experimentally measured room temperature (dashed) and 77 K (drawn) absorption spectra of the B820 complex of *Rhodospirillum rubrum* [from Koolhaas et al., Ref. 71]; (B) Calculated absorption spectra [71] for a disordered dimer using Eqs. 1–4 and assuming that the angle $\xi$ between the monomers is 10°, a monomeric bandwidth $\sigma_{inh} = 2V$ (mimicking the 77 K situation, drawn curve) and $\sigma_{inh} = 3V$ (mimicking the room temperature situation, dashed). $V$ was taken as 230 $cm^{-1}$ [72]; (C) Average dipole strength per state relative to the monomeric dipole strength (upper solid line) and the fluorescence anisotropy excitation spectrum (dashed) for $\sigma_{inh} = 2V$, $V = 230$ $cm^{-1}$ and $\xi = 10°$. The corresponding absorption spectrum is also shown (lower solid line). The anisotropy excitation function should be compared with the experimental spectrum shown in Ref. [423].

monomeric transition dipoles $\xi = 10°$) assuming $\sigma_{inh} = 3V_{12}$ at room temperature and $\sigma_{inh} = 2V_{12}$ at 77 K. Note the strong resemblance with the experimental spectrum (Fig. 1A). The other conspicuous feature of the calculated spectra is the presence of the high-energy exciton component. In this calculation this feature solely arises from the disordered nature of the dimer since the two contributing transition dipoles were chosen parallel. As a consequence the direction of the transition moment of the high-energy exciton component is parallel to that of the intense allowed transition at 820–825 nm. Assuming a small angle between the monomer transitions produces a small drop in the polarized fluorescence excitation spectrum, similar to what has been observed experimentally (see Fig. 1C). Fig. 1C also shows the average dipole strength per state. Note that in the peak this approaches 2 (as expected for a parallel degenerate dimer), but in the blue wing of the allowed transition the curve drops steeply.

The B820 BChl *a* dimer can be reaggregated into a large antenna complex, which strongly resembles the in vivo LH1 antenna [5,74]. The observed red-shift upon aggregation from 820 nm to 870–880 nm is probably not due to increased excitonic interactions, but largely protein-induced [75]. Energy transfer between these weakly coupled dimers probably occurs via the Förster mechanism (see below).

#### 2.2.2. Excitonic interactions in larger systems

The formalism given above for a dimer can easily be extended to larger systems. Good examples where this has been applied to model the spectral data are the Fenna-Matthews-Olson BChl *a* complex of *Prosthecochloris aestuarii* [76], the chlorosome BChl *c* aggregate [77], the reaction center of purple photosynthetic bacteria [78] and the CP-C phycobiliprotein [79]. For instance, for the FMO complex hole-burning [80] and singlet-triplet difference spectra [81] have shown that all absorption bands are coupled. The absorption spectrum of the FMO complex has been calculated from the crystal structure of the trimer taking into account all interactions between 21 BChl *a* molecules [76]. However, even for FMO the variation in site energies is of the same order of magnitude as the excitonic coupling, and also the disorder will be of similar size [82]. For all strongly coupled systems the excitonic wavefunctions are linear combinations of the locally excited states. In that case the relaxation between different exciton states is equivalent to excitation energy transfer, since the admixture of the locally excited states is different in the each exciton state. Two mechanisms for transitions between exciton states have been proposed:

(1) $\partial V_{ij}/\partial Q \neq 0$; that is, the coupling between sites $i$ and $j$ depends on variation in the nuclear coordinate $Q$ [80];

(2) $E_i$, the energy of site $i$, fluctuates as a function of time (Pullerits, T. and Larsson, S., unpublished data). It is possible that both mechanisms may lead to subpicosecond excitation transfer in the FMO-complex and in other strongly coupled systems.

### 2.3. Förster dipole-dipole transfer

For weakly coupled pigments the mechanism of energy transfer as proposed by Förster [36,37] is valid. The coupling is sufficiently weak that the spectra of donor and acceptor are not affected. The Förster mechanism depends on the square of the dipole-dipole coupling between the two transitions involved, and on the degree of overlap between the emission of the donor and the absorption of the acceptor, since the total energy of the system must be conserved during the transfer process. The Förster equation is given by:

$$k_{ET} = \frac{9\kappa^2(\ln 10)c^4}{128\pi^5 n^4 \, N\tau_R^D R_{DA}^6} \int f_D(\nu)\epsilon_A(\nu)\frac{d\nu}{\nu^4} \qquad (5)$$

In Eq. 5 $\epsilon_A(\upsilon)$ is the molar decadic extinction coefficient, and $f_D(\upsilon)$ the fluorescence quantum spectrum normalized to unity on a frequency scale ($s^{-1}$), $N$ is the number of molecules per millimole, $c$ the velocity of light ($ms^{-1}$), $\tau_R^D$ the radiative fluorescence lifetime, $R_{DA}$ the distance (m), $n$ the index of refraction and $\kappa$ is the orientation factor given by:

$$\kappa = \cos\alpha - 3\cos\beta_1\cos\beta_2 \qquad (6)$$

with $\alpha$ the angle between the transition moments of D ($\vec{\mu}_D$) and A ($\mu_A$), $\beta_1$ the angle between the vector connecting D and A ($\vec{R}_{DA}$) and $\vec{\mu}_D$, $\beta_2$ the angle between ($\vec{R}_{DA}$) and $\vec{\mu}_A$.

Eq. (5) is often written as:

$$k_{ET} = \frac{\kappa^2}{\tau_R^D}\left(\frac{R_0}{R_{DA}}\right)^6 \qquad (7)$$

in which $R_0$ is the Förster radius.

For example, for energy transfer from the B800 monomer to the B850 dimer in LH2 of *Rb. sphaeroides* the following numerical values can be calculated: $R_0 \approx 7.5$ nm, (at 4 K [1]), $\kappa^2 = 2$, $\tau_R^D = 15$ ns and $R \approx 2$ nm, since the B800 pigment is at the cytoplasmic side of the membrane and the B850's are coordinated to the histidines at a position about 2 nm away from the cytoplasmic side. These numbers yield for the rate of energy transfer from B800 to B850: $k_{ET} \cong 3.7 \cdot 10^{11}$ $s^{-1}$.

As will be shown below, the actually measured rate constant for this energy transfer step is about $4.2 \cdot 10^{11}$ $s^{-1}$ at 4 K. Similarly, for the rate of energy transfer between B875 dimers in the LH1 core antenna of

photosynthetic purple bacteria we estimate $R_{DA} \cong 2$ nm, $R_0 \cong 10$ nm, $\kappa^2 = 1$ and $\tau_R^D \cong 15$ ns which yields $k^{ET} \cong 10^{12}$ s$^{-1}$. If we assume that each dimer sees (at least) two neighboring dimers, the hopping time would be at most 0.5 ps. Hopping times of less than 1 ps are probably common in photosynthetic systems.

### 2.4. Migration and trapping

Energy transfer in a photosynthetic system involves a number of ultrafast transfer steps down an energy gradient until a pool of pigments is reached that is more or less isoenergetic with the reaction center excited state. In general, these pigments are organized around the primary donor, P, and energy transfer occurs among them until P is excited and charge separation takes place. The trapping time is then defined as the amount of time needed to equilibrate the charge separated state $P^+I^-$ with the antenna/P excited state. Examples of such core antenna-RC structures containing a set of iso-energetic pigments are the LH1-RC system of photosynthetic purple bacteria, with about 24 BChl *a* per P870, the core antenna of PS II with about 40 Chl *a* per P680 and the core antenna of PS I with about 60–100 Chl *a* per P700. We remark that the absorption bands of these (and other) core antennae show often significant fine structure (PSII, PS I), that the individual bands are inhomogeneously broadened, and that these effects have to be dealt with in a theory of excitation migration and trapping [43,84,85].

The processes of excitation migration and trapping in the core antenna systems of photosynthetic organisms are usually assumed to take place on a lattice, representing the core antenna, in which the primary donor P occupies a specific lattice site (we assume here the first lattice site). Then the master equation describing the process has the following form [84]:

$$\frac{dp_i}{dt} = \sum_{j=1}^{N} (p_j W_{ji} - p_i W_{ij}) - p_i k_1 - \delta_{1i}[p_1 k_{cs} - p_0 k_{cs} \exp(-\Delta E_{RC}/k_B T)] \quad (8a)$$

$$\frac{dp_0}{dt} = p_1 k_{cs} - p_0(k_{cs} \exp(-\Delta E_{RC}/k_B T) + k_Q) \quad (8b)$$

In Eqs. 8a en 8b $p_i$ is the probability that the excitation resides at lattice site $i$, $p_0$ denotes the probability that the excitation has formed the radical pair $P^+I^-$, $N$ is the number of lattice sites in the core antenna, $k_1$ is the rate of excitation decay due to all loss processes (including fluorescence), $\delta_{ij}$ is the Kronecker $\delta$, $k_{cs}$ is the rate of formation of $P^+I^-$, $k_Q$ is the rate constant for electron transport to the secondary acceptor Q, $\Delta E_{RC}$ is the free energy difference between the states P*I and $P^+I^-$, $k_B$ is the Boltzmann constant and $T$ is the absolute temperature. $W_{ij}$ is the rate of excitation transfer from site $i$ to site $j$, for instance given by the Förster equation (Eq. 7) using the single site emission ($F_i$) and absorption ($A_i$) spectra. These latter spectra can be calculated from the appropriate Franck-Condon factors and a model that describes the interaction of the pigment with the phonons of the lattice [84,86,87].

In principle, Eqs. 8a and 8b can be put into a more compact form:

$$\frac{d\mathbf{P}(t)}{dt} = \mathbf{R}\mathbf{P}(t) \quad (9)$$

in which **P** is a vector containing the site occupation probabilities $p_0 \ldots p_N$ as elements and **R** is the $(N+1) \times (N+1)$ rate matrix. The solution of this set of coupled first-order differential equations can be obtained using the Green's function method [84,88] and can be written as:

$$\mathbf{P}(t) = \mathbf{G}(t)\mathbf{P}(0) \quad (10)$$

**P**(0) reflects the initial distribution of excitations over all the lattice sites generated by the optical absorption properties of the pigments and the spectral distribution of the excitation light. The Green's function **G**($t$) is given by:

$$\mathbf{G}(t) = \mathbf{M}^{-1} \exp(\lambda t)\mathbf{M} \quad (11)$$

where **M** is the matrix of eigenvectors and $\lambda = \mathbf{M}\mathbf{R}\mathbf{M}^{-1}$ is the diagonal matrix of eigenvalues. The matrix **G**($t$) may be interpreted as follows: the element $\mathbf{G}_{ij}$ reflects the conditional probability that an excitation generated by the light pulse at site $i$ at $t = 0$ is found at site $j$ at time $t$. The matrix **G** evolves the initial distribution of excitations at time $t = 0$ into the distribution found at a later time $t$.

With Green's function **G**($t$) and known homogeneous site-specific absorption and emission spectra it is possible to calculate the time-dependent and time-integrated fluorescence transient absorption spectra. This is described in detail elsewhere [84,88].

It is not difficult to obtain the wavelength-dependent multi-exponential decays, even for a lattice containing many pigment sites. In practice, many of the $\lambda$-values are very large and reflect ultrafast equilibration of the initial excitation density among the spectral forms of the core antenna. This allows a simple and rather straightforward description of the trapping process, in which energy transfer to neighboring pigments is lumped into a single 'migration' time, $\tau_{mig}$, and the actual trapping process, including excitation transfer to the trap and charge separation, into a 'reaction center' time $\tau_{RC}$. Then, the total time required to trap the excitation is given by:

$$\tau_{trap} = \tau_{mig} + \tau_{RC} \quad (12)$$

For a two-dimensional regular lattice, the migration time is given by [43,89,90]:

$$\tau_{mig} = \tfrac{1}{2} N f_p(N) \tau_{hop} \quad (13)$$

where $N$ is the number of antenna pigments (or antenna dimers) per RC (including the RC-special pair), $f_p(N)$ is the structure-function characteristic for the lattice and $\tau_{hop}$ is the hopping time as given by Eqs. 5 and 7.

For $N = 13$, typical for the core antenna of photosynthetic purple bacteria (assuming that the basic spectroscopic unit is the bacteriochlorophyll dimer [72,73], $f_p(N) \approx 0.5$ for a square lattice and $\tau_{hop} \approx 1$ ps, as determined from singlet-singlet annihilation experiments [91,45]), we calculate that $\tau_{mig} \cong 3$ ps. For PS II with $N \cong 100$ it is easily calculated that $\tau_{mig} \cong 10$ ps. Note that these time constants are close to the experimentally observed equilibration times in the antenna of photosynthetic purple bacteria [92,93] and PS II [67]. These migration times are also much shorter than the observed trapping times, suggesting that migration (or equilibration) is not the rate limiting process.

The actual trapping time, $\tau_{RC}$, in Eq. 12 is given by:

$$\tau_{RC} = N\left\{\frac{1}{zW_1} + \left(\frac{W_2}{W_1}\right)\frac{1}{k_{CS}}\right\} \quad (14)$$

in which $W_1$ is the rate of energy transfer from one of the nearest neighbors to P, $W_2$ is the rate of back transfer from P to one of the nearest neighbors, $z$ is the number of nearest neighbors and $k_{CS}$ is the rate of charge separation (as in Eqs. 8a and 8b). It is of interest to investigate a few limiting cases of Eq. 10, since $\tau_{RC}$ probably determines the observed trapping time in photosynthetic systems:

(1) $W_1 \approx W_2 > k_{CS}$. This corresponds to the so-called trap-limited case and

$$\tau_{RC} = N k_{CS}^{-1} \quad (15)$$

The obtained trapping time may be interpreted in the following way. Since the excitation energy is transported over all lattice sites of the core antenna (including P) with a rate much faster than any of the processes that lead to deactivation, including charge separation, the probability to find the excitation on P ($p_1$) is $1/N$, assuming all sites to be energetically equivalent. In that case the trapping rate $k_{RC} = k_{CS}/N$, which is identical to Eq. 15.

For the core antenna of photosynthetic purple bacteria $k_{CS} = 3 \cdot 10^{11} s^{-1}$ and $N = 13$, yielding $\tau_{RC} = 39$ ps, which is close to the experimentally determined value (see section 4). For PS II with $N = 150$ and $k_{cs} = 3 \cdot 10^{11}$ $s^{-1}$, Eq. 15 would imply that $\tau_{RC} = 450$ ps, which is about twice as slow as experimentally measured (see section 3). Note however, that for the plant system there exists a weak funnel effect since on the average the antenna pigments absorb around 673 nm, while the primary donor P680 shows maximum absorption around 680 nm (see below). The same is true for PS I.

We finally remark that Eq. 15 predicts that the total time required for trapping the excitation, $\tau_{trap}$, scales linearly with the rate of charge separation in the RC ($k_{CS}$). Moreover, since $W_1$ and $W_2$ are both much larger than $k_{CS}$, we expect a significant contribution from the RC pigments in the fluorescence excitation spectrum of the core antenna. This latter experiment can be performed very elegantly in purple photosynthetic bacteria containing only RC-LH1 (such as *Rhodospirillum rubrum* and *Rhodopseudomonas viridis*). So far, this experiment shows that the relative probability of exciting the core antenna fluorescence upon direct excitation of the RC pigments is only 25% or less as compared to direct antenna excitation [94–96]. In addition, the effective trapping time, $\tau_{trap}$, was recently measured for a series of RC-LH1 mutants of *Rb. sphaeroides* in which the rate of charge separation, $k_{CS}$, was modified through mutagenesis of the RC residue M210. In these experiments it was demonstrated that $\tau_{trap}$ did not scale linearly with $k_{CS}$ [97].

(2) In the second limiting case (the so-called diffusion-limited case) it is assumed that the rate of energy transfer from the neighboring antenna pigments to P is rate-limiting or: $W_1 \approx W_2 < k_{CS}$. In that case Eq. 14 reduces to:

$$\tau_{RC} = \frac{N}{zW_1} \quad (16)$$

With $\tau_{trap} = \tau_{RC} = 60$ ps for photosynthetic purple bacteria, $z = 4$ and $N = 13$ we obtain $W_1 \approx 20$ ps and consequently $W_2$ is of the same order of magnitude. This result is consistent with the above mentioned low probability of observing core antenna fluorescence upon direct RC excitation and the relatively weak dependence of the measured total trapping time on the rate of charge separation. The physical reason for the slow transfer rate from the nearest neighbor antenna molecules to P in photosynthetic purple bacteria may be related to the relatively large distance.

To which extent excitation trapping in PS I or PS II is one of these two limiting cases is not known. Excitation transfer in PS I has been claimed to be diffusion-limited [46,98] and trap-limited [99,100]. The recently published 6 Å structure of PS I suggests that many of the core antenna Chl *a*'s may be quite distant from P700 [20]. The PS II excitation transfer kinetics have been described extensively by the trap-limited model [101,69,102] and, therefore, we will elaborate on that model. In particular we wish to take into account the effect of spectral heterogeneity. In a spectrally heterogeneous core antenna with fast energy transfer be-

tween all the pigments (including P) Eq. 15 can be modified into:

$$k_{RC} = \frac{1}{\tau_{RC}} = p_1 k_{CS} = \frac{1}{\sum_{i=1}^{N} \exp[(E_1 - E_i)/k_B T]} k_{CS} \quad (17)$$

The summation is over all the core antenna pigments, including P and the other isoenergetic pigments in the RC. In Eq. 17, $E_1$ and $E_i$ represent the excited state energy of site 1 and site $i$, respectively. Note that Eq. 17 reduces to Eq. 15 if $E_1 = E_i$ for all $i$.

Eq. 17 shows that in a core antenna with $E_1 < E_i$ the probability to find the excitation on P has increased relative to the isoenergetic case. This model has been applied successfully to PS II assuming a distribution of site energies $E_i$ corresponding with the measured absorption spectrum. Such a calculation shows that PS II is actually a weak funnel. Combining the measured trapping rate of $k_{RC} \approx 3 \cdot 10^9$ s$^{-1}$ [102,103] with the calculated value for $p_1 \approx \frac{1}{100}$, the intrinsic rate of charge separation is found to be $k_{CS} \approx 3 \cdot 10^{11}$ s$^{-1}$, close to the value reported by some authors for the rate of charge separation in isolated PS II reaction centers (see section 3).

### 2.5. The radical pair-exciton equilibrium model

In the previous review [1] it was pointed out that the multiphasic excited state decay kinetics observed in the decay of the PS II fluorescence might be explained by a model in which the trapping process results in a dynamic equilibrium between the core antenna excited state and the first stable radical pair state $P^+I^-$. Subsequently, this equilibrium may decay either due to electron transfer from I to the next acceptor or due to losses (including fluorescence) from the core antenna excited state. In the simplest version of this model, in which the initial formation of the state $P^+I^-$ is represented by a single rate constant, $k_{trap}$ (Eq. 12), this model results in biphasic excited state decay kinetics due to the reversibility of the trapping process. A schematic version of this model is shown in Fig. 2.

We can further assume that the energy transfer in the antenna is ultrafast (trap-limited case) and that $k_{trap} \approx k_{RC}$ as given by Eq. 17. The rate constant $k_{-1}$ is simply given by: $k_{-1} = k_{CS}\ e^{-\Delta E_{RC}}$. In case $k_{RC}$, $k_{-1} > k_Q > k_I$ the model yields the excited state decay kinetics. The fast phase represents the formation of the dynamic equilibrium with time constant $(k_{RC} + k_{-1})^{-1}$. The slow phase decays with time constant $\tau_Q \approx k_Q^{-1}$ and has the amplitude

$$(k_{-1}) \cdot (k_{RC} + k_{-1})^{-1} \approx e^{-(\Delta E^c_{RC}/k_B T)} \quad (18)$$

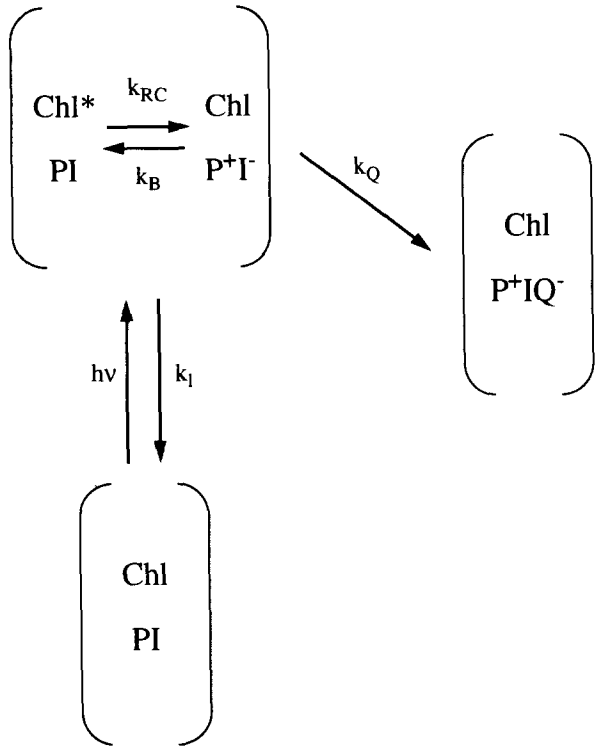


Fig. 2. Schematic representation of the exciton/radical pair equilibrium model in photosystem II. P is the reaction center pigment (P680) which is most probably a dimer of Chl *a*. I is the primary electron acceptor, a pheophytin. Q is the secondary electron acceptor, a quinone. State A reflects the ground state of the system, B the exciton-radical pair equilibrium and C the stable charge separation. The rate constants $k_{RC}$, $k_B$, $k_Q$ and $k_I$ are defined in the text.

where $\Delta E^c_{RC}$ is the free energy difference between the core antenna exited state and $P^+I^-$ given by:

$$\Delta E^c_{RC} = \Delta E_{RC} - k_B T \ln N \quad (19)$$

For instance, in PS II cores the chlorophyll fluorescence decay has been measured to be biphasic, with the amplitude of the slow phase (representing the formation of the state $P^+_{680}Q^-_A$ about 20% of the initial amplitude [101]. At room temperature this yields using Eqs. 18 and 19 that $\Delta E^c_{RC} \approx 0.042$ eV, close to the value calculated by Schatz et al. [69] using a more elaborate version of the radical pair-exciton equilibrium model.

## 3. Energy transfer in plants, green algae and cyanobacteria

### 3.1. Photosystem I

#### 3.1.1. Organization and structure

In plants and eukaryotic algae, the PS I complex consists of a cluster of more than 10 proteins. It can be

divided into two structural and functional parts: (1) the reaction center core complex containing all redox cofactors and a Chl *a* and β-carotene antenna system, and (2) the peripheral antenna LHC-I, which consists of a number of Chl *a*/*b* light-harvesting proteins. Cyanobacteria contain very similar reaction center core complexes compared to the eukaryotic systems, but lack Chl *b* and peripheral antenna complexes.

The major constituents of core complexes are two proteins with predicted molecular masses of 83 and 82 kDa. These proteins presumably contain the complete antenna system of the PS I core, and are thought to be organized as a heterodimer, sharing the iron-sulfur center $F_x$. There is no clear consensus about the number of Chl *a* molecules per core complex, and numbers between 25 and 120 have been reported (see, for example, Ref. [3]). Usually, these contents are determined by measuring the oxidized-minus-reduced difference spectrum of P-700. One cause of confusion was explained by Sonoike and Katoh [104,105] who found a pronounced sensitivity of the amplitude and shape of the P-700 difference spectrum to the specific detergent environment. In addition, certain detergents could extract some pigments from the complex. A special case is formed by diethyl ether extraction methods of core complexes introduced by Ikegami and co-workers [106,107]. This treatment removes a significant part of the Chl antenna, leaves the primary radical pair relatively intact, and thus results in a total Chl antenna size of 8–12 Chl/P-700. The native higher plant and green algal PS I complex consists of a core complex with associated peripheral antenna. This complex is usually denoted PS I–200 [108], the number indicating the estimated total Chl antenna size. The peripheral antenna probably contributes about 100 Chl $(a+b)$ molecules.

Information about the structural organization is rapidly growing. Three-dimensional crystals of cyanobacterial core complexes have been reported by a number of authors [109,110,111], and information about the general size and shape of several complexes has become available by electron microscopy and image analysis of isolated particles [112–116], two-dimensional crystals [117,118] and transient electric birefringence [119]. The general consensus of the data is that the core complex (when corrected for the detergent contribution in case of isolated particles) is a disk-like structure with dimensions of about $12.5 \times 7.0 \times 6.5$–9 nm, the latter dimension being the transmembrane distance, which is dependent on the presence of the psa-C, -D and -E gene products [120]. The native higher plant complex with connected antenna system has the same general shape as the PS I core, but significantly larger top view dimensions of about 16.5 $\times$ 12.5 nm. Isolated cyanobacterial cores have frequently been observed to be organized as trimeric complexes [112]. There is increasing evidence that this association represents the in vivo organization of the cyanobacterial core [121–123]. The results of Kruip et al. [123] suggest a dynamic equilibrium between the monomeric and trimeric states that depends on the specific salt conditions. The existence of such an equilibrium may explain why in some EM studies the trimeric form could not be observed in the membranes [124].

Recently, the three-dimensional structure at 6 Å resolution has been reported of the cyanobacterial reaction center core complex [125,20]. The three Fe-S clusters could clearly be resolved, as well as about 28 α-helical stretches and 45 chlorophyll molecules at 8–15 Å minimal center-to-center distances. Most of the chlorophylls are at relatively large distances to the center of the system, in which a dimer-like structure was tentatively attributed to P-700 and two symmetry-related structures to monomeric chlorophylls, one of which was thought to be the electron acceptor $A_0$.

From the estimations of Chl contents and particle dimensions, the average distances between Chl molecules in the complexes can be calculated. The numbers given above revert to volumes of 7.0–7.5 $nm^3$ per Chl in core complexes and of 6.5–7.0 $nm^3$ per Chl in native complexes of higher plants. This could mean that the complexes are composed of Chl building blocks with dimensions of, for instance, $2.5 \times 2.5 \times 1.1$ nm, suggesting average distances between the Chl π-electron systems on the order of 1.0–1.2 nm, which seems in agreement with the recently published structure at 6 Å resolution [20].

*3.1.2. Steady-state spectroscopic properties*

The absorption spectrum of purified PS I core complexes reveals the presence of several pools of Chl absorbing at about 666, 671, 677, 680, 684 and 693 nm (see, for example, Ref. [126]). In addition, there are various spectral species absorbing above 693 nm (apart from P-700). These long-wavelength spectral species largely determine the steady-state fluorescence properties at low temperatures. Based on site-selected fluorescence experiments it has been suggested that these spectral species arise from dimeric Chl *a* molecules [127]. In plants, the red-most species occur in the peripheral antenna and are called C716 [127]. In the core antenna the number of red pigments per reaction center and their absorption spectra seem to be variable, i.e., they depend on the particular cyanobacterial or plant species. PS I from the cyanobacterium *Synechocystis* PCC 6803 probably contains one Chl *a* dimer peaking at 708 nm (C708) [127], while in the thermophilic cyanobacterium *Synechococcus* sp. probably more long-wavelength species are present (Schlodder, E., personal communication). Holzwarth [128] resolved in *Synechococcus* sp. four Chl *a* pigments at 712 nm and

one at 725 nm by a Gaussian deconvolution of the room temperature absorption spectrum. Note, however, that usually several solutions of Gaussian deconvolutions of absorption spectra are found [126], and that therefore the presence of a special 725 nm pigment is not without doubt. In *Spirulina*, however, there is more evidence that one or more Chl's are present that absorb at about 730 nm [129]. Monomeric cyanobacterial core particles sometimes contain lower amounts of red pigments than trimeric particles [121,126,129]. The reason for this difference could originate from a somewhat greater lability of the (detergent)-isolated monomers. The red pigments do not contribute to a significant extent to the (low-temperature) CD spectrum. From LD studies on various PS I preparations it has been concluded that P700, Chl *a*-686 (= acceptor $A_0$), C-708 and C-716 are oriented predominantly with their $Q_y$ transitions in the plane of the membrane [130,131]. The more blue absorbing Chl molecules are characterized by more random orientations.

The room-temperature fluorescence yield of PS I is low (< 1% for highly purified PS I particles). In such particles, the emission maximum is between 680–690 nm (F685) with a pronounced red shoulder at 720–730 nm; the latter is in fact dominating the emission spectrum of cores of *Synechococcus* sp. [99]. Holzwarth [128] calculated the steady-state emission spectrum using the deconvolution of the absorption spectrum (including the far-red pigments) and assuming a full equilibration of the excitation density over all pigments. Upon cooling (to 77 K or below) the red emission increases dramatically and in intact PS I (core plus LHC-I) a fluorescence peak at 735 nm (F735) can be distinguished in addition to F685 while in isolated core complexes a fluorescence peak at 720 nm (F720) is observed. It is generally agreed that F720 and F735 emissions arise from the core and peripheral antenna, respectively [14]. F685 probably has a heterogeneous origin and arises from both core and LHC-I chlorophylls. For most cyanobacteria the maximum fluorescence at 77 K is at about 720 nm (F720) with a weak contribution from shorter wavelengths, but *Spirulina* probably contains a very long-wavelength pigment fluorescing at 760 nm (F 760). *Chlamydomonas* LHC-I and core give F715 and F720, respectively. Most core complexes are susceptible for detergents like Triton X-100 and SDS (although cores from thermophilic cyanobacteria are relatively stable); in their presence fluorescence bands at 670–685 nm occur, which disappear upon removal of these detergents [132].

### *3.1.3. Time-resolved excitation decay at room temperature*

The low yield of the PS I fluorescence at room temperature suggests that the excited state lifetime is short. Indeed, picosecond time-resolved fluorescence measurements in intact algae and cyanobacteria have revealed a short-lived decay component ($\tau$ = 70–120 ps) with a broad fluorescence spectrum peaking at about 700 nm [133,134]. This decay component was assigned to excitation migration and trapping in PS I, also because it was unaffected by the state of the PS II (closed or open) and because it was observed in a PS II less mutant as well [134]. Since 1985, a large number of excited state decay measurements were reported on intact PS I and on purified particles of variable composition (with or without LHC-I), antenna size and quality, which will be discussed below.

*3.1.3.1. Trapping in the Photosystem I core complex.* Many recent studies have revealed fluorescence lifetimes between 15 and 40 ps in PS I core complexes [46,98–100,135,136–144]. In several cases, long-lifetime (~ 5 ns) components with low amplitudes (< 15%) were observed as well. In the most intact preparations these slow components were virtually absent, suggesting that they may have been caused by badly connected or free Chl *a*. From all these results, we may safely conclude that trapping (presumably by P-700) in PS I core complexes takes about 20–40 ps.

Experiments by Owens et al. [46] suggested a linear relationship between the fast dominant decay phase and the antenna size. The authors interpreted this result in terms of the relation given by Pearlstein [43] for the average trapping time, which assumes energy transfer on a homogeneous lattice and yields numbers for the microscopic rate constants of excitation migration and charge separation. Thus, time constants of single-step excitation energy transfer and charge separation were calculated to be 0.2 ps and about 3 ps, respectively. Note that the former number is remarkably similar to the value estimated for single-step transfer in the purple bacterial light-harvesting antenna [45,145,146] and that the latter number equals the time constant for charge separation in isolated bacterial reaction centers [147,148]. From a recent femtosecond fluorescence upconversion study, Du et al. [52] concluded that 0.18 ps is the upper limit for the average single transfer step in the PS I core, in line with the earlier suggestion of Owens et al. [46].

A detailed analysis of the PS I fluorescence decay as a function of excitation and detection wavelength by Owens et al. [98] suggested that the excitation density was spectrally equilibrated in the PS I antenna within the time resolution of the experiment (10 ps), and found to be not fully concentrated on low-energy (red-shifted) pigments. This finding, combined with the fact that all steady-state and time-resolved spectral features seem to be independent of the PS I core size, suggested to these authors that the various Chl *a* spectral forms that occur in the PS I antenna are organized more or less randomly around P700. A similar conclu-

sion was drawn by Causgrove et al. [138] from time-resolved depolarization studies on small PS I particles and by Owens et al. [149] on mutants of *Chlamydomonas reinhardtii*. These studies have suggested that trapping by P700 may be described as an intermediate between a trap-limited and a diffusion-limited process, with the excitation visiting P700 on the average 2–3 times before charge separation.

In contrast, several groups have interpreted their results from time-resolved fluorescence to show that initially a rapid energy transfer takes place between the major fraction of antenna Chl *a* and a minor pool of relatively red-shifted pigments (responsible for the F720 emission) [100,136,139,140,142–144] and time constants in the range of 5–20 ps have been estimated for this process, much slower than the estimated hopping time between 'identical' Chl *a* molecules. In this view, the 20–40 ps decay that follows the energy transfer phase reflects the trap-limited decay of the equilibrated excitation density due to charge separation by P700. It was assumed or proposed by several authors [12,86,99,100, 136,140–142] that the transfer to P700 occurs only from the red-shifted minor antenna pool (see, however, Van der Lee et al. [126]). We note in this respect that the trap-limited model predicts a linear relationship between antenna size (assuming that all spectral species increase in proportion) and the fluorescence lifetime, since the effective trapping rate in this case is simply given by the product of the molecular rate of charge separation and the probability to find the excitation on P700.

*3.1.3.2. Trapping in large Photosystem I complexes.* Larger PS I complexes (150–200 Chl/P700) consist of a reaction center core complex and a number of peripheral Chl *a*/*b* containing LHC-I complexes. In general, fluorescence decay times between 50–120 ps have been reported and probably the average is between 70–90 ps; this time constant has been ascribed to trapping and in all cases shows in addition to 685 nm emission a significant amount of long-wavelength fluorescence (720–740 nm) [98,99,134,143,149–152] of about equal intensity. In some cases additional faster phenomena were observed, which at least in part can be ascribed to equilibration before trapping takes place (see 3.1.3.4). By measuring trapping by P700 directly through generation of a membrane potential, Trissl et al. [150] concluded that for intact PS I the trapping time was 70–80 ps, independent of the excitation wavelength between 700 and 720 nm, which supports the idea of ultrafast equilibration followed by a trap-limited charge separation. The wide variation in reported fluorescence lifetimes may in part be due to the heterogeneous nature of these 'intact' PS I preparations used for the experiments. 'Slow' decay phases in the 100–300 ps time range have been observed quite often, and were ascribed to 'badly' or 'differently' coupled LHC-I [134,46,98]. Holzwarth et al. [99] suggested that the trapping time is heterogeneous due to the fact that PS I–200 preparations contain smaller (fast decaying) and larger (slow decaying) fractions. Such a heterogeneity may also explain the deviations observed by Owens et al. [98,149] in the linear relation between antenna size and trapping time for LHC-I-containing particles. For a homogeneous, well-coupled PS I preparation the additional LHC-I complexes should contribute to the effective antenna size as shown by Trissl et al. [153] and in contrast to the claim by Owens et al. [98,149].

*3.1.3.3. Excitation decay in intact Photosystem I.* Fluorescence kinetics recorded with sufficient time-resolution indicated that in intact algae and thylakoid membranes the PS I excited state decay is of the order of 100 ps [1,14]. Recently, a full global analysis was performed of the room temperature fluorescence decay of pea chloroplasts at a variety of wavelengths, which led to the assignment of 10–20 ps equilibration phase [67,99,102], followed by the 80–120 ps decay. In these chloroplasts the decay associated emission spectrum (DAS) of the main PS I fluorescence decay shows broad contributions near 690 and 730 nm, of which the 690 nm contribution may be partly contaminated with PS II emission. In general, these results are quite consistent with those obtained for the large PS I complexes.

*3.1.3.4. Spectral and spatial equilibration in Photosystem I.* The timescale and degree of distribution of excitation energy over the various spectral forms of PS I and their possible role in funneling excitation energy to P700 have been the subjects of a long discussion. The results by Owens et al. [46,98,149] on a variety of PS I preparations never gave any indication of an equilibration process on a timescale slower than 10 ps. The emission spectra were shown to be rather similar for the various decay components and were interpreted to represent the emission spectrum of a thermally equilibrated excited state involving all spectral forms. It was shown that the relative amplitude of the fluorescence recorded at different wavelengths was independent of the emission wavelength and close to that expected from thermal equilibrium. The excitation wavelength dependence of the fluorescence kinetics for large PS I preparations indicated that equilibration between LHC-I and the core occurred within less than 5 ps. Computer simulations of the PS I excited state kinetics using 'reasonable' numbers suggested that most spectral equilibration would occur within 10 ps and probably within 1 ps, and therefore hard to detect using single photon timing [88,154]. It is important to note that the PS I particles investigated in these studies may have lost a (large) fraction of the red pigments, since the room temperature emission spectra peak around 685 nm and exhibit only a weak shoulder around 720 nm. The absence of red pigments may have

obstructed the detection of a 10–20 ps equilibration phase.

Causgrove et al. [138,152] were the first to observe fast decay processes in PS I by using time-resolved isotropic and polarized absorption spectroscopy. Their experiments indicated that in PS I core complexes and in PS I–200 preparations an equilibration process of a few picoseconds preceded trapping. This absorption anisotropy decay was interpreted to be the result of relatively slow hopping between certain clusters (and ultrafast spectral equilibration within a cluster). Indeed, several groups reported time-resolved absorption measurements that indicated the localization of the excitation energy on red-shifted pigments within at most a few picoseconds [139,155]. From more recent two-color pump-probe measurements by Lin et al. [68] using PS I core complexes from *Synechococcus* sp., it was concluded that within the time-resolution of the experiment ( < 2 ps) the excitation distribution equilibrated almost completely among the spectral forms, as manifested by the ultrafast redshift of the zero-crossing of the transient absorption difference spectrum. The ultrafast decay was associated with a strong depolarization of the transient absorption signal. A slower phase of about 10 ps, associated with a blue-shift of the zero-crossing of the transient absorption difference spectra and correlated with a weak depolarization, probably represents a further equilibration between the bulk of the PS I core and some of the far red pigments.

Time-resolved fluorescence measurements by Holzwarth et al. [99,100] suggested a 10–20 ps equilibration phenomenon in PS I cores of *Synechococcus sp.* It was shown that the decay associated fluorescence spectrum of the first fast phase of 10–20 ps had positive (decay) amplitude at the blue side of the emission spectrum and negative (rise) amplitude at the red side, characteristic for an energy transfer process. More recently, the same group [142] presented evidence that in fact the 10–20 ps equilibration between the bulk core Chl *a* and the minor pool responsible for F720 was preceded by < 3 ps equilibration between the bulk Chl *a* emitting at 685–690 nm and another pool emitting at about 710 nm. This latter pool may originate from pigments absorbing at 693 nm that are oriented at large angles with the long-wavelength pigments responsible for the F720 emission [126]. Transient absorption data suggested that the < 3 ps kinetics are dominated by a few hundred fs process [68], in agreement with the above-mentioned fluorescence depolarization kinetics with a time-constant of about 0.2 ps [52]. Similarly, for large PS I complexes from spinach stroma lamellae, evidence from time-resolved fluorescence kinetics was presented that demonstrated the existence of an energy transfer process of about 20 ps preceding trapping by P700. Probably, the faster (few hundred fs) equilibration process has escaped registration in larger particles and intact systems so far.

In conclusion, ultrafast equilibration among the bulk of the PS I pigments occurs on a sub-picosecond timescale. Slower equilibration processes ( ~ 10 ps) occur between the 'red' and the bulk PS I pigments; these kinetics may be determined by the migration time, in view of the low concentration of the red pigments. An additional element, which also holds for the situation in purple bacteria (see section 4.1), is that the transfer from the antenna Chl *a* molecules to P-700 may be relatively slow in comparison to the Chl *a* → Chl *a* transfer among the antenna Chl's. The 6 Å PS I structure suggests that most of the antenna Chl's are rather far from P-700, due to which the energy transfer time from a bulk PS I pigment to P-700 could easily be in the order of 10 ps. Thus, in this sense trapping and equilibration compete, and probably the excitation density in PS I is not fully equilibrated on the timescale of trapping.

### *3.1.4. Energy transfer in Photosystem I at low temperatures*

At all temperatures between 300 K and 10 K the emission decay of the 685–690 nm components is fast ( < 100 ps) and the associated fluorescence yield (F690) is almost constant with temperature [1,14]. In higher plants, the fluorescence decay at 735 nm (F735), ascribed to the minor pigment pool C716, slows down upon cooling (it has a characteristic ~ 3 ns decay time at 77 K) and, in addition, gains amplitude [151]. Similarly, in core particles, the F720 emission was found to slow down with decreasing temperature to 200–400 ps at 77 K [1,14]. In chloroplasts from higher plants F735 was observed to exhibit a finite risetime upon excitation of the main pool of Chl *a* with a short light pulse. A variety of values for the F735 rise kinetics have been reported, and evidence has been presented by Wittmershaus et al. [156] that in intact chloroplasts at 77 K the F735 rise kinetics are in fact biphasic with components in the 10–20 ps and 100 ps ranges. Similarly, the dominant F720 emission in core preparations exhibited a 10–20 ps risetime at 77 K, which was correlated with the 10–20 ps decay of the emission at 685–690 nm (F690) from the major Chl *a* pool.

Based on these results, Wittmershaus [157] presented a kinetic model for the PS I excitation decay kinetics, in which F720 reflects the emission of a minor red-shifted pool of Chl *a* (designated now as C708) that links the major fraction of Chl *a* to P700. In this model the rise of F720 is directly correlated with the decay of the excitation density in the major pool of Chl *a*. The temperature dependence of the energy transfer from C708 to P700 is the major cause for the increase in the PS I fluorescence yield in these isolated particles. The model could easily be extended to explain the

kinetics observed in chloroplasts of higher plants by including a second parallel path for feeding excitations into P700. In this second path, the F735 emitting species C716 connects P700 via a peripheral fraction of core Chl *a* to LHC-I. The energy transfer from C708 is responsible for the fast (10–20 ps) part in the rise of F735, while the energy transfer from C716 on LHC-I is responsible for the slow (100 ps) part. The model was numerically fitted to the available experimental data. Again, the temperature dependence of the energy transfer from C708 and C716 to P700 is the main cause for the dramatic increase of the long-wavelength fluorescence of PS I. The model assumes that C708 and C716 are not connected via energy transfer, which is mainly based on the observation that the lifetime of F720 (200–400 ps) is insensitive to the presence or absence of C716 [157]. Note that the model originally presented by Wittmershaus [157] is very similar to that proposed recently by Turconi et al. [142] (at least with respect to the PS I core), in which the pool responsible for F720 is proposed to be intermediate between P700 and the bulk chlorophylls. The major difference is that Turconi et al. place a third emitting state (F710) between the bulk antenna and F720 (vide supra).

Several alternative schemes have been suggested that indicate a different spatial organization of the red pigments around P700. Searle et al. [137] studied the temperature dependence of the fluorescence emission of an SDS-purified core preparation with 40 Chl *a*/P700. At 77 K their observations are quite similar to those of Wittmershaus [157], but Searle et al. performed measurements over a much larger temperature range. They fitted their data with a model that includes a direct connection between the major pigment pool responsible for F690 and P700. The transfer of excitations to P700 via C708 represents in their view a parallel and less favored path that acts as a trap for excitations at low temperature. They base their choice of the model mainly on the hypothesis that, even below 77 K, P700 is still oxidized with a relatively high quantum efficiency.

The temperature dependence of the fluorescence yield and decay of LHC-I containing particles was investigated by Mukerji and Sauer [151,159]. Again, the F690 contribution to the emission spectrum was found to be short-lived at room temperature ($< 30$ ps) and only slightly longer-lived at 77 K (50 ps), while the F690 fluorescence yield was found to be almost temperature independent. At 77 K, the 50 ps component clearly reflects energy transfer from F690 to F735, as shown by the fluorescence DAS with positive (decay) and negative (rise) contributions. At least 4 other components were required to fit the wavelength resolved fluorescence decays at 77 K. Apart from a slowly decaying contribution from unconnected Chl *a*, 250–300 ps (F720) and 1 ns and 2.5 ns (F735) decay components were observed. The F735 fluorescence is specifically excited by Chl *b*. Separate experiments on isolated LHC-I complexes demonstrate unequivocally that F735 originates from the Chl *a*/*b* LHC-I antenna [158,159,143]. These authors suggested a model that differs from the scheme by Wittmershaus [157] but is similar to that of Searle et al. [137] discussed above. Mukerji and Sauer assume that the core Chl *a* transfers its excitation energy to P700 either directly or via C708. Upon lowering the temperature the transfer to C708 is favored over the direct transfer to P700, due to a slight slowing down of the direct transfer process. This would explain the observed increase in amplitude of the F720/F725 emission upon lowering the temperature. In addition, and in contrast to Wittmershaus, LHC-I was supposed to feed excitations to P700 through a serial arrangement of C716 (F735) and C708 (F720).

The most extensive study on the temperature dependence of the PS I emission was performed by Werst et al. [141], who recorded time-resolved fluorescence decays of core complexes from the green alga *Chlamydomonas reinhardtii* between 36 K and 295 K. At room temperature, a strong 15–20 ps decay component was observed. Upon lowering the temperature, the emission decay slowed down, in particular at the long-wavelength side of the emission spectrum (around 720 nm). Notably, even at 36 K the 720 nm fluorescence decay kinetics occurred in about 100 ps, indicative of some trapping process that still occurs from these low-energy states. The authors fitted the temperature dependencies with a model that assumes a regular two-dimensional pigment arrangement and includes the various spectral forms of PS I and their distribution around P700. The 'only' model that fitted the observations reasonably well was one in which two red pigments (C708) are placed close to P700 and mediate excitation energy transfer from the bulk, randomly distributed pool of Chl a to P700. Also based on a regular two-dimensional pigment arrangement Trinkunas and Holzwarth [160] modelled exciton migration in PS I from *Synechococcus* sp. using the various spectral forms. *Synechococcus* is probably special because it shows extended red wing absorption in comparison to PS I cores from most other photosynthetic organisms (see 3.1.2). From the modelling it was concluded that the long-wavelength pigments form a cluster in the corner of the lattice relatively close to P700. The assumption of a regular lattice including P700, however, may not be justified in view of the 6 Å structure [20]; this structure suggests that there is, as in photosynthetic complexes from purple bacteria and probably also in PS II, a considerable distance between P700 and most of the antenna pigments.

Stationary polarized fluorescence measurements have suggested that in the core antenna excitations are

not transferred among low energy pigments at low temperature [161,126,127]. Van der Lee et al. [126] have shown that at 77 K the polarization of the fluorescence of trimeric PS I cores of *Synechocystis* approaches the theoretical maximum for $\lambda_{exc} > 690$ nm.

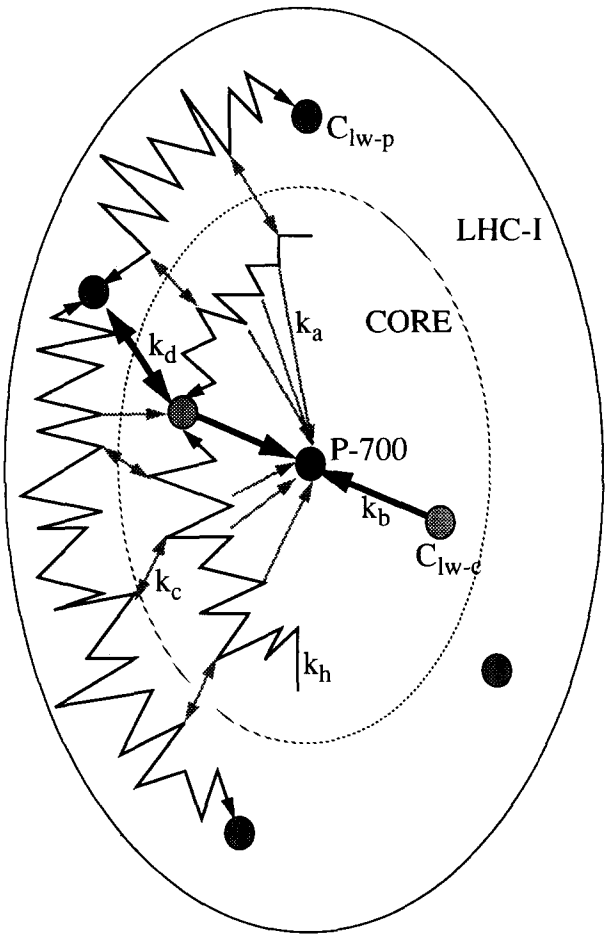


Fig. 3. Schematic model of the energy transfer and trapping processes in PS I. The overall structure is based on electron microscopic results of [115] and represents a top view of the native PS I complex in plants. In the core complex a large number of bulk Chl *a* molecules are involved in ultrafast hopping with average rate $k_h$. At a few places within this structure of Chl molecules, long-wavelength species $C_{lw-c}$ are located (from which recently the absorption maxima were determined at 708 nm [127]). Note that *Synechocystis* probably contains one dimeric $C_{lw-c}$ per complex [127]. The excitations on the bulk Chl *a* molecules may have an equal chance [126] to reach one of the $C_{lw-c}$ molecules via fast hopping or to reach P-700 directly with rate $k_a$. The rate constant $k_a$ is assumed to be in the 10–20 ps range. The excitations on $C_{lw-c}$ finally reach P-700 via the temperature-activated uphill energy transfer rate $k_b$. P700 is represented as an irreversible trap in accordance with results in Refs. [126,141]. In LHC-I, the bulk chlorophylls are also connected by fast hopping. Here, they either reach one of the LHC-I long-wavelength pigments $C_{lw-p}$, or they reach one of the bulk pigments of the core antenna with rate $k_c$. Some of the long-wavelength pigments on the core and peripheral antenna may be interconnected by the temperature-dependent rate $k_d$.

Site-selected polarized fluorescence experiments at 4 K showed a remarkable dependence of the fluorescence emission maximum on the excitation wavelength [127], which is explained by inhomogeneous broadening of the long-wavelength absorption band. Since the fluorescence is predominantly excited by the pigments absorbing at $\lambda_{exc} > 690$ nm [126], the long wavelength pigments are not a necessary intermediate for EET from the bulk Chl *a* to P700, in agreement with the models proposed by Searle et al. [137] and Mukerji and Sauer [151,159]. In larger PS I–200 particles from spinach the rise of the fluorescence polarization and the onset of the shift of the emission maximum occurred at much longer wavelength than in the core [126,127] and in isolated LHC-I [158], suggesting that at and below 77 K downhill energy transfer takes place from the core antenna to the peripheral antenna.

Localization of excitations in PS I upon lowering the temperature has also been observed using time-resolved single-wavelength absorption anisotropy [155] and spectral hole-burning [162]. In the former experiments, the absorption anisotropy decay at 680 nm was found to slow down from 7 ps at 300 K to 60–65 ps at 38 K, with most of the slowing down occurring between 65 K and 38 K. If the anisotropy decay is due to single EET steps, the temperature dependence can be modelled by assuming that localized low-frequency ($\omega = 20$ $cm^{-1}$) phonons (from the surrounding protein) are coupled to the energy donor and acceptor (note that a careful analysis of these phenomena taking into account the possible *T*-dependent admixture between excited state absorption and ground state bleaching at the wavelength used for these experiments still has to be performed). Non-photochemical hole-burning of PS1–200 at 1.6 K in the wavelength range between 670 and 680 nm by Gillie et al. [163] resulted in ZPH-widths of 0.02–0.03 $cm^{-1}$, or a $T_1$ of about 300 ps, again suggesting localized excitations. However, the hole-burning result may in part have been due to a detergent-induced disruption of the PS I particle that was studied in these experiments (Small, G.J., personal communication).

In Fig. 3 we show a schematic model that may account for many of the time-resolved and stationary spectroscopic results obtained as a function of temperature for cores and intact PS1. The crux of the model is (i) localization of the excitation on low-energy pigments in the core and/or the peripheral antenna, (ii), due to their relatively low concentration it may take 5–20 ps for an average excitation to reach the low-energy pigments, (iii) from many pigments there exists a slow (20–40 ps) and essentially irreversible energy transfer process to P-700, and (iv) the energy transfer from the low-energy pigments to P-700 (and of course to neighboring antenna Chl *a*'s) is strongly temperature dependent.

### 3.2. Photosystem II

#### 3.2.1. LHC II

*3.2.1.1. Organization.* Green plant thylakoid membranes contain a number of peripheral antenna complexes, which all contain Chl *a* and Chl *b*, belong to the same family of proteins (in view of the homologies in the primary amino acid sequences) with molecular masses in the range of 25–30 kDa, are in most cases present in variable amounts, and are generally only loosely associated with the photochemical reaction centers of the Photosystems I or II [4].

By far the best studied Chl *a*/*b* complex is the major light-harvesting complex II (LHC II), which binds close to 50% of all chlorophylls in green plants. Its three-dimensional structure has been determined by electron diffraction on two-dimensional crystals to a resolution of 6 Å [18], and recently to 3.4 Å [19]. The protein crystallizes as a trimer, which is also believed to be the native form. Each monomer contains 3 transmembrane $\alpha$-helices and most likely 7 Chl *a* and 5 Chl *b* molecules [19]. The positions and relative orientations of the planes of the porphyrin rings of the chlorophylls have been determined [19]. All porphyrin rings were found to be oriented almost perpendicularly to the plane of the membrane, and arranged in two levels near the upper and lower surfaces of the thylakoid membrane. These levels were reported to contain 7 and 5 Chl's, respectively [19]. The data suggest that all Chl *b* molecules are in close contact with Chl *a*, and that most Chl *a* molecules are in close contact with carotenoids, thus providing the framework for rapid EET from Chl *b* to Chl *a* and efficient triplet energy transfer from Chl *a* to the carotenoids. The shortest center-to-center distances between the chlorophylls range from 9–14 Å within one plane and from 13–14 Å between planes. This points to a very densely packed pigment structure, in which relatively strong exciton couplings between pigments and relatively fast energy transfer rates are expected.

*3.2.1.2. Spectroscopy.* The 4 K absorption spectrum of trimeric LHC II shows several peaks and shoulders in the $Q_{y(0-0)}$ absorption region of Chl *a* and Chl *b* (i.e., between about 680 and 635 nm) [164–167]. Low-temperature LD spectra have indicated that Chl *b* transitions at 656 and 649 are at angles larger than 35° (magic angle), and that the Chl *a* transitions at 676 nm are at small angles with the plane of the membrane (between 0° and 12° [168]). The 4 K CD spectrum shows negative peaks at 676, 651 and 639 nm, positive peaks at 667 and 645 nm and shoulders near 660 and 673 nm [166], suggesting that in LHC II a complicated set of excitonic interactions occurs between several Chl *a* and Chl *b* molecules. Some of the spectral bands are not observed in monomeric LHC II, which indicates that some of the excitonic bands arise from interactions between chlorophylls on different monomers [169].

The 4 K emission spectrum consists of a narrow (fwhm 5.5 nm) transition peaking at 681 nm and a number of vibrational transitions at higher wavelengths [170]. In the Chl *b* absorption region, the polarized excitation spectrum (at 77 K) showed fine structure that clearly resembled the LD spectrum [164]. This was explained by assuming that the emitting species form a circularly degenerate oscillator in a plane, which is reflected similarly by the fluorescence polarization and the LD spectra. This suggests that the plane of the circularly degenerate oscillator is (almost) the same as the plane constituted by the two long axes of the particle (and of the plane of the membrane). The observed low value of the polarization at 676 nm ( $\sim 0.1$ [164]) is in agreement with the idea of a circularly degenerate oscillator, provided that the energy transfer between the several $Chl_{676}$ molecules is efficient. The gradual rise of the polarization upon raising the excitation wavelength above 680 nm may in this context be explained by inhomogeneous broadening of the 676 nm transition and less efficient back-transfer once a relatively red-absorbing species is excited (see also the extensive discussions in section 4). Recent polarized fluorescence and hole-burning experiments suggest that in addition to the inhomogeneously broadened pool of $Chl_{676}$ molecules a small pool (one pigment per trimer) of chlorophyll molecules absorbing at 680 nm is present [168,171].

Until recently the spectroscopy of LHC II was analyzed in terms of the so-called trimeric Chl *b* exciton model by van Metter, Shepansky and Knox [172, 173,174]. These authors assumed a structure consisting of a core of three excitonically coupled Chl *b* molecules surrounded by three more distant Chl *a* molecules. The more recent data on the pigment structure [18,19] suggest that such a core of excitonically coupled Chl *b* molecules, if present, can only exist in the center of the LHC II trimer, while the more recent spectroscopic data suggest a considerably more complex framework of excitonic interactions than predicted by the trimeric Chl *b* exciton model.

Some of the spectroscopic properties of trimeric LHC II change drastically upon aggregation due to detergent-removal. Most conspicuous are the more than 20-fold quenching of the steady-state fluorescence, the shift of the peak wavelength of the 77 K fluorescence to about 700 nm, and characteristic changes in absorption, linear dichroism and circular dichroism spectra (Refs. [175–177]; Ruban, A.V., Kwa, S.L.S., Van Grondelle, R., Horton, P. and Dekker, J.P., unpublished data). Recent experiments indicate that at 4 K almost no quenching of steady-state fluorescence occurs in aggregated LHC II, and that the peak of this fluorescence blue-shifts to about 685 nm (Ruban, A.V.,

Calkoen, F., Peterman, E.J.G., Van Grondelle, R., Dekker, J.P. and Horton, P., unpublished data). This effect may be rationalized by a small number of quenchers in the aggregates and a small effective cluster size at 4 K (which is due to the difficulty for the excitation to escape from local low-energy traps at low temperature – see also [70]).

It has been proposed [176] that a reversible aggregation of LHC II would be the primary cause of 'high-energy quenching' of fluorescence in leaves and thylakoids. This high-energy quenching offers a physiologically important regulation mechanism of Photosystem II when in intact thylakoids excess light is absorbed [178] and is related to the so-called xanthophyll cycle [179]. The nature of the fluorescence quencher, however, is not known yet. In addition, it is not yet generally accepted that the fluorescence quencher resides on LHC II; other hypotheses propose a fluorescence quencher near the reaction center of PS II [180]. However, the evidence that the quenching also occurs in $F_0$ [181] can not easily be explained by a quencher near the reaction center of PS II and thus favors LHC II aggregation as the primary cause of high-energy quenching.

*3.2.1.3. Energy transfer dynamics.* The dynamics of excitation energy transfer in the LHC II complex has been investigated by several groups using time-resolved one-color and two-color absorption and fluorescence spectroscopy. Earlier experiments reported multiphasic fluorescence decays with characteristic lifetimes of 3.5 ns and 1.1 ns for the trimeric form of LHC II [182]. Under conditions leading to aggregation only sub-ns lifetimes were observed [182,183,184], which is in line with the strongly decreased steady-state fluorescence yields of these aggregates (vide supra).

Earlier one-color pump-probe experiments on LHC II in Triton X-100 [185] indicated Chl *b* → Chl *a* and Chl *a* → Chl *a* transfer times of about 6 and 20 ps, respectively. In these experiments the Chl *b* → Chl *a* transfer time was derived from the isotropic absorption decay in the Chl *b* spectral region, where no depolarization was found. The Chl *a* → Chl *a* transfer time was inferred from the absorption depolarization at 665 nm. We note that such measurements are notoriously difficult since the observed signal may be composed of signals with opposite sign and different polarization. Time-resolved singlet-singlet annihilation experiments suggested that extensive energy transfer occurred and pointed at a nearest-neighbor transfer time of less than 5 ps and probably faster than 1 ps [183]. These transfer times are closer to those extracted from time-resolved excited state lifetime measurements on cores of PS I, PS II and LH1-RC's from purple bacteria.

Using time-resolved fluorescence upconversion to study the transfer from Chl *b* to Chl *a* in a PS I/PS II-less mutant from *C. reinhardtii* led Eads et al. [49] to conclude that the timescale of energy transfer from Chl *b* to Chl *a* was approximately 0.5 ps, about an order of magnitude faster than suggested before by Gillbro et al. [185]. Sub-picosecond kinetics of energy transfer are expected in case of Chl-Chl separations of up to 1.2 nm [18,49], and were also observed in PS I [52].

Recently, the LHC II excitation transfer dynamics was investigated using one- and two-color picosecond pump-probe spectroscopy [50,186]. It was found that the Chl *b* to Chl *a* energy transfer kinetics were strongly multiphasic, with a large fraction of the transfer occurring with a time constant of less than a picosecond, corresponding to the ultrafast process observed by Eads et al. [49]. It was suggested that the ultrafast phase may be attributed to Chl *b* → Chl *a* transfer within a layer of pigments in the monomer [50]. Polarized one-color absorption measurements in the red part of the spectrum showed that also the Chl *a* → Chl *a* transfer within such a layer occurs at a similar high rate. A slower process (2–6 ps) was tentatively assigned to Chl *b* → Chl *a* transfer and further Chl *a* (671 nm) → Chl *a* (676 nm) equilibration between the layers in the monomer. In addition to the subpicosecond and 2–6 ps lifetime components, decay phases with lifetimes of 14–36 ps and several hundreds of picoseconds were observed. The former group of lifetimes may arise from exciton equilibration between pigments of different monomers [50]; the latter remained unassigned. Recent time-dependent fluorescence depolarization studies by Du et al. [51] provided more details about the ultrafast processes. Most of the depolarization was found to occur in the 150–300 fs time range, suggesting that the Chl *b* → Chl *a* energy transfer proceeds in this time range. A 5–10 ps depolarization time was found as well, in agreement with the heterogeneous kinetics reported by Kwa et al. [50]. Pålsson et al. [187] recently interpreted their sub-picosecond pump-probe experiments in a similar way.

Similar experiments at 23 K and lower [186] resulted in spectra that were red-shifted compared to those at 300 K. At these low temperatures both the residual anisotropy and depolarization time increased upon exciting towards longer wavelengths in the red-wing of the absorption spectrum. Both the temperature and wavelength dependence of the anisotropy decay could be explained by the assumption that at low temperatures energy transfer between the pigments within the inhomogeneously broadened 676 nm is possible. However once pigments in the red tail are excited energy transfer to other red pigments can only take place via pigments that absorb a few nanometers to the blue, which 'explains' the activation by temperature. Both at room temperature and at low temperatures an intensity-dependent annihilation process was observed to take place on a timescale of approximately 30 ps upon excitation in the Chl *a* absorption peak [50,186]. This

result provides an indication of the time that the excitation needs to 'walk' through the trimer.

We finish this discussion by emphasizing the point that energy transfer within the LHC-II trimer is a strongly multi-phasic process with kinetics that range from less than some hundreds of femtoseconds to about 30 ps.

### 3.2.2. The Photosystem II reaction center (D1-D2-Cyt.b559)

*3.2.2.1. Organization.* The photochemical reaction center (RC) of Photosystem II is bound by two transmembrane proteins called D1 and D2. The amino acid sequences of these proteins and of those of the RC proteins of purple bacteria show in some regions pronounced homologies [188], suggesting a common evolutionary origin of these reaction centers. It is generally accepted that the electron transport chains of both systems are very similar at the reducing sides with comparable pheophytin/quinone/non-heme iron organizations. The electron transport chains, however, differ essentially at the oxidizing sides. In PS II the redox potential of the primary electron donor P680 is extremely high, due to which water can be used as ultimate electron donor and oxygen is released as a byproduct.

The isolation of a complex of D1, D2, cytochrome *b*-559 and the psb-I gene product has first been reported in 1987 by Nanba and Satoh [2]. It was shown that the preparation is photochemically active [189] and that the small cyt.*b*-559 and psb-I proteins are not essential for pigment binding and photochemical activity [190]. Satoh's work induced a large amount of research by many groups. The first progress (1987–88 papers) was, however, hampered by the instability of the preparations. It is generally believed that the instability is caused by the formation of singlet oxygen, which is formed as a result of oxygen quenching of Chl triplet states [191]. The second-generation preparations are more stable, which is due to the exchange of the detergent Triton X-100 by mild detergents as dodecyl maltoside or digitonin [192–194], to the application of oxygen-free conditions, to the reduction of the time of Triton-exposure [195] and/or to the application of new methods that completely avoid the use of Triton X-100 [196].

In all PS II RC preparations obtained thusfar the plastoquinones $Q_A$ and $Q_B$ were removed from their binding sites, implying that photochemistry does not proceed beyond the primary radical pair. The pigment stoichiometry has been the subject of considerable debate. Presently most researchers accept the notion that each D1-D2-cyt.*b*559 complex binds Chl *a*, Pheo *a* and $\beta$-carotene in a stoichiometry of 6 : 2 : 2 [197,198,195]. About 2 Chl *a* and 1 $\beta$-carotene molecules are probably removed from the complex by excess detergent treatment [199].

*3.2.2.2. Spectroscopy.* In the Chl $Q_{y(0-0)}$ region (around 675 nm), the 4 K absorption spectrum is characterized by a sharp peak at 679.5 nm, a much broader peak with slightly smaller amplitude near 670 nm and a shoulder near 683 nm [200,201]. The shoulder at 683 nm has not been observed in all studies; research in our laboratory has suggested that this shoulder appears in particular when the isolation procedure is carried out in complete darkness. Contamination by CP47 (as suggested by Jankowiak and Small [202]) may be regarded as less likely in view of the constant amplitude of this component in different preparations (Ref. [201]; Eijckelhoff, C. and Dekker, J.P., unpublished data), of the absence of CP47 emission, and of the absence of light-inducible CP47 carotenoid triplets [203].

It is currently believed that the long-wavelength region (679–683 nm) is dominated by P680 and that the 670 nm region is dominated by accessory Chl. The $Q_y$ transitions of the pheophytins were reported between 676.5 nm [200] and 680–1 nm [204,205]. The pigment organization has been studied by low-temperature polarized light spectroscopy by a number of groups [206–209]. The general consensus is that the orientations of the pheophytins are similar in the reaction centers of PS II and of purple bacteria (see also Refs. [210–212]) and that the average orientations of the accessory Chl molecules are significantly different in both systems [208].

There is considerable debate about the nature of the primary electron donor P680, which is thought to be either a Chl *a* monomer, a (weakly coupled) dimer of Chl *a* molecules or even a set of interacting Chl *a* molecules. The *D* and *E* values of the P680 triplet suggest that the triplet is not delocalized over more than one Chl *a* molecule (see, for example, Refs. [213,205]). The heme plane of the triplet was found at an angle of 30° with the plane of the membrane, suggesting an orientation similar to the accessory BChl molecules in the bacterial reaction center [213]. Also the $Q_y$ and $Q_x$ optical axes are probably similarly oriented [214]. Some observations suggest the presence of a dimer in PS II: Durrant et al. [48] and Schelvis et al. [215] noted a significantly higher oscillator strength of the long-wavelength Chl molecules upon excitation and suggested the formation of a coherent excitonic state shortly after excitation. Recent experiments with polarized site-selection excitation suggest the presence of a small high-exciton band at about 665 nm [216], indicating a true dimer (or multimere) structure. Results from FTIR spectroscopy were also interpreted in favor of a dimeric structure [217]. The small amplitude of the high-exciton band [216] and the LD-ADMR experiments by Van der Vos et al. [205] suggest almost

parallel orientations of the constituting monomer transitions. Because the orientations of these transitions are near the magic angle with the membrane plane, this might indicate that there is no $C_2$-symmetry relation between the original monomer transitions of the primary donor in PS II. Van Gorkom and Schelvis [218] and Kwa [214] suggested a pigment structure that accounts for the broken $C_2$ symmetry, the similarity with the protein structure of the bacterial reaction center and the observed spectroscopic features in a straightforward way. This structure consists of a Chl *a*

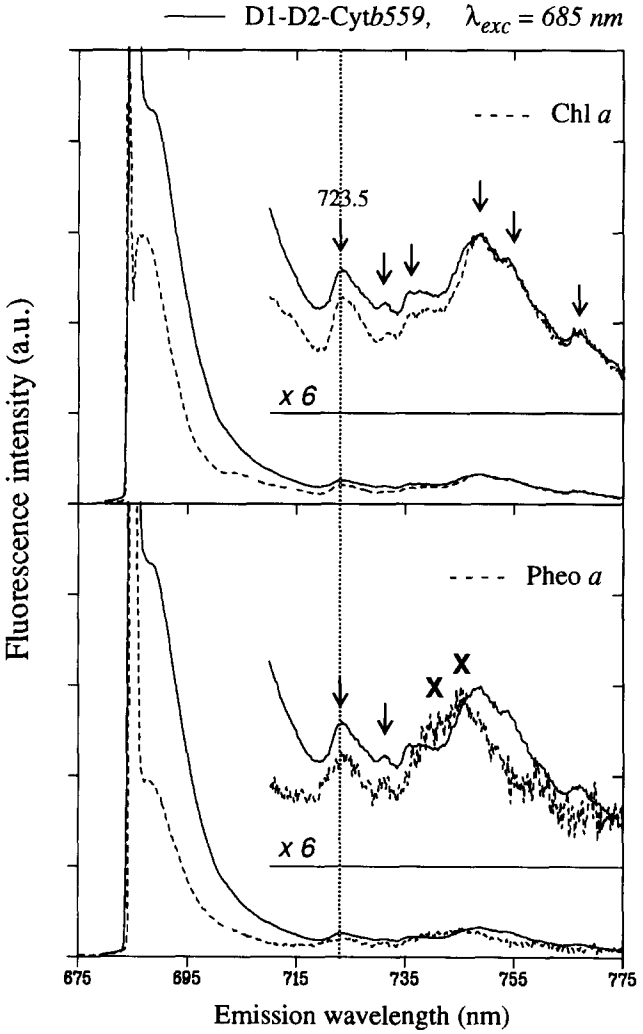


Fig. 4. Fluorescence emission spectrum of D1-D2-cyt.*b*559 at 4 K excited at 685 nm (solid curve in upper and lower panels). For comparison the emission spectra at 4 K of Chl *a* excited at 676 nm (dashed curve, upper panel) and of Pheo *a* excited at 670 nm (dashed curve, lower panel) are also shown. The Chl *a* and the Pheo *a* spectra were shifted on computer to the red to align the vibrational bands with those of D1-D2-cyt.*b*559. Exact alignment was performed for the vibrational band at 723.5 nm. All spectra were normalized to the vibrational emission band at around 735–750 nm. The vibrational regions of the spectra were also enlarged by a factor of 6 (insets). Coinciding vibrational bands are indicated with arrows, while bands which are clearly different are indicated with crosses (taken from Ref. [220])

molecule oriented as one of the special pair molecules in the bacterial reaction center, a Chl *a* molecule oriented as the accessory BChl molecule on the oher branch and a Pheo *a* molecule oriented as the BPheo on the same branch as the BChl molecule.

Some observations suggest a heterogeneity of P680 with discrete forms absorbing near 680 and 684 nm [209,205,216]. Recent absorbance-difference measurements on the P680 triplet of more intact PS II preparations (Ref. [219], and Schlodder, E. and Hillman, B., unpublished results) suggest that the form at 684 nm is caused by the native form of P680 and that the form at 680 nm is caused by structural changes during the purification procedure.

In carefully prepared PS II RC complexes, the 4 K steady-state fluorescence spectrum is characterized by a narrow band peaking at 684 nm without apparent shoulders [203,206,220]. The presence of unconnected pigments in partially destabilized preparations usually gives rise to a clear peak or shoulder at 672 nm in the fluorescence emission spectrum. Above about 80 K, the low-temperature fluorescence arises mainly from recombination luminescence. The temperature dependence of the steady-state fluorescence yields suggested the presence of an antenna pigment absorbing at about 680 nm that at very low temperatures (e.g., 4 K) may act as a trap of excitation energy and is responsible for most of the steady-state fluorescence [203]. Recent hole-burning experiments suggested a pigment absorbing at 682 nm with a lifetime of about 4 ns and thus confirmed it as a trap of excitation energy (Groot, M.L., Den Hartog, F.T.H., Dekker, J.P., Van Grondelle, R. and Völker, S., unpublished results). As shown in Fig. 4, a comparison of the vibrational fine-structure of this fluorescence with those of Chl *a* and Pheo *a* identified this antenna trap as (predominantly) Chl *a* in relatively native preparations with a 6:2 stoichiometry of Chl and Pheo [220]. In less gently treated preparations with a 4–5:2 stoichiometry of Chl and Pheo the low-temperature emitting species is most likely a Pheo *a* [220]. These results suggest that P-680, one or both Pheo *a* residues and a third Chl molecule contribute to the absorption at about 680 nm in the reaction center of PS II.

*3.2.2.3. Energy transfer dynamics and trapping.* The dynamics of excitation energy transfer and trapping in isolated D1-D2-cyt.*b*559 complexes of different degrees of intactness has since 1987 been studied by several groups using pump-probe absorbance-difference, single-photon-timing fluorescence and transient and permanent hole-burning techniques at a variety of temperatures.

Generally, the radical pair state $P^+I^-$ is formed with relatively high efficiency and decays (for a large part to the triplet state) with an almost *T*-independent lifetime of up to about 100 ns [221–225], which may be

heterogeneous [226–228]. In less intact material, a 6.5 ns component is usually attributed to uncoupled Chl fluorescing at 672 nm [224] which, due to the high quantum yield, will readily dominate the steady-state fluorescence. In relatively intact preparations, deconvolution routines of fluorescence kinetics also yielded an about 6.5 ns phase but peaking around 683 nm [228]. This could suggest that at least part of the 6 ns phase is also the result of recombination luminescence of the radical pair. Fluorescence decay phases with lifetimes in the range between a few hundreds of picoseconds up to about 1 ns also appeared after deconvolution, and also peak around 683 nm [228]. They represent relatively minor percentages of the total emission yields, and their origins are not clear. The heterogeneity of the fluorescence kinetics may be explained by one or more of several mechanisms: (i) inhomogeneous distribution of the primary reactants, leading to a distribution of energetically different states of the $P^+I^-$ radical pair [70] and a broad distribution of lifetimes [226]; (ii) decay of the total equilibrated $C^*PI \Leftrightarrow CP^*I \Leftrightarrow (CP^+I^-)^S \Leftrightarrow (CP^+I^-)^T$system (see below for a more detailed description); if the rate constant of the recombination of the (singlet) radical pair to $C^*/P^*$ is of the same order as singlet-triplet mixing, one expects to observe the 2–6 ns decay of $C^*/P^*$ in the fluorescence and radical pair kinetics (see also Ref. [203]).

The fastest and most detailed transients were recorded thusfar by Durrant et al. [48,229,230] using femtosecond pump-probe absorbance difference spectroscopy under anaerobic conditions at room temperature. The basic result was that excitation energy transfer from pigments absorbing at 670 nm to pigments absorbing at 680 nm and vice versa proceeds with $(100 \pm 50)$ fs lifetimes. The authors suggested the following kinetic scheme for exciton equilibration [48]:

$$^1C670^* \underset{k_{-1}}{\overset{k_1}{\rightleftharpoons}} {}^1P680^*$$

with $k_1 \sim k_{-1} \sim (200\ \text{fs})^{-1}$. If the Förster mechanism of energy transfer is applicable in this system, this would imply that the nearest neighbor distance between the 670 and 680 nm pigments does not exceed 1.2 nm (see the discussions in Ref. [49]).

There is considerable debate about the attribution of observed decay phases in the about 1–50 ps time range. In the following, we will discuss results concerning these processes separately at room temperature and at cryogenic temperatures. At low temperatures, the back-transfer ($k_{-1}$ in the scheme above) is expected to be retarded considerably, due to which charge separation will arise from the 680 nm pigments alone, while at higher temperatures charge separation is expected to proceed from a completely equilibrated 670–680 nm pigment complex.

The first ultrafast absorbance difference measurements at room temperature by Wasielewski et al. [231] revealed a 3 ps lifetime that was attributed to primary charge separation. Roelofs et al. [232] interpreted their fluorescence lifetime measurements as indicative for a 1–6 ps charge separation process. It should be noted, however, that both studies were done with relatively unstable preparations. Later results by Hastings et al. [233] using ultrafast pump-probe techniques at 545 nm (which monitors a pheophytin $Q_x$ ground-state absorption band) and 460 nm (which monitors a pheophytin anion absorption band) dispute these conclusions by showing that at least part of the pheophytin reduction takes place with a rate constant of $(21\ \text{ps})^{-1}$. This rate constant was observed both with 612 nm excitation (which basically excites all pigments) and with 694 nm excitation (which presumably excites P680 directly). The identification of the 21 ps component as due to the decay of (P/Chl *a*)* hinges heavily on the observed kinetics of a weak stimulated emission sideband at 740 nm [230]. An about 200 ps phase was observed with 612 nm excitation only, and attributed to slow energy transfer. The 1–6 ps phase was also detected and tentatively assigned by the London group as exciton scattering (see also Ref. [230], where 600 fs and 3.7 ps phases were observed). Alternatively, when the 3 ps phase is ascribed to the charge separation process the 21 ps phase has to be attributed to energy transfer from C-670 to C-680 pigments, which is, according to Ref. [215], just possible in view of the Förster mechanism of energy transfer and the size of the PS II reaction center complex, although it seems hard to believe that *all* C-670 pigments are located at a distance of about 30 Å from *all* pigments absorbing at about 680 nm.

The problem of the attribution of the decay phases may also relate to the lack of knowledge about the spectral shape of the charge separation reaction. The disappearance of the equilibrated (CPI)* state is expected to cause an absorbance increase peaking at 680 nm with a shoulder at 670 nm and an additional absorbance increase due to the disappearance of stimulated emission, while the appearance of $P^+I^-$ is expected to cause bleaching at 680 nm of the ground state absorbances of P and I. The appearance and disappearance of the 680 nm features depend on the oscillator strengths of the components involved and on the stimulated emission contribution. The 21 ps phase is characterized by a positive-going 670 nm contribution and a small negative-going 680 nm contribution [233], which indeed might favor attribution to a (CPI)* $\rightarrow P^+I^-$ change (with I being the active pheophytin). The 3 ps phase is characterized by a strong positive-going 680 nm contribution (upon 694 nm excitation [230]), which in a first approximation resembles a disappearing P* contribution without the appearance of the charge separated state, and therefore tentatively

was attributed to exciton scattering within the P-680 dimer [230]. However, it is not clear to us how that would give rise to a strong recovery of the ground state absorption of P-680. If the comparison between the bacterial and plant reaction center actually holds two crucial aspects of the initial charge transfer process should be considered: (1) the intrinsic multiphasic decay kinetics of P* and (2) the possible formation of a true short-time intermediate with unknown (possibly Chl *a*-like) spectral properties, but not involving Pheo *a*.

Durrant et al. [229] concluded from their experiments, and from the scheme outlined above with $k_1 \sim k_{-1} \sim (200\ \text{fs})^{-1}$ that the intrinsic rate of charge separation takes place with a rate constant of about $(10.5\ \text{ps})^{-1}$. We note that this estimation is rather arbitrary. If excitation energy transfer proceeds with similarly fast ($\sim 100$ fs) rates between all pigments, one could calculate a rather different intrinsic rate of charge separation: if there are four 670 nm and four 680 nm absorbing pigments (the latter includes at least one of the pheophytins, P-680 and an accessory Chl-680 [220,203]), and if the excitation has a 2-fold higher chance of residing on a 680 nm pigment, then one expects an intrinsic rate of charge separation of $\{21/(4 + 4/2) = 3.5\ \text{ps}^{-1}\}$. It would therefore be possible that the charge separation kinetics contain both $\sim 3$ ps and $\sim 20$ ps phases, the relative amplitudes of which depend on $k_{-1}$ and thus on features like sample intactness and excitation wavelength.

At 4 K kinetics of about 2, 10–20 and $\sim 50$ ps have been observed with transient absorption, fluorescence lifetime and hole-burning techniques [234,235,204,236, 228,237]. The interpretation of most of these experiments points rather consistently to the following: primary charge separation in about 1.5–2 ps, energy transfer from (a) 670 nm absorbing pigment(s) to (a) 680 nm absorbing pigment(s) (perhaps pheophytin) in about $\sim 10$ ps, and energy transfer from the latter pigment(s) to almost isoenergetic pigment(s) (presumably a chlorophyll absorbing around 681 nm) in about $\sim 50$ ps. This interpretation does not necessarily disagree with the results obtained at room temperature: due to the retardation of energy transfer to higher energy pigments, a large fraction of the excitation density will rapidly be localized on P680 and the intrinsic rate of charge separation will be measured. The relatively slow (10–50 ps) energy transfer steps may be rationalized by long-wavelength energy traps other than P680 out of which escape will be relatively hard. The fact that the transfer appears slower in the red wing of the PS II RC absorption band [204] is in line with this idea. In addition, probably all the species absorbing around 680 nm (P680, Pheo *a*, Chl *a*) are inhomogeneously broadened; for individual particles with $E_{\text{P680}} < E_{\text{Pheo}}, E_{\text{Chl}}$ one expects a very fast energy transfer to P680, but for individual particles with $E_{\text{P680}} > E_{\text{Pheo}}, E_{\text{Chl}}$ one could easily get relatively long (10–50 ps or even longer) energy transfer times (see also the discussions in 3.2.2.2).

### *3.2.3. PS II core complexes (CP47-CP43-D1-D2-Cyt.b559 and CP47-D1-D2-Cyt.b559)*

*3.2.3.1. Organization.* In PS II, the photochemical reaction center complex D1-D2-Cyt.*b*559 is surrounded by fixed amounts of two highly conserved Chl *a* containing proteins CP47 and CP43 [238], which are generally denoted as the core antenna proteins. Together with a water-soluble 33 kDa protein involved in oxygen evolution, the purified so-called PS II core complex (CP47-CP43-D1-D2-Cyt.*b*559) may be regarded as the minimal, fully functional PS II complex capable of charge stabilization, plastoquinone reduction and oxygen evolution [30].

In certain cyanobacteria, the complex is organized in dimers in vivo [239,240]. The monomeric complexes appeared fully functional [241] and are characterized by exponentially shaped fluorescence induction curves, whereas for the dimeric complexes sigmoidally shaped curves were found (Schatz, G.H., Rögner, M., Dekker, J.P. and Holzwarth, A.R., unpublished observations), suggesting energy transfer from closed to open centers within one dimer. The dimeric organization was proposed to be related to the structure of the cyanobacterial phycobilisomes [239,241]. Also in green plants a dimeric association of the PS II core was proposed [242,243]. Holzenburg et al. [244] presented an analysis of two-dimensional arrays of PS II in thylakoid membranes and interpreted the results in terms of a monomeric PS II core structure. Recent EM studies on several types of isolated particle, however, suggest that the interpretation in [244] is not correct and that the data should be interpreted in terms of a dimeric PS II core structure [31,245]. The EM studies indicate that the dimeric association of PS II is virtually identical in green plants and cyanobacteria and that it represents the native association of PS II in both types of organism [245].

In absence of the extrinsic 33 kDa protein, CP43 is removed from the complex by detergent (dodecyl maltoside) incubation at room temperature [246]; the detergent treatment also releases the plastoquinones from the complexes [247]. It was shown by Rögner et al. [248], however, that the CP43 protein is not essential for $Q_A$ binding. Other detergents were reported to remove $Q_A$ but not the core antenna proteins [249]. CP47 and CP43 each contain 6 putative transmembrane $\alpha$-helices [238]. The CP47 protein contains approximately 13 Chl *a* and 2 $\beta$-carotene molecules [250,251]; in view of sequence homologies, about the same amount is expected for the CP43 protein. The most purified oxygen-evolving core complexes were

reported to contain 30–35 Chl *a* per photochemically active $Q_A$ [241,195].

*3.2.3.2. Spectroscopy.* The isolated CP47 and CP43 complexes were reported to contain several spectral forms of Chl *a* [206,252,253] with main $Q_y$ absorption maxima (in case of CP47) at about 683, 676, 670 and 660 nm and a minor one at ~690 nm. The LD of CP47 suggested that the average orientations of the Chl *a* $Q_y$ and $Q_x$ transitions are parallel and perpendicular, respectively, to the plane of the membrane [206,252,251] indicating perpendicular orientations of most of the heme planes. The $Q_y$ transitions of the 683/676 nm forms are more parallel to the plane of the membrane than of the other forms, whereas the $Q_y$ transition of the 690 nm spectral form is almost perpendicular to the plane of the membrane.

The low-temperature steady-state fluorescence from the PS II core complexes originates from long-wavelength pigments on the core antenna: emission peaking near 695 nm (F695) presumably arises from the 690 nm pigment of CP47 (one pigment per complex [254] with orientation perpendicular to the plane of the membrane [206,255,256]), whereas emission peaking near 685 nm (F685) arises from several ~683 nm pigments (with orientation parallel to the plane of the membrane) of CP43 and/or CP47. A Chl antenna triplet of CP47 has been detected by ADMR [257] and by absorbance difference spectroscopy [253]. It arises from Chl *a* peaking at ~683 nm, is characterized by a relatively short lifetime (~0.8 ms) and by almost identical D and E values compared to those observed in PS II reaction center complexes and in Chl *a* in solution. At 77 K, CP47 triplets can also be photo-induced in CP47-RC complexes, which was explained by energetic sinks of low-energy transitions in CP47 [258].

*3.2.3.3. Energy transfer dynamics and trapping.* In view of energy transfer dynamics and trapping, the CP47 and CP43 containing PS II core complexes differ in two main respects from the isolated D1-D2-cyt.*b*559 complexes: they contain an at least 5 times larger Chl *a* antenna, and (if prepared properly) a functionally active plastoquinone acceptor $Q_A$. Thus, in these complexes charge stabilization by electron transfer from reduced pheophytin to $Q_A$ will occur. Several groups have analyzed this reaction by transient absorption spectroscopy and reported lifetimes of about 300–500 ps [259,101,260], suggesting similar kinetics of this reaction in the reaction centers of PS II and purple bacteria (vide infra).

A detailed study of the Chl *a* excited state decay kinetics in PS II core complexes of *Synechococcus sp.* was performed by Schatz et al. [101] using picosecond transient absorption and fluorescence spectroscopy at room temperature under non-annihilating conditions. The assumed Chl antenna size (~80 Chl/RC) was based on oxygen flash yields, which generally yield overestimated values; antenna size determinations based on $Q_A$ quantitations yielded ~50–60 Chl/RC for similar preparations [241,14]. With open reaction centers (in state PIQ) fluorescence decay phases of about 80–100 ps and 520 ps were observed. The biphasic decay was explained by a model that describes trapping in terms of the decay of an equilibrium between the radical pair $P^+I^-$ and the excited antenna (C-PI)* ([1,101], see also section 2.4). This model was extended by Holzwarth and co-workers into the so-called 'exciton/radical pair equilibrium model' [69], who further assumed that the initial excitation equilibration between the Chl *a* antenna and P680 takes place within 10 ps or less (the recent ultrafast experiments of Durrant et al. [48] on PS II RC's support this assumption), and thus describe the model by a 'trap-limited' exciton decay. In this model the 80–100 ps decay phase is ascribed to charge separation (formation of $P^+I^-Q$) and the 520 ps phase to charge stabilization (formation of $P^+IQ^-$). When corrected for the assumed antenna size (80 Chl/P680) and the energy of excited state of P680 relative to that of the antenna, the intrinsic rate of charge separation in open complexes was calculated to be about $(2.7\ ps)^{-1}$ [101]. An antenna size of 50 Chl/P680, a very crude approximation of antenna composition of equal amounts of 680 and 670 nm pigments and a 2-fold higher chance for the exciton to reside on a 680 nm pigment (see above) would similarly lead to an intrinsic rate of charge separation of $(2.9\ ps)^{-1}$.

PS II core particles have also been studied by Hodges and Moya [261] by single photon timing spectroscopy. In open centers the decays appeared somewhat faster (30–60 ps and 150–210 ps) than reported by Schatz et al. [101]. Fluorescence kinetics as a function of single or double reduction of $Q_A$ have recently been studied by van Mieghem et al. [262]. The main decay phases in open centers (about 60 and 250 ps) were also observed in closed centers with doubly reduced $Q_A$, suggesting that double protonation of the doubly reduced $Q_A$ results in neutralization of the negative charges and thus leads to a radical pair that is energetically similar to that in open centers. The occurrence of a 250–300 ps phase in centers with doubly reduced $Q_A$ indicates that in this case the phase can not be attributed solely to charge stabilization ($P^+IQ^-$ formation). Hodges and Moya [261] suggested perturbation of energy migration by detergent molecules as a possible cause for the heterogeneous kinetics.

With PS II in the closed state ($PIQ^-$) the decay components slowed down to 200–250 ps and 1300 ps, respectively [101], or to about 100, 500 and 1500 ps [262]. Analysis of these decays in terms of the exciton/radical pair equilibrium model resulted in an about 6-fold lower rate constant of charge separation [69], which was explained by Coulomb repulsion due to

the presence of the negative charge on $Q_A^-$. The results implied that the free energy difference of charge separation ($\Delta G_{ChlP^*,P^+I^-}$) for open centers is −38 meV and for closed centers + 12 meV [69].

A consequence of the formation of the equilibrium between the radical pair $P^+I^-Q_A$ and the antenna/P680 excited state is that the transiently formed amount of radical pair after a flash is not 100%. In particular, in closed RC's the amount of radical pair $P^+I^-$ was calculated to be only 20% [69]. This was confirmed by fast photovoltage experiments on intact pea chloroplasts [263], which showed very low amounts of radical pair in closed centers. Note that in intact chloroplasts the Chl/P680 ratio exceeds 200, which will shift the excited state-radical pair equilibrium even further to the excited state.

Summarizing, the exciton/radical pair equilibrium model [1,264,69] describes energy transfer and trapping in PS II rather well, and provides good evidence that the energy difference between the equilibrated excited state of the antenna and the primary radical pair state is sufficiently small to cause the biphasic decay of the excited antenna state in open centers, as observed by many authors. Nevertheless, the high variability in radical pair yield and triplet yield observed under a variety of conditions and the extremely multiphasic radical pair decay indicate that the kinetic model may be more complex than suggested by Schatz et al. [69]. For instance, the rate constants reported by these authors assume simple monophasic kinetics for $P^+I^-Q$ formation and could require modification in case of more complex kinetics [261,262] and/or inhomogeneous broadening of the relevant energy levels ($P^*$, $P^+I^-$, etc.). Also the possible existence of energetically 'relaxed' radical pairs [265] would seriously complicate the model.

### *3.2.4. Energy transfer dynamics and trapping in intact PS II*

Excited state decay and excitation trapping in intact PS II has since 1985 been investigated by a variety of authors [67,102,103,133,134,262,266–274]. Considering the total body of experimental results that have been obtained, the data are remarkably consistent. The decays show three groups of components: one or more fast phases (50–100 ps), one or more middle phases (0.4–1.0 ns) and one or more slow phases (1.2–2.2 ns). The actual numbers and relative amplitudes depend on the absence/presence of multivalent cations, the presence and phosphorylation state of LHC-II, open/closed reaction centers, etc. There is general agreement that at least a large part of the fast phase is due to PS I and that the middle and slower phases are due to PS II.

Several kinetic models have been proposed to describe the experimentally observed excitation decays. The models can be divided into two groups: (1) 'diffusion-limited' models [266,267,275], in which the energy transfer processes between the various pigment pools and the reaction center are considered to be reversible but in which the charge separation process is considered to be irreversible. The heterogeneous kinetics were explained by antenna heterogeneity (the tripartite model [267]) or by PS II heterogeneity ($\alpha,\beta$ centers, the heterogeneous bipartite model [266]), and the slower kinetics in closed centers were ascribed to recombination luminescence, following earlier suggestions from Klimov [276]. (2) 'trap-limited' models [1,264,69,14], in which trapping is described in terms of an equilibrium between the radical pair $P^+I^-$ and the excited antenna $(C\text{-}PI)^*$. Holzwarth and co-workers used the exciton/radical pair equilibrium model introduced by Schatz et al. [69] for PS II core particles as the basis for the kinetic model and introduced PS II $\alpha/\beta$ heterogeneity to explain the multi-exponential decays [133]. Recently, Roelofs et al. [102] reported an extended description of this model (see below). The slower kinetics in closed centers were explained by a shift of the equilibrium between the excited antenna and the radical pair to the antenna due to electrostatic repulsion of the negative charge on $Q_A^-$ and the radical pair.

In the following, we will discuss some recent results on energy transfer dynamics and trapping in intact PS II in more detail and concentrate on the kinetic modeling of the decays. This is quite essential, because the attribution of the specific phases depends on the specific model used. We will omit detailed discussions about the influences of salts, pH, state transitions, protein phosphorylation, etc., because the interpretations of these experiments also depend on the specific kinetic models used. See for a review Karukstis [277].

Hodges and Moya [270] have investigated PS2 membranes (the so-called 'BBY' [278] or 'K&M' [279] preparations) using single-photon timing spectroscopy. The decay showed its maximum emission at 685 nm and could be well represented by three exponentials with time-constants of 40–50 ps (small amplitude), 175–200 ps (2/3 amplitude) and 380–450 ps (1/3 amplitude). In closed centers the latter two decay phases slowed down approximately 6-fold (to 1.2–1.3 ns and 2.4–2.5 ns, respectively), whereas the small fast phase was no longer observed. The slow components were similar to those attributed to PS II in intact chloroplasts [268]. The authors did not interpret their multi-exponential decays in terms of $\alpha/\beta$ heterogeneity ($\beta$-centers were supposed to be absent in BBY's [280]). In contrast, they suggest that the fast phase represents the trapping process in PS II cores, that the variable 175–200 ps (1.2–1.3ns) component is due to reexcited PS II cores and that the variable 380–450 ps (2.4–2.5 ns) component is due to reexcited LHC-II. The model seems to be a variation of the homogeneous

PS II tripartite model [266], in which apparently the various components (PS II core, LHC-II) are equally sensitive to the redox state of the reaction center.

The problem seems to point to the attribution of the ~ 400–500 ps component: is it due to a decay of the excitation density as a result of reduction of Q [1], to a slow trapping process (perhaps caused by some remote LHC-II), or to both? The phase was clearly detected in PS II core particles in fluorescence and transient absorption, and could well be explained by charge stabilization (see above - [101]). Light-induced photovoltage experiments by Trissl et al. [281] showed that in destacked chloroplasts ('blebs') the PS II contribution consisted of a 50 ps trapping process (with many photons present – under low-intensity conditions trapping occurred in about 200 ps) and a 350–400 ps charge stabilization process. The latter phase accounted for 1/2–2/3 of the signal. However, Van Mieghem et al. [262] reported fluorescence decays of PS II membranes with doubly reduced $Q_A$ and found ~ 220 ps (4/5 amplitude) and ~ 600 ps (1/5 amplitude) lifetimes. Vass et al. [274] found in addition to a 150–250 ps phase also 600 ps, 2–3 ns and 10 ns phases in membranes with doubly-reduced $Q_A$. Because in these membranes charge stabilization can not occur, one almost inevitably has to propose some slow or very multiphasic trapping process. Thus, it seems possible that the ~ 400–500 ps component in PS II membranes or thylakoids with open reaction centers is caused by a combination of independent charge stabilization and slow trapping processes.

The most extensive data set was collected for intact pea chloroplasts by Roelofs et al. [102] using a combined global and target analysis of all decays observed in $F_0$ and in $F_{max}$ (open and closed centers) in the wavelength range 680–730 nm. Global lifetime analyses indicated PS II lifetimes of 290 and 630 ps for open centers and 0.55, 1.75 and 2.9 ns for closed centers. Roelofs et al. [102] discussed their results in terms of $\alpha/\beta$ heterogeneity [133] combined with the exciton-radical pair equilibrium model [69]. Table 1 lists the resulting kinetic and energetic parameters for PS II$\alpha$ and PS II$\beta$. Remarkable is that PS II$\alpha$ accounts for twice as much Chl as PS II$\beta$ in this analysis (suggesting a PS II$\alpha$/PS II$\beta$ reaction center stoichiometry of about 1), that the results extracted for PS II$\alpha$ are similar to those obtained earlier for purified PS II cores [101], and that the calculated intrinsic charge separation lifetime for PS 2$\beta$ is unexpectedly slow (11 ps).

Recently, Dau and Sauer [103] reported electric field effects on the fluorescence kinetics of PS II membranes, found field dependencies of the primary charge separation and recombination processes, and concluded that the data could well be explained in terms of the exciton/radical pair equilibrium model. However, a pronounced electric field effect on the charge stabilization reaction could not be detected.

We may conclude that in general the exciton/radical pair equilibrium model describes excitation energy decay and trapping in intact PS II rather well, and that at least some kind of heterogeneity has to be proposed to explain the data. Roelofs et al. [102] assumed different PS II centers ($\alpha/\beta$ centers) to explain the multiphasic kinetics, but whether this represents a realistic description of the data remains to be qualified. The similarity of the kinetics in thylakoids and in PS II membranes does not seem to favor $\alpha/\beta$ heterogeneity, because one would in a first approximation assume that PS II membranes are devoid of $\beta$ centers [280] (if not, one consequently also has to assume $\alpha/\beta$ heterogeneity in PS II core and reaction center particles, since these are prepared with high yields from PS II membranes [195,246]). A second point of concern regarding $\alpha/\beta$ heterogeneity is the about 4-fold slower intrinsic charge separation time (11 ps) of PS 2$\beta$ centers [102], which is unexpected in view of the presumably identical amino acid backbones of the reaction center polypeptides.

Two alternative explanations for the observed heterogeneous kinetics may be suggested: (i) a part of the peripheral LHC-II antenna is thought to be only loosely associated with the 'reaction center/core antenna/firmly bound peripheral antenna' complex [282], and could therefore give rise to perturbations in the equilibration of energy transfer. Moreover, a distribution of antenna sizes would give rise to a distribution of trapping times (see section 2, Eq. 14), which easily may be fitted by a two- or three-exponential decay, (ii) the heterogeneous kinetics may also be related to the

Table 1
Kinetic and energetic parameters for open and closed PS II$\alpha$ and PS II$\beta$ centers (from Roelofs et al. [102])

| | $\alpha$ open | $\beta$ open | $\alpha$ closed | $\beta$ closed |
|---|---|---|---|---|
| $\Phi(P^+Q^-)$ | 90% | 86% | | |
| $(P^+I^-)_{max}$ | 38% | 35% | 17% | 18% |
| $\tau_i$ (in ns), (amplitude) | 0.25 (68%) | 0.32 (59%) | 0.65 (22%) | 0.38 (26%) |
| | 0.52 (32%) | 0.67 (41%) | 1.79 (78%) | 2.92 (74%) |
| $\Delta G_{cs}$ (in meV) | −55 | −46 | −8 | +21 |
| $\tau_{cs,int}$ (in ps) | 2.9 | 11 | 19 | 34 |

observed heterogeneity of charge separation kinetics in bacterial reaction centers [283], where 3 and 11 ps intrinsic time constants for charge separation were extracted. Note that these kinetics are virtually identical to those extracted for PS II (see Table 1), due to which there would be no need to propose $\alpha/\beta$ heterogeneity in PS II.

### 3.3. Phycobilisomes

#### 3.3.1. Intact phycobilisomes

Phycobilisomes form the major light-harvesting antenna in red algae and cyanobacteria. The phycobilisomes are complex, but highly organized structures that are loosely attached to the thylakoid membrane. They are composed of aggregates of small pigment-protein complexes and their organization has been the subject of various reviews [284–288]. The chromophores are open chain tetrapyrroles (bilins) that are covalently attached via cysteine linkages to specific sites in the protein. The absorption spectra of the bilins are sensitive to the precise conformation (more or less extended) of the tetrapyrrole backbone.

The basic structural building blocks of the phycobilisomes are trimers and hexamers of pairs of the small $\alpha$- and $\beta$-polypeptides. In vivo, colorless linker polypeptides are essential for the formation of the complex phycobilisome structure. In vitro the smaller aggregates are stable without linkers and these building blocks are suitable for structural and spectroscopic studies. In the extensively studied phycobilisomes of *Mastigocladus laminosus*, which contain the biliproteins phycoerythrocyanin (PEC), phycocyanin (C-PC) and allophycocyanin (APC), it is well established that the transfer of excitation energy proceeds in the order PEC → C-PC → APC → Chl *a* [289–294]. The biliproteins absorb (and emit) progressively more to the red in the order given above, and the emission of APC overlaps very well with the Chl *a* absorption spectrum. The most likely energy acceptors are the core-antenna pigments of PS II and the overall energy transfer efficiency is > 95%.

The kinetics of energy transfer in the phycobilisomes and between the different phycobiliproteins were established by the work of the Porter and co-workers, who detected the rise of the various emitting species in the 30–50 ps following the order given above. The overall energy transfer time was about 100 ps in the case of whole cells of the red alga *Porphyridium cruentum* [295,296] and less than 50 ps for the cyanobacterium *Anacystis nidulans* [297,298]. Similar times were more recently observed by Yamazaki et al. [299]. These energy transfer times depend probably on the size of the phycobilisome (see below).

Most of the work on phycobilisomes has been done on isolated systems, in order to describe the main routes of excitation energy migration in relation to our relatively detailed understanding of the overall organization of the individual biliproteins in the phycobilisome. In this section we will concentrate on phycobilisomes of *Synechococcus* 6301 (*Anacystis nidulans*), since its structure has been studied in detail by Glazer and co-workers [300] and also because the rods only contain phycocyanin. Moreover, it has been possible to generate mutants of this cyanobacterium with different number of hexameric units per rod. In the early experiments on this system it was clear that there was a delay in the APC emission which corresponded to the decay of the C-PC emission [301–306]. It was also observed that the C-PC excited state lifetime increased as the length of the rod increased. The data obtained thus far are plotted in Fig. 5, where the C-PC lifetime is shown as a function of the number of C-PC chromophores per rod (black circles). The most remarkable observation is that there is an almost linear relationship between lifetime and size of the rod. The rod to core transfer time varies from 17 ps in 18 S particles with just a single C-PC trimer connected to a core fragment to about 85 ps for a wild type rod consisting of three C-PC hexamers. These data can most easily be explained by a model which assumes that the transfer of energy within an aggregate is faster than the transfer step in the junction between the rod and the core. In this case a fast equilibration of the excitation energy of all the phycocyanins is predicted. This seems very likely in view of the results on isolated trimers of C-PC, APC

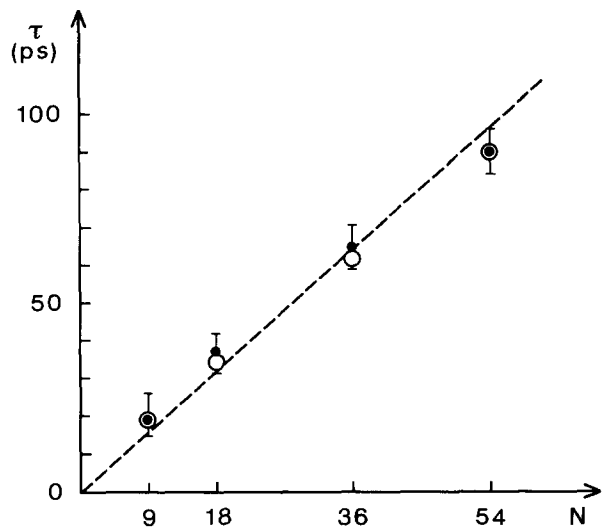


Fig. 5. Time constant for energy transfer from the C-PC rod to the APC core in different mutants and different preparations of *Synechococcus* 6301. N shows the number of phycocyanin chromophores in each rod ($N = 54$ corresponds to the intact rod containing three hexameric units of C-PC). The filled circles are the measured lifetimes for the various rod lengths, the dashed line reflects the best linear fit through the experimental data, while the open circles were calculated assuming that the rod pigments that transfer the excitation to the core are about 3 nm red-shifted in comparison with the bulk of the C-PC chromophores.

and PEC that we will discuss below. According to calculations by Sauer and Scheer [79] based on the C-PC structure of Schirmer et al. [21] the fastest transfer is on the sub-picosecond timescale between neighboring $\alpha$-84 and $\beta$-84 chromophores. Based on the same data Demidov and Borisov [307] calculated the fastest tansfer between trimers to be approx. 5 ps between $\alpha$ chromophores and that between $\beta$ chromophores in different hexamers to be less than 10 ps. These results strongly suggest that a fast equilibration of the excitation energy within a rod could occur in about 20 ps. This conclusion was also reached in the work of Suter and Holzwarth [305], where a trimer-trimer rate of 100–300 $ns^{-1}$ is predicted. The rate-limiting step should then originate from the chromophores ($\alpha$-84 or $\beta$-84) in the C-PC trimer closest to the core to one or more APC chromophores. The effective rate of this step is, however, dependent on the number of chromophores over which the excitation energy is distributed. If we, for instance, assume that the distribution is equal over $\alpha$-84 and $\beta$-84 and that all $\beta$-84 chromophores of the nearest trimer couple to the core, we obtain a transfer time of 8–9 ps for this step, which in fact is close to the value calculated for the $\beta$-84 $\rightarrow$ $\beta$-84 energy transfer between hexamers [307]. As can be seen in Fig. 5, there is a slight deviation from a straight line and the rates for larger phycobilisomes are somewhat larger than expected from statistical considerations alone. We can, however, modify our model by assuming a small red spectral shift for the chromophores situated in the trimer closest to the core. The open circles were obtained for a 3 nm shift assuming a Boltzmann distribution of the energy over the whole phycobilisome (cf., the theoretical section). A red shift in the trimers closest to the core has been observed by Lundell et al. [308].

We should also mention the opposite view taken by Glazer et al. [309,310] that actually the disk-to-disk transfer is the rate-limiting step for the energy flow in phycobilisomes. Also in this case each hexameric disk increased the total rate with ca. 30 ps, which agrees well with the data presented in Fig. 5. However, this type of diffusion-limited process would lead to a non-exponential decay as was also noted in the work by Demidov and Borisov using a Monte Carlo method [307].

### 3.3.2. *Phycobiliproteins*

In this section we will discuss the most recent results on time-resolved studies of isolated phycobiliprotein aggregates. We will focus our attention on the phycobiliproteins from cyanobacteria, since these have been the most intensely studied systems thus far. One important reason for this is the detailed structural information available for trimers and hexamers of C-PC [21,22,311,312] and PEC trimers [313]. From these studies it was found that the chromophore binding sites are similar and that the closest distance in the trimers is 2.1 nm between the $\alpha$-84 and $\beta$-84 bilins in adjacent monomer units. From the amino acid sequences of allophycocyanin [314] one can further conclude that the $\alpha$-81 and $\beta$-80 binding sites have homology to the corresponding $\alpha$-84 and $\beta$-84 of C-PC [315] and of PEC [316]. Some of the earlier picosecond fluorescence and absorption experiments on isolated phycobiliproteins were done on aggregates of C-PC [317–320]. From these studies it was obvious that the kinetics was complex and strongly dependent on the aggregate size. In the work of Holzwarth et al. [319] it was shown that the shortest lifetime decreased from 50 to 10 ps in going from monomeric to hexameric aggregates of C-PC. These authors also showed by symmetry considerations that in all cases three exponential terms are expected. In terms of the terminology sensitizing (s) and fluorescing (f) chromophores [321], the $\beta$-155 chromophore absorbing at 590 nm [322] is most likely 's' and thus connected to the fast lifetime.

The model calculations by Sauer-Scheer [79] and recently by Demidov and Borisov [307] predict that the transfer time from $\beta$-155 decreases from 48 to 35 to 11 ps in going from monomer to trimer to hexamer. This is in reasonable agreement with the experiments (see also Ref. [323]) considering that these values are based on best exponential fits to non-exponential decays. The interesting point to be stressed here is the increase of the total transfer rate as the number of interacting neighbors increases.

Since this field was reviewed last time several new and relevant papers have appeared [53–55,324–328]. The main new finding is that in addition to earlier picosecond kinetics in the 10–25 ps range a new sub-picosecond transient has been observed in trimers of C-PC, APC and PEC. Sharkov et al. [53,324] for the first time reported a 440 fs signal in APC trimers excited with 75 fs pulses at 615 nm. Later, a 500 fs anisotropy relaxation in C-PC trimers from the same species (*Mastigocladus laminosus*) was also reported [54]. Xie et al. [55] reported sub-ps fluorescence kinetics from both APC and C-PC trimers. A shorter than 2 ps lifetime was observed by Beck and Sauer [325] in APC trimers. Recently a 500 fs transfer time was observed in PEC trimers by Hucke et al. [327] and Pålsson et al. [328]. It thus seems to be a general property of phycobiliproteins to display an ultrafast non-radiative process. In the following we will attempt to present a general explanation of this process.

As mentioned above, Scheer and Sauer calculated the Förster transfer rate between the $\alpha$-84 and the $\beta$-84 chromophores in the C-PC trimer, based on the structural data by Schirmer et al. [21]. They obtained the rates 1400 and 1180 $ns^{-1}$ for the forward and back transfer, respectively [79]. This yields an equilibration

lifetime of about 400 fs between these chromophores, in excellent agreement with the experimental results, in particular considering the uncertainly in the absorption spectra of the different chromophores in the complexes. In the work of Gillbro et al. [54] the 500 fs process was detected as an anisotropy relaxation and this could be well interpreted as due to excitation transfer between $\alpha$-84 and $\beta$-84. The anisotropy of 0.23 obtained after a few picoseconds agreed well with the value calculated from the crystal structure. Xie et al. [55] also inferred from the rather small interaction of 56 $cm^{-1}$ [79] between the chromophores that a Förster model could not be excluded. These authors, however, suggested that the interaction might be sufficiently strong to put this interaction in the intermediate range [37,329,330].

At this point it is of interest to mention the theory recently developed by Gülen and Knox [63] for an excitonically coupled dimer. If the arrangement of the original dipoles is such that two new exciton states are produced with approximately equal dipole strength in each state, then simultaneous excitation of both excitonic states with a spectrally broad laser pulse (e.g., a 50 fs pulse) will result in a localized excited state and an initial fluorescence polarization of somewhat less than 0.7, depending on the precise angle between the two transition dipoles (for a more detailed discussion see Ref. [64]). In this model a fast anisotropy relaxation to 0.4 should result as a loss of coherence in the originally prepared mixture of excitonic states, which occurs with the Förster rate. This will be followed by a decay of the non-equilibrium distribution of excited excitonic states resulting in the final polarization of 0.1 (for this specific geometry). It will be of interest to look for these highly polarized phenomena and the possible involvement of coherent and/or delocalized excitonic states in future experiments on phycobiliproteins with even better time-resolution.

Strong excitonic interactions have been inferred to play a crucial role in the APC-trimers [331,332]; the absorption maximum of the trimeric particle has been shifted to 650 nm, although a clear shoulder remains in the spectrum at 620 nm, the absorption maximum of the APC-monomer. Nevertheless, both the strong homology between APC and C-PC/PEC [315,316] and the intensity of the observed CD spectrum [331–333] do not support this interpretation. Alternatively, a structural change upon trimer formation may be proposed, in which the conformation of one of the bilin chromophores is modified [286]. A similar variation in the protein environment underlies the blue shift of the $\beta$-155 chromophore in C-PC relative to the absorption of $\alpha$-84 and $\beta$-84 [21,22]. We also note that Resonance Raman [334,335] and CARS [336,337] experiments have demonstrated structural differences between C-PC and APC trimers and between monomers and trimers of the latter. It was suggested that the main conformational change occurred in the C15 methine bridge of the bilin chromophore.

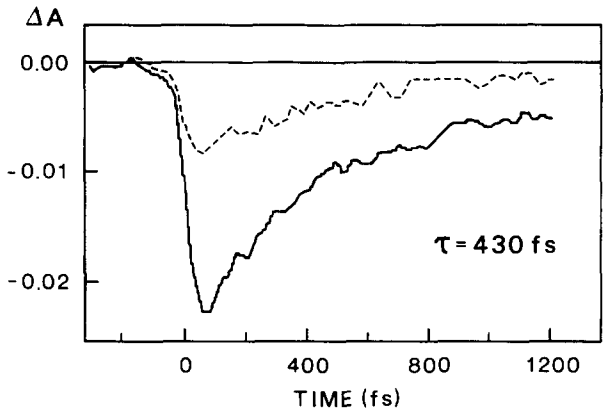


Fig. 6. Single wavelength pump-probe experiment on APC trimers of *Synechococcus* 6301. The excitation source was a CPM laser, pulse width 75 fs, $\lambda_{exc} = 615$ nm. The absorption was recorded parallel (solid curve) and perpendicular (dashed curve) the excitation wavelength. The resulting anisotropy was high and constant. The isotropic groundstate recovery was characterized by a single exponential component of 430 fs (for further details see Ref. [53].

The fs work on APC trimers [53–55,324–326] demonstrated a 440 fs relaxation of the chromophore excited at 615 nm, a constant high (0.4) anisotropy during the decay and a fast sub-ps bleaching of the main absorption band at 650 nm. An example of a single wavelength pump-probe experiment at 615 nm is shown in Fig. 6. The most straightforward interpretation of these results is that the two chromophores of APC have different spectra in the trimer with one chromophore still absorbing at about 620 nm, while the other has been shifted to 650 nm. In this model the energy transfer could proceed by a similar Förster mechanism as in C-PC trimers. This model should give rise to only one energy transfer component, however, in contradiction with earlier picosecond fluorescence and absorption studies where relaxation times in the order of 14–45 ps were observed [325,333,338] together with an approx. 1.8 ns emission. In the work by Sharkov et al. [53] it was pointed out that the slower components seem to be more pronounced in older samples. It was suggested that this at least in part could explain the slower components as a result of destroyed chromophore-chromophore interaction. There are, however, two alternative explanations of the sub-picosecond and picosecond kinetic components that have been proposed by Holzwarth et al. [333] and Beck and Sauer [325], respectively. The first authors assign the 14 ps lifetime to a relaxation between closely situated excitonic states, while the second group interprets the sub-picosecond component as an interexcitonic level transition and the 45 ps decay process as a direct relaxation from the upper excitonic state to the ground

state. However, also in the latter work heterogeneity is suggested to play a role in understanding the complexity of the overall excited state relaxation.

A relatively slow anisotropy decay of 45–70 ps has been observed in APC trimers [325,338] and might be interpreted as slow excitation transfer between different $\beta$ or $\alpha$ chromophores. Clearly more work needs to be done on different APC trimer preparations in order to understand this important system. Unfortunately, structural studies have so far been hampered by the poor quality of the crystals.

Recently, two reports have appeared on ultrafast energy transfer in PEC trimers and also in this case lifetimes in the order of 0.5 ps were found [327,328] which were ascribed to a transfer from the $\alpha$-84 phycobiliviolin to the $\beta$-84 phycobilin chromophore. It was further concluded that $\beta$-155 should absorb at the longest wavelength in contrast to the situation in C-PC [322]. Note that these conclusions remain rather uncertain since the spectra of the individual chromophores are less well known.

Before ending this section it should be mentioned that interesting work has been done on the cryptomonad chromoproteins phycocyanin 645 and phycocyanin 612 [339–341] and phycoerythrin [342,343]. In the former two biliproteins Malak and MacColl have proposed that two of the four chromophores in an $\alpha_2\beta_2$ structure form a strongly interacting pair. In phycocyanin 645 the excitonic states are located at 585 and 650 nm and a 2 ps fluorescence signal is supposed to represent a relaxation between them. Slower components of 9 and 15 ps are interpreted as energy transfer from weakly coupled chromophores at 558 and 624 nm, respectively. As in the case of APC trimers, no structural data on these phycobiliproteins are available, which makes a detailed discussion of these interesting systems premature.

## 4. Photosynthetic bacteria

### 4.1. Purple photosynthetic bacteria

At the time of a previous overview of this field [1], very few time-resolved measurements existed on purple photosynthetic bacteria, and the knowledge of energy transfer was mainly derived from steady-state spectroscopic experiments. With the advent of laser systems producing stable (sub-)picosecond light pulses of low energy and with high repetition rate, and tunable throughout the infrared absorption bands of the various BChl pigments (780–1050 nm), this situation has changed drastically. Today, the excitation transfer dynamics within isolated pigment-protein complexes, the transfer between different pigment pools in the in vivo antenna and the interaction between the antenna and the reaction center have been studied extensively and a detailed picture exists of these processes in a variety of bacterial light-harvesting systems.

#### 4.1.1. Pigment-protein organization in LH1 and LH2

Purple photosynthetic bacteria contain bacteriochlorophyll *a* (BChl *a*) or bacteriochlorophyll *b* (BChl *b*) as dominant pigment in the light-harvesting antenna and the reaction center (RC). Of the BChl *a*-containing bacteria many different species have been characterized, whereas for BChl *b*-containing bacteria only *Rhodopseudomonas (Rps.) viridis* has reasonably well been studied. The high-resolution crystallographic structures of *Rps. viridis* [16,344] and *Rb. sphaeroides* [17,345,346] reaction centers suggest that reaction centers of different purple bacteria are quite similar. The reaction center is surrounded by the LH1 core antenna, which consists of pairs of small transmembrane polypeptides ($\alpha$ and $\beta$) to which BChl is non-covalently attached in a 1:1 stoichiometry [32,33]. Most likely, the highly conserved histidines in $\alpha$ and $\beta$ are used as 5th ligand [32,33,293,347]. The BChl *b* containing bacteria have an additional $\gamma$-polypeptide, which is not involved in pigment binding [348].

In vivo, the LH1-RC core has a constant number of 24 BChl per RC (12 $\alpha$ and 12 $\beta$), although some uncertainty and variation in this number is possible [349,350,351]. Electron micrographs of membranes of *Rps. viridis* and other BChl *b*-containing species [352–355] and, recently, the BChl *a*-containing species *Rps. marina* [357] show that LH1 surrounds the RC in a circular way. The diameter of the RC-LH1 complex was estimated to be about 11 nm for the BChl *b*-containing and 10 nm for the BChl *a*-containing species; the difference is possibly due to the absence of the $\gamma$-polypeptide in the latter. A recent electron microscopy and image analysis study of purified RC-LH1 core particles of *Rhodospirillum molischianum* resulted in very similar structure, in which the 12 $\alpha\beta$-pairs were distinguished quite well [356]. Ring-like structures with approximately the same dimensions have also been observed for concentrated solutions of purified LH1 [357]. For the purified LH1 complex isolated from *Rb. sphaeroides* M2192 in detergent solution (octyl glucoside), the particle appears to consist of two closely linked $(\alpha\beta)_6$ units, and therefore may reflect a collapsed ring [358]. All these results are compatible with a model for the organization of the $\alpha$ and $\beta$ polypeptides in the membrane in which the minimal structural unit is a $(\alpha\beta BChl_2)$ complex [13,293]. These minimum units form a circular structure with the centers of all BChl pigments and their $Q_y$-transition moments in a single plane parallel to the membrane [1,359]. Spectroscopic measurements have shown that the RC-LH1 cores aggregate further into extended networks containing more than 10 RC's over which, at

least at room temperature, the excitation can freely diffuse [45,83,360–367]. At low temperature the excitation diffusion is restricted to, possibly, a single RC-LH1 core [364,366,368].

Various models have been suggested for the detailed structural organization of the $\alpha$ and $\beta$ polypeptides of the LH1 antenna [13,32,33,369–374]. It is believed that pairs of $\alpha$- and $\beta$-polypeptides form a minimum unit which aggregates further to form the fully functional in vivo antenna. Such a minimal unit was first isolated by Loach and co-workers [5,375,376] and spectroscopically analyzed in detail (see section 4.1.3.4). A molecular weight determination of this so-called B820 subunit by gel filtration showed that B820 had a considerably lower molecular weight than the reassociated B873 form. Similar subunits could be purified from various photosynthetic purple bacteria [377–381]. The B820 subunit prepared from *Rps. marina* [380] has a molecular mass of 33 kDa, about 1/6 of the molecular mass of purified LH1 from the same species. From this biochemical result the $(\alpha\beta)_2$-form was considered to be the most likely aggregation form for B820 [357,380]. The spectral properties, however, show that B820 arises from a single $\alpha\beta$-pair (see below).

Several species of purple bacteria contain, in addition to the LH1 core antenna, a peripheral LH2 antenna at higher excited state energy, with major BChl absorption between 820 nm, and 860 nm, depending on the species, and a second major BChl *a* $Q_y$-transition around 800 nm (see Ref. [382] for an overview). The ratio of LH2 to LH1/RC depends strongly on the growth conditions. For instance, in *Rb. sphaeroides* grown under low-light conditions LH2 is by far the dominant spectral species. It is now well established that some species (*Rps. palustris, Rps. acidophila, C. vinosum*) have the ability to change their antenna polypeptide composition (and consequently their absorption) in response to light and/or temperature [32,33,382]. Simultaneously, they can adapt the relative amount of pigment absorbing around 800 nm [382]. The LH2 protein backbone also consists of transmembrane $\alpha$-and $\beta$-polypeptides, which bind three BChl *a* per $\alpha\beta$-pair [32,33]. LH2 may have a complex carotenoid composition and the carotenoid to BChl *a* ratio may vary between 1:1 and 3:1 [382,383]; for instance LH2 of *Rb. sphaeroides* contains sphaeroidene as the major carotenoid and the BChl/carotenoid ratio is 2/1 [384].

The organization of the pigments in LH2 of *Rb. sphaeroides* (B800–850) was extensively studied [385–388] and detailed arrangements of the pigments have been proposed (see below). Nevertheless, up to now no agreement exists about the aggregation state and minimum functional unit ($\alpha\beta$, $\alpha_2\beta_2$, etc.). A unit composed of $(\alpha\beta)_2$ containing 6 BChl *a* molecules and three carotenoids explains most of the steady-state and time-resolved spectroscopic properties of LH2 [1,388]. Zuber [32,33,293] has proposed the cyclic $(\alpha\beta$ BChla3$)_6$ structure based on structural considerations. An EM and image analysis study of LH2 from *Rb. sphaeroides* isolated in the detergent LDAO gave a similar result [358]. Crystals of the B800–850 LH2 complex of *Rps. acidophila* suggest a trimeric $(\alpha\beta)_2$ structure as the basic unit [390], which in the crystal are further arranged as $[(\alpha\beta)_2]_3$ units, in agreement with a suggestion originally proposed by Scherz and co-workers [372–374].

In vivo, light absorbed by LH2 is efficiently transported to the RC, probably via LH1, although a mutant of *Rb. sphaeroides* lacking LH1 but containing LH2 and RC's shows trapping kinetics closely similar to those observed for RC-LH1 species [389]. For *Rb. sphaeroides*, LH2 connects cores of LH1/RC units, containing at most a few RC's [363,391]. Recently, it was shown for *Rps. acidophila* that the LH2 antenna interconnects individual LH1/RC units. In case of a B800–820 connecting antenna, the LH1/RC units were effectively isolated (even at room temperature), while in case of a B800–850 antenna excitations were able to migrate between different LH1/RC units [392].

### *4.1.2. Spectroscopy of the LH1 and LH2 light-harvesting antennae*

*4.1.2.1. In vivo spectral properties of LH1 and LH2.* The major BChl (*a* or *b*) absorption in LH1 and LH2 is strongly red-shifted relative to the absorption of BChl in organic solvents. In case of BChl *a* containing LH1, room temperature absorption maxima are observed in the wavelength range 870–890 nm, which shift even further to the red upon lowering the temperature. For some species, e.g., *Ectothiorhodospira mobilis* [393,394] and *Chr. tepidum* [395], the long wavelength maximum may be above 900 nm. For each species the precise maximum depends somewhat on the particular conditions; for instance, the absence (or type) of carotenoid in LH1 of *Rb. sphaeroides* may shift the absorption maximum almost 10 nm to the blue (Ref. [376] and Olsen, J.M., Beekman, L.M.P., Somsen, O.J.G., Van Grondelle, R. and Hunter, C.N., unpublished data). For the BChl-*b*-containing species the major absorption at room temperature is around 1015 nm, which sharpens and shifts to about 1040 nm upon cooling to 4 K.

Typically, the major LH2 absorption in purple bacteria is between 820 and 860 nm with a second peak around 800 nm. For instance, LH2 of *Rb. sphaeroides* absorbs at about 800 and 850 nm; LH2 of *Rps. acidophila* 7050, grown under dim light conditions absorbs maximally around 800 and 820 nm [32,33,382].The precise location of the peaks is also here sensitive to the presence and type of carotenoid. Recently, Fowler et al. [25] succeeded in blue-shifting the major absorption

transition of LH2 of *Rb. sphaeroides* by site-directed mutation of the double tyrosine motive ($\alpha$Tyr44Tyr45) in the $\alpha$-polypeptide. The single ($\alpha$Tyr44 → Phe) and double ($\alpha$Tyr44Tyr45 → PheLeu) mutants absorbed around 839 and 828 nm, respectively. This particular mutation was inspired by the PheLeu motive in the 800–820 complex of *Rps. acidophila* and demonstrated that this pair of residues is indeed responsible for the spectral tuning, possibly by the formation of an H-bridge between $\alpha$Tyr44 residues and the c-2-acetyl group of one of the BChl molecules [430].

Both LH1 and LH2 are believed to have a quite similar organization of their pigments. Consequently, their spectroscopic properties are also closely related. In particular, the organization of the BChl *a* of LH2 absorbing at 820–860 nm is believed to be rather similar to that of BChl *a* of LH1, with a dimer of BChl *a* as basic structure. All BChl molecules in LH1 and LH2 have their major $Q_y$ transitions in the plane of the membrane [385,386,388,396–398]. Within this plane there is, however, no preferential orientation. The $Q_x$-transitions belonging to B870 in LH1 and B820–860 in LH2 absorb around 585–595 nm and are oriented perpendicular to the membrane plane (or make at most a small angle with the normal). In LH2 of *Rb. sphaeroides* the B800:B850 ratio is 1:2, but the B800 peak is markedly sharper than the B850 peak and asymmetric in low-temperature absorption spectra [387,399].

The B800 pigment is assumed to be 'monomeric' and is possibly not liganded to histidine [347], but rather weakly attached to the LH2 structure [398–400]. The B800 absorption shows a predominant orientation in the plane of the membrane; its $Q_x$ transition (at 580 nm) is at a small angle with this plane [386,388]. Species with an increased absorption around 800 nm (e.g., *Rps. palustris*) usually exhibit complex CD, LD and polarized fluorescence excitation spectra reflecting stronger interactions between the B800 pigments [394,401–404]. Of particular relevance is the fact that the organization of the major $Q_y$ transitions leads to ultrafast depolarization of the transient excited state during energy transfer (see below).

*4.1.2.2. Site inhomogeneous broadening in LH1 and LH2.* Previously, the low-temperature (< 100 K) spectroscopic and excitation transfer properties of the purple bacterial antenna have been described in terms of the 'two-pool' hypothesis, in which the LH1 spectrum of *Rb. sphaeroides* was proposed to be composed of a major form (B880) and a minor long-wavelength form (B896) [83,398,405–409]. Fast excitation energy transfer was proposed to take place from B880 to B896, leading to strong depolarization of the fluorescence. Similarly, for LH2 of *Rb. sphaeroides* the existence of a

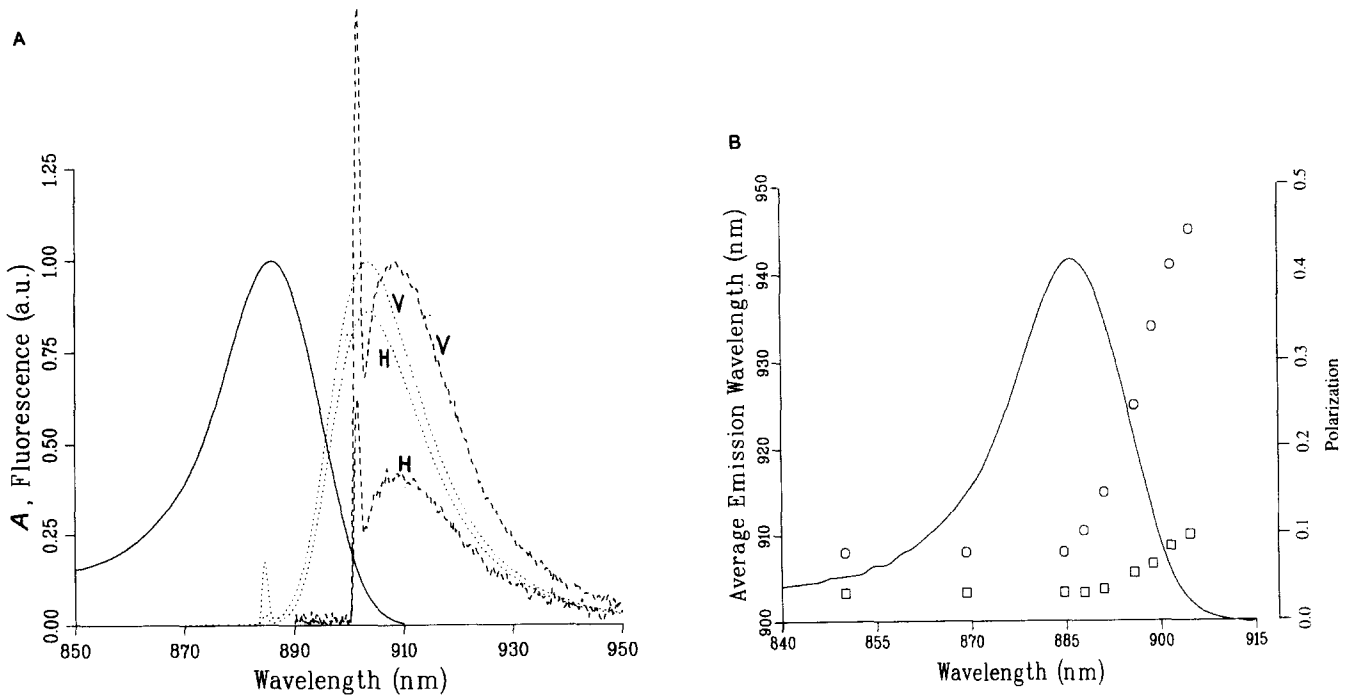


Fig. 7. (A) 4 K site-selected emission spectra of LH1 antenna complexes from *Rb. sphaeroides* M2192. Excitation at 884 nm (dotted) and 902 nm (dashed) detected parallel (V) and perpendicular (H) to the polarization of the excitation light. The solid line is the 4 K absorption spectrum (from Ref. [411]) (B) Dependence on the excitation wavelength of the maximum of the emission (squares) and the polarization of the emission (circles). The solid line is the 4 K absorption spectrum (from Ref. [411]).

major B850 and a minor B870 form has been forwarded [409,410].

Recently, however, low-temperature fluorescence [73,411], time-resolved fluorescence [92,93], absorption [368] and spectral hole-burning experiments [58,409, 412,413] have demonstrated that the LH1 and LH2 absorption spectra are in fact inhomogeneously broadened. Van Mourik et al. [411] applied narrow-banded laser excitation to study the polarized fluorescence properties of purified LH1 complexes at 4 K and measured as a function of the excitation wavelength ($\lambda_{exc}$) the position of the LH1 emission maximum ($\lambda_{max}$) and the fluorescence polarization. It was observed that $\lambda_{max}$ was unchanged at 904 nm for $\lambda_{exc} \leq$ 886 nm. For $\lambda_{exc} >$ 886 nm, $\lambda_{max}$ shifted linearly with $\lambda_{exc}$ to the red and the polarization increased from about 0.1 to close to maximal (see Fig. 7B). An example of the polarized emission spectra obtained for two different choices of $\lambda_{exc}$ is shown in Fig. 7A. Similar results were also obtained with purified LH2 of *Rb. sphaeroides* and *Rsp. molischianum* (Visschers, R.W., Germeroth, L., Monshouwer, R., Van Mourik, F., Michel, H. and Van Grondelle, R., unpublished data). In contrast to earlier observations [414,415], also for LH1-RC complexes and intact membranes of *Rps. viridis* the increase in fluorescence polarization in the long-wavelength part of the absorption spectrum was detectable using narrow-banded laser excitation. For *Rps. viridis* membranes this could only be observed upon excitation in the very red edge of the absorption band ($\lambda_{exc} >$ 1050 nm) [416]. For neither LH1-RC nor membranes could any shift of the emission maximum with excitation wavelength be detected, which is probably due to a specific narrow distribution of the low-energy emitting states. All observations suggest that in membranes at 4 K excitation energy transfer occurs over at least a few photosynthetic units, in agreement with results from singlet-singlet annihilation [367].

These results are not consistent with the two-form hypothesis, but can be fully explained by assuming inhomogeneous broadening as the dominant factor in determining the shape of the LH1 and LH2 absorption spectra. Within the framework of this concept, LH1 and LH2 may be regarded as clusters of weakly coupled BChl *a* dimers among which fast excitation energy transfer takes place. Each individual cluster is supposed to be a random sample from the total inhomogeneously broadened pigment pool. For small clusters, with efficient energy transfer leading to rapid thermalization of the excited state, the effects of site-selection depend on the cluster size only, and consequently, site-selective excitation yields information about the number of coupled BChl *a* molecules in a cluster. It was demonstrated that this model explains the observed emission polarization excitation spectrum unequivocally [411]. Within the context of this model B896 represents the distribution of energetically lowest cluster states. It is not difficult to demonstrate that the width of this distribution narrows and the maximum shifts to lower energy with increasing cluster size [411]. Thus the model proposed by Van Mourik et al. predicts that for large clusters, in which even at 4 K efficient excitation energy transfer is possible, the increase in polarization will occur only in the very red edge of the absorption spectrum and will be rather steep. This was indeed observed in LH1-only membranes [410] and in reconstituted LH1 preparations [73].

Spectral hole-burning experiments at 1.2 K have recently been reported for LH1 and LH2 of *Rb. sphaeroides* [412,409] and *Rps. acidophila* [413]. Excitation in the middle or blue wing of the main LH1 ($\sim$ 875 nm) or LH2 ($\sim$ 850 nm) absorption bands only resulted in broad, featureless spectra, whereas excitation of the red wings of these absorption bands resulted in narrow holes (3.2 $cm^{-1}$), implying a process with a 5–10 ps lifetime. Plotting the burning efficiency as a function of laser frequency mapped out a profile with a width of 70 $cm^{-1}$ peaking around 895 nm in LH1 and around 870 nm in LH2. The narrow (5–10 ps) hole was always accompanied by the rather broad feature, with a width of about 200–210 $cm^{-1}$, close to half the bandwidth of the original LH1/2 absorption band, and a strong absorption increase (anti-hole) in the blue wing. In contrast to the 'weak coupling of dimers' model introduced above [70,411], the B850 and B875 hole-burning results were interpreted in terms of a 'strong exciton coupling' model in which all ($\alpha\beta BChl_2$) pairs are organized in a cyclic unit cell and strongly excitonically coupled. Further (weaker) coupling was supposed to occur between the interacting unit cells. We note that this interpretation is remarkably similar to that proposed by the same group for the complex spectral hole-burning pattern observed for the BChl *a*-containing FMO-complex of green sulphur bacteria [80,417] (see below). Within the context of this model, B896 and B870 are the lowest exciton states of the LH1 and LH2 unit cells, respectively, and the 70 $cm^{-1}$ profile reflects the inhomogeneous linewidth of these lowest exciton states. In contrast to the FMO complex, no further exciton level structure was observed on the ground state and hole-burning spectrum. The broad profile observed in the hole-burning spectrum was ascribed to a special form of homogeneous broadening caused by the close spacing of the many exciton levels, the lifetime broadening of each exciton level due to fast inter-exciton level relaxation ($\pm$200 fs) and disorder [34,80,409]. However, the fact that for LH1 and LH2 of purple photosynthetic bacteria no exciton level fine structure is distinguishable in the high-resolution spectra seems to argue against the applicability of the strong coupling model for these sys-

tems. Alternatively, the excitation profile of the narrow hole could be correlated with the probability of exciting a lowest energy state in a cluster. It is of interest to note that the limiting wavelength for observing the narrow hole in LH1 and LH2 coincides with the onset wavelength of the fluorescence redshift and polarization increase observed in the site-selection experiments described above [411,416]. In that case the broad feature in the hole-burning spectra is explained by a phonon sideband, possibly including both low- and high frequency phonons, accompanying the zero-phonon hole obtained at the burning wavelength [87,92].

Hole-burning experiments on LH2 complexes from various organisms have shown that the B800 absorption band is inhomogeneously broadened. The hole-width in the red edge of the band yields a linewidth that corresponds with the estimated time-constant for B800 → B850 excitation energy transfer (see below), which is 2.4 ps ($\Gamma_{hom}$ = 70 GHz [58,409,412,413,418]) in LH2 of *Rb. sphaeroides* between 1.2 and 30 K. If the burning wavelength is tuned to the blue edge of the band, the holes become progressively broader, reaching a value of 250–300 GHz upon burning at 795 nm or lower [419]. In the case of blue excitation in LH2 of *Rps. acidophila*, a broad hole is obtained in the red edge of the B800 band. All these features can be interpreted as resulting from subpicosecond downhill energy transfer within the B800 band, in agreement with earlier measurements of the polarized fluorescence of the B800 band [388] and with more recent time-resolved data [57]. The hole-burning spectra of LH2 have demonstrated a 750 $cm^{-1}$ vibronic of the major B850 band, which coincides with the strong 800 nm transition [409,412,413]. A study with a set of spectrally modified LH2 mutants indicated that the 750 $cm^{-1}$ vibronic may be crucial in the low-temperature excitation transfer from B800 to B850 [417].

*4.1.2.3. Stark spectroscopy of LH1 and LH2.* Stark spectroscopy of BChl *a* in films has yielded a value for the difference (between excited and ground state) dipole moment of $|\Delta\mu_A| = 1.3–2.0$ D/*f* [420], in which *f* is the local field correction factor. For BChl *a* in the FMO complex rather similar values were obtained, suggesting that the BChl *a* molecules in FMO behave as a set of non-interacting pigments with respect to the electric field.

For LH2 of *Rb. sphaeroides* the B800 band has $|\Delta\mu_A| = 0.8–0.9$ D/*f*, while the B850 band shows an unusually large $|\Delta\mu_A| = 3.4$ D/*f* [420]. Stark spectra of both components have anomalous lineshapes and the spectra do not match the second derivative of the absorption spectrum (as expected for a single transition with a single value for $\Delta\mu_A$). The complex spectrum may (in part) be explained by assuming that red-shifted species are hidden under the LH2 absorption profile with enhanced charge transfer character. The amplitude of the B850 Stark spectrum shows that the BChl *a* chromophores are strongly coupled, giving rise to enhancement of $|\Delta\mu_A|$. $|\Delta\mu_A|$ for B850 is not affected by the disappearance of B800 upon LDS-treatment. The B800 Stark effect is consistent with the idea that B800 represents weakly coupled BChl *a*, susceptible to perturbations in the external environment. Surprisingly, LH2 shows an unprecedented large decrease in fluorescence yield in an applied electric field. It was suggested that the proposed charge transfer character of (part of) the B850 absorption is responsible.

For B875, the Stark absorption and emission spectra are dominated by a strong first derivative contribution [420]. Fitting the Stark absorption spectrum to a sum of derivative components yielded $|\Delta\mu_A| = 3.3 \pm 0.2$ D/*f* and in addition a very large polarizability difference. Although the Stark absorption spectrum does not hint at special red states in the B875 profile, it is still possible that the observed effects are due to overlap of transitions within the LH1 absorption band, with different responses to the applied electric field. In comparison with the special pair of the RC ($|\Delta\mu_A| = 7$ D/*f* [421]) the Stark effect is 'weak', which may indicate that for LH1 not all of the redshift is due to an increase in electronic coupling, but rather to 'local' effects (see 4.1.2.4).

*4.1.2.4. Spectral properties of the B820 LH1 subunit and the nature of the redshift.* The isolation of a subunit form, B820, of LH1 of Rs. rubrum and *Rb. sphaeroides* [5,375–381,422] has added significantly to our understanding of the spectroscopy of LH1 in relation to the aggregation state. From absorption, CD and fluorescence polarization spectra it was concluded that two excitonically interacting BChl *a* molecules are responsible for the spectral properties of B820. Recent triplet-minus-singlet spectroscopy, singlet-triplet annihilation and fluorescence site-selection studies [72, 422,73] have demonstrated that the B820 spectral properties are those of a BChl *a* dimer, with little or no interaction between different dimers. The dimer was proposed to have a head-to-tail arrangement, putting most of the oscillator strength in the red-shifted transition [423]. The high-energy component could only be observed by a small dip in the polarized excitation spectrum around 790 nm. The 'monomer' transition is located at 808/809 nm, which shows that in B820 more than 2/3 of the redshift (from 777 nm) is non-excitonic. Within the B820 dimer the monomer transition dipoles are quasi-equivalent and they make a small angle of about 20° to account for the observed CD [423,71]. Low-temperature site-selected fluorescence experiments [73] have shown that the B820 absorption band is inhomogeneously broadened and in fact behaves like a 'single state' system, as expected for a strongly coupled dimer. In addition, the major B820 absorption band is narrower with a factor of about $\sqrt{2}$

than the estimated monomer transition, which is consistent with the idea that each B820 dimer is composed of two BChl *a* monomers that are randomly selected from the total inhomogeneous distribution. An attempt to calculate the absorption, CD- and polarized excitation spectrum assuming that B820 is composed of a 'disordered dimer' of BChl *a* was rather successful (Refs. [70,71]; see theoretical section).

Recently, the time-resolved association of B820 into B875 using stopped flow has strongly suggested that only two B820 units are required to form B875 [424]. A spectroscopic intermediate could not be detected and further aggregation only marginally affected the spectrum. The CD spectrum of the reassociated B873 is, apart from the red-shift, not very different in shape and intensity from that of B820, which suggests that the interactions within the dimer have not been altered much during the tetramerization. These experiments have been taken to imply that the nature of the red-shift of BChl in LH1 (and probably also in LH2) is largely non-excitonic. This is supported by low-temperature triplet-minus-singlet spectra [368], which seem red-shifted copies of the B820 triplet-minus-singlet spectrum and do not show the appearance of a strong monomer absorption band far to the blue of the original LH1 absorption.

An earlier model that was proposed to explain the in vivo LH1 and LH2 spectra was based on model studies, which showed that artificially prepared dimers of BPheo *a* have absorption and CD spectra that are strongly reminiscent of those of LH1 and LH2 [372,373,425,426]. On the basis of these results it has been proposed that the major species of LH1 and LH2 consists of dimers of BChl *a* in a configuration similar to that of the special pair of the bacterial RC. The red-shift would be purely excitonic. The strong CD of LH1 and in particular LH2 was ascribed to much weaker interaction between various dimers. However, also in the case of the special pair of the RC the origin of the redshift is certainly not purely excitonic, since even the proposed high energy exciton component [427] is still very red-shifted relative to the absorption of BChl *a* in organic solvents. Experiments by Picorel and co-workers [428,429] provide further evidence that this model is not correct. It was demonstrated that the cross-section for $\gamma$-radiation inactivation of the spectroscopic unit of LH1 corresponds with the size of the ($\alpha\beta$-$BChl_2$) pigment-protein complex. The product of the inactivation has the size of a single polypeptide plus one molecule of BChl *a*. Despite its small size, the product formed by the radiation inactivation of LH1 still has a highly red-shifted absorption spectrum.

Then what is the cause for the redshift observed in LH1/2 and how is it related to the redshift of B820 upon formation of B873? In the B820 complex a molecule of the detergent octyl glucoside may occupy the position of the carotenoid [75]. Consequently, the interaction between the detergent molecule and BChl *a* may have some effect on the BChl *a* absorption band. As discussed earlier, Fowler et al. [25] have shown that in LH2 of *Rb. sphaeroides* the B850 absorption band can be shifted more than 20 nm to the blue upon mutation of a Tyr pair in the $\alpha$-polypeptide. Resonance Raman spectra have shown that the spectral shift upon formation of B820 and in LH2 upon mutagenesis of the Tyr pair in the $\alpha$-polypeptide are accompanied by dramatic changes in the H-bonding pattern of the BChl molecules [75,430]. Similar effects have been observed in LH1 (Olsen, J.D. et al., unpublished). These observations are in line with the view that non-excitonic factors, such as charge effects [431,432], deviations in planarity of the porphyrin ring systems [433] or the change in dielectric constant in close environment of the pigments [434] may largely determine the site-absorption of the pigments. Similar ideas have been put forward for the interpretation of the spectrum of the FMO-complex [76,82,433].

### *4.1.3. Energy transfer in LH2-less purple bacteria*

*4.1.3.1. Rhodospirillum rubrum and Rhodobacter sphaeroides (LH1-RC only mutants).* *Rs. rubrum* and RC-LH1-only mutants of *Rb. sphaeroides* may be regarded as photosynthetic systems in which excitation energy transfer and trapping occur in a 'homogeneous' core antenna. The original results of Vredenberg and Duysens [360] have shown that at room temperature such systems should be viewed as 'lakes' in which many reaction centers are connected through very efficient excitation energy transfer. These ideas were further substantiated by singlet-singlet and singlet-triplet annihilation experiments [44,45,391,363,435].

The actual time required to trap an excitation by photochemically active ('open') reaction centers at room temperature was measured to be 50–70 ps with both picosecond absorption [145,436,437] and fluorescence [438–440] techniques. In 'closed' centers (with oxidized primary electron donor), the excited state lifetime lengthens to about 200 ps, showing that even in the state $P^+$ the reaction center efficiently quenches the excitations in the antenna. Picosecond absorption kinetics [145] also displayed an additional 20–50 ps decay component, which at that time was ascribed to the equilibration of excitation density among different spectral forms in the LH1 antenna, but also may have included a contribution from singlet-triplet annihilation [96,441,442].

Selective picosecond excitation and probing in the redwing of the LH1 absorption band has shown that in the temperature range 100–200 K energy is transferred to the RC with a time-constant of 35–40 ps [443,444], which was considered to reflect excitation transfer from (one of) the nearest neighbors of the RC to P. At room

temperature a slightly shorter time constant (about 20 ps) was estimated. The weak temperature dependence suggests that LH1 is nearly resonant with P; the localization of the excitation energy on P, however, may be somewhat more favorable at lower temperatures. From the measured rate constant a distance of about 3 nm between the nearest neighbor and P was calculated, in reasonable agreement with the distance estimated on the basis of the dimensions of the RC.

Early low-temperature fluorescence measurements have indicated that below 100 K the fluorescence yield of (open or closed) *Rs. rubrum* starts to rise dramatically [445] and that the fluorescence polarization of LH1 and LH1-RC cores of all purple bacteria shows a marked dependence on the excitation wavelength [396,398], suggesting that below 100 K the LH1 antenna behaves like a spectrally heterogeneous system. Low temperature (77 K) picosecond absorption [446], fluorescence [93,440,447,448] and absorption anisotropy [406,408,446] kinetics have supported this interpretation. The fluorescence and absorption decays indicated the presence of a 10–20 ps component on the high energy side of absorption/emission spectrum that preceeds trapping. Hence, LH1 is spectrally heterogeneous and consists of at least two, but possibly many spectral forms, as was discussed in 4.1.2.2. In all models fast ($\sim$ 10 ps) energy transfer occurs from the major BChl *a* pool to the low-energy fraction.

At ultralow temperature (4 K), the trapping efficiency for excitations by P drops to about 60% of its value at $>100$ K in *Rs. rubrum* membranes [445]. Picosecond absorption measurements indicated an increase in the trapping time upon far-red excitation [444]. 4 K annihilation experiments showed that the major part of the fluorescence quenching occurred in the red wing of the emission spectrum [83]. Time-resolved fluorescence measurements at 4 K [93] on *Rs. rubrum* membranes, in which the primary donor was accumulated in the triplet state, revealed at least 10–20 ps components in the blue part of the emission spectrum, 100–200 ps components in the center and very slow components (1 ns) in the red-edge. All these results can well be explained by the 'inhomogeneous broadening' model described in 4.1.2.2 [84,85,92,368, 449].

In contrast to the relatively slow transfer between P and its nearest neighbors (20–30 ps at room temperature) and the slow equilibration phenomena observed at 77 K and 4 K, there are strong indications that the transfer among identical LH1 dimers is much faster. From singlet-singlet annihilation measurements, the residence time of an excitation on a B880 molecule was estimated to be less than 1 ps [45,363] and a recent detailed analysis of the annihilation experiment suggested a $\tau_{hop}$ of 0.65 ps [91]. Time-resolved absorption anisotropy measurements of *Rs. rubrum* and *Rb. sphaeroides* showed that at room temperature during the first few picoseconds after excitation the polarization of the excited state is largely lost, independent of the excitation and probing wavelength [145,406,408]. It was proposed that a time-dependent depolarization occurs as a result of ultrafast (sub-ps) energy transfer among spectrally similar but not identical BChl *a* dimers (assuming that the dimer is the basic spectroscopic structure of LH1 – see above). The 'final' value of the anisotropy of 0.1 is in agreement with earlier polarized spectroscopy results and consistent with models proposed for LH1. Some further depolarization took place on a slower timescale (10–30 ps), possibly reflecting the diffusion of the excitation through the LH1 domain. Also at 77 K the absorption anisotropy was about 0.1 after a few picoseconds in the main LH1 absorption band and its blue wing. Only upon excitation and probing in the low-energy wing ($\lambda > 900$ nm) highly polarized decays were observed $\{r(0) = r(\infty) = 0.25\}$ [446,406]. This agrees with earlier fluorescence polarization measurements [398] and supports the idea that a minor fraction of the pigments in the low-energy wing of the LH1 absorption band acts as a trap for excitation energy. Direct excitation of these red-shifted pigments results in immobile excitations and consequently a highly polarized emission. Finally, the transient absorption measurements after picosecond excitation exhibit a strong bleaching at the red side of the LH1 absorption band and strong excited state absorption in the blue wing.

In the earlier picosecond experiments around the isosbestic point fast additional absorption changes have been observed [92,406,446,450], which, due to the duration of the excitation pulse could not be time-resolved, but indicated a spectral equilibration process within LH1 on a timescale of at most a few picoseconds. We recently obtained direct evidence for sub-picosecond energy transfer in the LH1 antenna. Recording the absorption difference spectrum shortly after a 200 fs laser flash in membranes of *Rs. rubrum* demonstrated that spectral equilibration of the excitation density occurred on a time scale of 320 fs (see Fig. 8). Similarly, time-resolved fluorescence anisotropy decay measured via fluorescence upconversion gave an initial anisotropy of 0.4 and an anisotropy decay time of about 300 fs [451].

Earlier models based on homogeneous lattices have suggested that the escape probability for an excitation arriving on P is high, as a consequence of the near degeneracy of P and LH1 and of the assumed fast transfer rate from neighboring LH1 to P [45,439,452] (see for a discussion Refs. [1] and [442]). On the other hand, early measurements of fluorescence excitation spectra of purple bacteria in which the reaction center absorption was well separated from the major LH1 band indicated that the probability of observing the

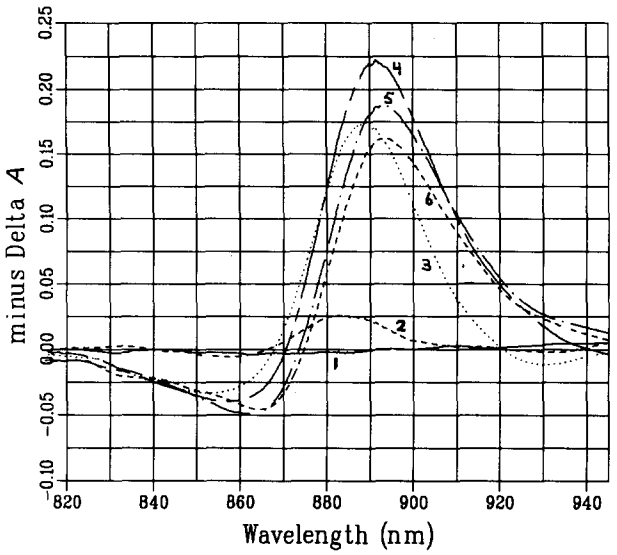


Fig. 8. Transient absorption difference spectra observed in membranes of *Rs. rubrum* obtained with a variable delay after excitation by a 200 fs 605 nm laser pulse at room temperature. The spectra are recorded at 0 fs (1), 166 fs (2), 333 fs (3), 500 fs (4), 1166 fs (5) and 1833 fs (6). Following the rise in spectra 1–4, resulting from the apparatus response time, the spectrum progressively shifts to longer wavelengths as the excitation density begins to approach a Boltzmann distribution among excited states. The 12 nm dynamic redshift of the isosbestic point follows a quasi-single exponential time course with a characteristic time of 325 fs. Data obtained by H.M. Visser, F. Van Mourik and R. Van Grondelle.

LH1 fluorescence through excitation of the reaction center is low ($< 0.25$ at room temperature) [94,453]. Recent time-resolved absorption experiments on *Rs. rubrum* by Timpmann et al. [96] showed that the relative efficiency of formation of the LH1 excited state was at least a factor 3–4 less upon reaction center excitation. In Ref. [95], however, an even lower escape probability ($< 5\%$) was obtained for a variety of photosynthetic purple bacteria down to low temperatures. It is not clear what causes the discrepancy with the results in [96]. Here we will use the number of Timpmann et al. [96] for further calculations.

The low escape probability can only be explained by assuming that the time constant for energy backtransfer from P to LH1 (7–9 ps) is about 3-times smaller than the time constant for charge separation (2.8 ps). This implies of course that also the rate of energy transfer into the RC is (much) slower than the rate of charge separation The precise value will depend on the relative energy of P* vs. LH1* and the coordination number ($z$) of the RC [85], but a reasonable estimate ($z = 6$) yields a value of about 20 ps; rather similar to the number extracted from direct measurements of the trapping time upon excitation of red pigments at 77 K [443,444]. This conclusion was recently experimentally verified by Beekman et al. [97] who studied the rate of excitation trapping in LH1-RC-only mutants of *Rb. sphaeroides* in which the Tyr M210 residue in the RC was mutated into Phe, Leu or His. The first two of these mutations induced a reduction of the rate of charge separation in the isolated reaction center by a factor of 4 (Phe) and 6 (Leu), probably by raising the energy level of $P^+I^-$ relative to that of P* [454,455]. Charge separation in the RC of the His mutant was actually slightly faster. For the intact LH1-RC cores, the trapping time increased only marginally in membranes of the Phe and Leu mutants, while on the other hand in both systems a phase in the decay of the LH1 excited state reflecting the electron transfer from $I^-$ to Q increased in amplitude. The His mutant exhibited virtually unchanged trapping kinetics. All these results are consistent with a 30–40 ps energy transfer time from one of the RC nearest neighbors to P. Consequently, the excitation transfer from a neighboring LH1 to P and not the rate of charge separation dominates the trapping time. This would make the trapping in LH1-RC cores of photosynthetic purple bacteria 'diffusion limited', although the rate of excitation diffusion in LH1 itself is exceptionally high.

*4.1.3.2. Rhodopseudomonas viridis.* Until quite recently there was an almost complete lack of knowledge about the energy transfer dynamics in the LH1 antenna of *Rps. viridis*. The main reason for this was the absence of a suitable picosecond laser source in the wavelength range of BChl *b* absorption (960–1030 nm). In the meantime, however, mode-locked dye lasers and solid state lasers have become available that operate in the desired part of the spectrum and, consequently, many new results on *Rps. viridis* may be expected in the near future.

Using the picosecond photo-induced electric gradient technique, Trissl and co-workers [365,456] reported a trapping time of 40 ps in *Rps. viridis* whole cells with open RC's. Bittersman et al. [457] employed low-intensity excitation pulses and time-resolved fluorescence detection and reported a 80 ps fluorescence decay time. This difference in lifetimes may at least partially be ascribed to the fact that the electric measurements by Trissl et al. were performed with high intensity pulses due to which the excited state lifetime could have been slightly shortened by singlet-singlet annihilation. Picosecond absorption measurements using low-intensity, tunable infrared (960–1020 nm) pulses provided more detailed results about the *Rps. viridis* excitation transfer dynamics [458]. It was shown that the room temperature excited state lifetime is 60 ps in open centers, 90 ps in centers with reduced secondary acceptor ($PIQ_A^-$) and 150 ps in centers with oxidized the primary electron donor. Measurement of the time-resolved absorption anisotropy and isotropic absorption kinetics at several wavelengths at 77 K did not reveal any multi-exponential decay at the blue edge of the LH1 absorption spectrum (as observed for the

BChl *a* containing purple bacteria). The initial polarization of the absorption changes was low, $r(0) = 0.1$, in agreement with earlier steady-state measurements [414]. The observation of a low, on a picosecond timescale constant ($r(0) < 0.1$), polarization is consistent with rapid (sub)picosecond energy transfer between differently oriented BChl *b* antenna molecules.

Trapping of excitation energy by *Rps. viridis* reaction centers is probably quite different from the corresponding process in the BChl *a*-containing purple photosynthetic bacteria in view of the strongly blue-shifted absorption of P (980 nm at 300 K; 1010 nm at 6 K [459]) relative to the major absorption of LH1 (1015 nm at 300 K; 1040 nm at 6 K [459]]). Using these results as the input for set of equations as given by Pearlstein [29] (see also section 2) yields a first passage time of 40–80 ps with a reasonable choice of all the parameters (with a LH1-P distance 2 nm and a coordination number $z = 6$, the rate of transfer to and from LH1 to P is assumed about 6 ps [365,458]). In view of the energy of P* relative to LH1* and the well-established time-constant of charge separation (2.8 ps) escape of the excitation from the RC and retrapping will contribute significantly to the calculated overall excitation lifetime. The best estimate given by Zhang et al. [458] was about 60–100 ps for the overall trapping time. An improvement relative to the experimentally obtained lifetime was possible by assuming (i) a very tight coupling between LH1 and the RC, (ii) an ultrafast deactivation of P*, or (iii) a much better overlap between P absorption and LH1 emission. Although at this point it is difficult to decide between these alternatives, it may be worthwhile to put more effort in establishing the precise position and shape of the P → P* transition (see below).

A study of the efficiency of charge separation by the *Rps. viridis* LH1-RC's as a function of temperature [459] showed, surprisingly, that the quantum yield of charge separation was independent of the excitation wavelength at 300 K and at 6 K, but the absolute efficiency dropped to 55% at 6 K. The fluorescence excitation spectrum showed no contribution from direct RC excitation in the wavelength range 780–860 nm. The effective rate of transfer from neighboring pigments to the special pair was estimated to be $(1.3\ \text{ns})^{-1}$ at 6 K. Note that, combined with a maximum backtransfer rate of at the most $(40\ \text{ps})^{-1}$, this implies that P* and LH1* are almost isoenergetic.

Recent low-temperature polarized fluorescence experiments on isolated LH1-RC complexes and membranes of *Rps. viridis* [416] revealed highly polarized emission only upon excitation (with a narrow-banded laser) in the very red wing of the absorption spectrum, suggesting a similar behavior as the LH1 absorption bands of BChl *a* containing purple bacteria [398,411]. Inhomogeneous broadening of the main absorption bands remained so far undetected and will further complicate the problem of excitation trapping at low temperatures. In membranes, the polarization effects are limited to the very red tail of the absorption band and therefore probably difficult to detect with broadband excitation [415]. Since time-resolved absorption [458] and fluorescence experiments at 23 K [460] only yielded a single decay time, the time for excitation energy transfer to these lowest states must be faster than a few picoseconds.

In general, we believe that the observed trapping kinetics and temperature dependence of the quantum yield for charge separation are not compatible with the proposed large energy difference between P* and LH1* [365,458,460]. The calculation of this energy difference and of the relevant overlap integrals using the $P^+$-P difference spectrum is strongly dependent on the assumed spectral shapes and intensities. The difference spectrum measured in *Rps. viridis* membranes, which is taken to represent the P-P* transition, contains an unknown contribution of a BChl *b* bandshift, which may have caused an apparent blue shift to 1010 nm relative to the main absorption band (max. at 1040 nm at 6 K). Also the use of the spectrum of the isolated RC is not correct because that certainly is blue-shifted in position. The fact that trapping still has an efficiency of 55% at 6 K suggests that on the average P* and LH1* are about equal in energy (apart from the entropic contribution). If both P and LH1 are inhomogeneously broadened, the number of 55% may simply reflect the fraction of LH1-RC cores in which P* is the lowest energy state.

Excitation annihilation experiments [367,456] have indicated significant competition between trapping by reaction centers and annihilation. The general theory for trapping, loss and annihilation [1,42] describes these results correctly if the finite duration of the laser pulse is accounted for [415]. At room temperature, the domains for annihilation are large (> 15 LH1-RC cores). At ultralow temperature, the annihilation becomes less efficient (which could be due to inhomogeneity), but still sizable annihilation domains ($N_D > 100$) are estimated. This is consistent with the observation that the increase in fluorescence polarization occurs only in the very red edge of the absorption spectrum. Three effects may contribute to the relatively efficient energy transfer and annihilation at 4 K in *Rps. viridis*: (i) the LH1-RC structure is highly organized and probably well connected, (ii) the width of the inhomogeneous distribution function is probably relatively small in the case of *Rps. viridis* [416] mitigating the effects due to lowering the temperature, and (iii), the Stokes' shift of *Rps. viridis* is probably quite small, resulting in a higher average transfer rate (see for a discussion Ref. [85]). Since in the excited state decay no 10–20 ps component is observed reflecting energy transfer within the

inhomogeneous band [458,460] we conclude that this energy transfer process occurs at a rate of less than a few picoseconds, even at 4 K.

*4.1.3.3. Heterogeneity of LH1 and its role in energy transfer and trapping*. Recently, Pullerits and Freiberg [84] extensively modelled energy transfer and trapping on the basis of inhomogeneously broadened LH1 and RC spectra. A hexameric arrangement of six $(\alpha\beta\text{B-Chl}_2)_2$ units around the RC analogous to the electron micrographs of *Rps. viridis* was taken as the structural basis of this model. The spectral properties of each unit were chosen randomly from the total inhomogeneously broadened pool and only three fitting parameters remained: the interunit hopping time, the hopping time to the RC and the homogeneous linewidth. At 77 K, a satisfactory fit was obtained with a single hopping time of 60 ps (implying a mean residence time of 12 ps) and a hopping time to the RC of 70 ps; extrapolating these results to room temperature yielded a perfect fit of the fluorescence data. At 4 K the fit was only qualitatively correct, in part due to the uncertainty about the homogeneous absorption and emission spectra at 4 K. The width of the inhomogeneous distribution function (20 nm) was estimated to be about half of the bandwidth (40 nm).

The extrapolated hopping time of 60 ps between tetrameric clusters of BChl a, however, seemed too slow to be consistent with the annihilation experiment. It was argued [368] that due to the use of periodic boundary conditions the simulation of Pullerits and Freiberg missed a phase in the relaxation due to energy transfer between different LH1-RC cores. Consequently, Pullerits and Freiberg had to attribute the observed 10–20 ps decay to an intra-LH1-RC core energy transfer process, which resulted in the slow hopping time. A simulation in which periodic boundary conditions were applied to a unit containing several LH1-RC cores resulted in a satisfactory fit of the 77 K picosecond absorption and fluorescence data using a hopping time of 3 ps [92]. Although still larger than the value extrapolated from annihilation experiments, the relative numbers are sufficiently close to make us confident about the correctness of the basic concepts. In this respect, a reevaluation of the annihilation experiment using a spectrally and spatially inhomogeneous antenna would be well timed. In addition, if the transfer from LH1 to P was assumed to occur from one B880 BChl dimer (monocoordinate RC [461]), the transfer time for this process was estimated to be about 10 ps; consistent with the estimated escape probability (see 4.1.3.1). Of course, models in which the transfer from LH1 to P is not restricted to one specific site are also possible, but in that case the individual transfer rate from one B880 dimer to P would have to be slower (note that in case P is degenerate with LH1 the ratio $k_{in}/k_{out} = z$, with $z$ the coordination number). In conclusion, we believe that the intrinsic inhomogeneous broadening of the spectra of the light-harvesting antenna is pertinent to the interpretation of the spectral and energy transfer properties as a function of temperature. Nevertheless, the question whether or not the RC is coupled to the LH1 antenna via the red-most pigment(s), as has been suggested for purple bacteria [462] (and recently also for P 1 [86]) remains to be answered.

*4.1.4. Energy transfer in LH2-containing purple bacteria*

*Rhodobacter (Rb.) sphaeroides* is the best studied LH2 containing purple bacterial species. At room temperature and with open centers, picosecond absorption [145] and fluorescence [407,448,463] techniques generally revealed a non-exponential decay with lifetime components of 10–40 and 70–100 ps. In the fluorescence studies, the faster (< 10 ps) energy transfer component was dominant while a minor 40 ps phase corresponded to the decay observed in single-wavelength transient absorption experiments. The bi- (or multi-) exponentiality of the decay is partly a consequence of the complex antenna structure of this bacterium, and probably reflects the equilibration of energy between LH1 and LH2. Using a simple two-step equilibrium model involving LH2, LH1 and the RC it was shown [145] that the measured trapping time of about 70–100 ps corresponds to an actual trapping time of 50–60 ps for the LH1-RC core, i.e., the same value as observed for *Rs. rubrum* [145] and LH1-RC only mutants of *Rb. sphaeroides* [97,408].

In centers with oxidized primary electron donor ($P^+$), charge separation cannot occur and the excitation lifetime increases to 200–250 ps [145,407,448,463], similar to that which was observed for *Rs. rubrum*. This shows again that the closed RC quenches antenna excitations rather efficiently. The LH1 ↔ LH2 equilibration appeared not to be affected by the RC redox state. Time-resolved absorption anisotropy experiments revealed a low 'initial' anisotropy $\{r(0) = 0.1\}$ of the absorption changes recorded in the major LH2 and LH1 absorption bands, consistent with (sub-)picosecond energy transfer between neighboring BChl molecules in LH1 and LH2 [145].

Measurements of energy transfer kinetics at low temperature (77 K) enabled, due to improved spectral resolution, a much better resolution of the individual energy transfer steps (narrower spectral bands) and effectively unidirectional energy transfer. Recently, two-color pump-probe experiments were reported for *Rb. sphaeroides* at 77 K, in which the probing wavelength was varied over the 790–910 nm wavelength range [464]. Absorption and detection in the B800 band showed that the approximate lifetime of the B800* excited state was between 1–2 ps at 77 K. The absorption changes in the B800 band were moderately

polarized $\{r(0) = \pm 0.25\}$. Exciting the high-energy pigments (B800) and probing the arrival of the excitations on the low-energy pigments through the rise-time of the 910 nm ground state bleaching/stimulated emission revealed a major time-constant of about 10–12 ps, while the remaining part had a considerably slower rise of about 30–40 ps. Selective excitation of B850 in the wavelength range 830–860 nm and probing the arrival of excitations at 885 nm (in the middle of the LH1 band) or at 910 nm (at the red edge of LH1 spectrum) showed that this biphasic risetime is the result of the spectral heterogeneity of B850, because excitation in the blue wing of the B850 spectrum resulted in a slower energy transfer to LH1. This wavelength dependent energy transfer can be represented by two spectral components with two different B850 → B875 transfer times of 10 ps and 30–40 ps, respectively [464]. The 30–40 ps component probably corresponds to the decay observed before in single-wavelength pump-probe experiments in the same wavelength region [145,462]. The 10 ps rise of the 910 nm signal implies that the major part of the LH2 → LH1 transfer occurs in 5 ps or less.

The biphasic B850 excited state decay does not necessarily imply that there exist two different forms of B850. The more likely explanation is that excitation in the blue wing of B850 results in more and possibly slower transfer steps than excitation of the main peak. Time-resolved fluorescence measurements have been interpreted in a similar way [407,448,463] and Freiberg et al. [463] proposed a model with two parallel pools of LH2, i.e., an inhomogeneity of both B800 and B850. However, from the available experimental results there seems no indication for heterogeneity in B800. For instance, hole-burning experiments on LH2 showed that at 4 K the B800 band is inhomogeneously broadened and that the B800 → B850 transfer time is constant over the 800 nm absorption band [58].

Finally, an accurate analysis of the absorption kinetics of *Rb. sphaeroides* [446] and studies of the polarized spectroscopic [410] and time-resolved absorption properties [408] of an LH2 only mutant of *Rb. sphaeroides* suggested that at 77 K there is a pool of 'red' pigments in LH2 (called B870) is involved in the coupling of LH2 and LH1. It is highly likely that this 'B870' fraction reflects the pool of low-energy pigments within the total inhomogeneous distribution of LH2, where the excitation becomes trapped, before transfer to LH1 occurs.

Time-resolved fluorescence data have been obtained at 290 K for membranes of *Rhodobacter capsulatus* [465], a species assumed to have a light-harvesting antenna organization very similar to that of *Rb. sphaeroides*. From a five-component global analysis fit and a target analysis including a simulation of the time-resolved fluorescence data, it was concluded (i) that the overall antenna excitation decay kinetics is limited by the rate of charge separation (trap-limited kinetics), (ii) that the excited states of LH1 and P are equilibrated on a timescale of $< 3$ ps, and (iii) that the LH2 → LH1 energy transfer at room temperature occurs in about 9 ps. The first of these observations is difficult to reconcile with the experiments described above for other purple bacteria. The trap-limited model would predict a high probability of escape for excitations upon direct excitation of the RC pigments, contrary to the observations. The relatively slow 9 ps LH2 → LH1 transfer time may be due to the limited response time of the experimental set-up, or alternatively to a larger ratio of LH2/LH1.

We will briefly summarize the results obtained with other LH2 containing purple bacteria. *Chromatium minutissimum*, which has a pigment system very similar to that of *Rb. sphaeroides*, was studied with time-resolved fluorescence spectroscopy [448,463] and the results were very similar to those obtained with *Rb. sphaeroides* on all essential points. Membranes of low-light *Rhodopseudomanas palustris*, in which the B800 band shows a pronounced exciton structure (possibly due to a tight packing of several B800 pigment molecules – see below) show ultrafast relaxation within the 800 nm exciton band, followed by excitation transfer via B850 to LH1 in at most a few picoseconds [404]. The bacterium *Erythrobacter sp.* strain Och 114, having the unusual pigmentation B806–870, was investigated with time-resolved fluorescence spectroscopy [466,467]. Despite the large energy difference between the two antenna species, energy was found to be transferred from B806 to B870 within the time resolution of the experiment (about 6 ps) at room temperature [466], but significantly slower at 77 K [467]. A low-energy pigment component of B870, B888, contributing approximately 3 BChl/RC was also observed, with properties closely related to those reported for the low-energy components of *Rs. rubrum* and *Rb. sphaeroides*. The observed risetime of the B888 fluorescence of 9 ps at room temperature agrees well with the observed risetime of red-edge excitation in *Rb. sphaeroides*. A slower decay component in the B806 fluorescence, which was not observed as a corresponding risetime in the B888 fluorescence, suggested a heterogeneous decay pattern of B806, somewhat reminiscent of the situation for LH2 in *Rb. sphaeroides*. Low temperature experiments suggest that also in the B806 band energy transfer to low-energy pigments precedes transfer to B870 [467].

#### *4.1.5. Energy transfer in isolated light-harvesting complexes and mutants*

*4.1.5.1. LH1.* If detergent-purified LH1 is analyzed on an LDS-PAA gel, a discrete set of complexes $(\alpha\beta)_n$ is observed with $n \geq 3$ [468,469]. All complexes absorb around 870 nm and slightly further to the red with

increasing n [468,470]. Excitation annihilation [435] and polarized fluorescence [468,470] experiments have shown that the various BChl molecules in these LH1 complexes are well coupled. For the LH1-only mutant of *Rb. sphaeroides* M2192, annihilation experiments indicated large domains at room temperature ($N_D >$ 100) [364].

The excited state decay of LH1 is slow, even at room temperature, and takes about 650 ps for the detergent isolated form [406,471,473] and 450 ps for the LH1-only mutant M2192 [408]. At 77 K, excitation of LH1 of *Rb. sphaeroides* in the major absorption peak resulted in a biphasic decay with a fast 20 ps phase dominant in the blue edge of the spectrum followed by a slow decay of the excited state on one of the red-edge pigments (900 ps in the detergent isolated LH1 complex, 400 ps in M2192 mutant of *Rb. sphaeroides*). Time-resolved absorption anisotropy of detergent isolated LH1 [406] and the LH1-only mutant M2192 [408] showed that (sub)picosecond depolarization occurs, probably as a result of very fast ($\geq 10^{12}$ $s^{-1}$) energy transfer within a minimum unit of LH1. Time- and spectrally resolved fluorescence experiments of detergent-isolated LH1 of *Rs. rubrum* were performed at low temperatures up to 4 K [473]. The observed kinetics depended strongly on the excitation wavelength; the shortest decay times of 10–20 ps were observed on the blue side of the emission spectrum, whereas above 940 nm the emission was essentially monoexponential with a decay time of 940 ps at 4 K. In all cases the kinetics were taken to reflect energy transfer in a spectrally heterogeneous system. Measurement of the polarized LH1 fluorescence spectrum as a function of narrow-banded excitation at 4 K showed a characteristic shift of the emission maximum which was interpreted to reflect energy transfer within an inhomogeneously broadened cluster of coupled BChl *a* molecules [411].

*4.1.5.2. LH2.* Energy transfer properties of a variety of LH2 complexes have been studied extensively over the past few years, and they all demonstrate rather similar characteristics. Both stationary and time-resolved absorption and fluorescence experiments have indicated that energy transfer among the B850 pigments is fast ($< 1$ ps) and leads to ultrafast depolarization of the excited state. At 77 K additional spectral equilibration phenomena were observed to take place on a 10–20 ps time-scale [450], very similar to LH1. Recent sub-picosecond pump-probe measurements show that the initial depolarization occurs with a time constant of 200–300 fs [472], similar to what was observed for LH1.

The most conspicuous feature of LH2 is the energy transfer process from B800 to B850, which probably is the best studied photosynthetic single step energy transfer process. At room temperature, the emitting B800 excited state is fully equilibrated with the B850 excited state [387]. From early fluorescence yield measurements it was estimated that at 4 K this energy transfer process occurs within 2–3 ps [387]. Later experiments with picosecond time-resolution indicated a time-constant of 1–2 ps at 77 K and a somewhat faster rate at room temperature [146,450]. In the so-called B800–820 complex of *Rps. acidophila* strain 7050 the energy transfer from B800 to B820 was observed to take place within 0.5 ps at 77 K, consistent with the improved spectral overlap for B800 → B820 as compared to B800 → B850 transfer [450]. From a transient absorption experiment with 0.2 ps time-resolution using the B800–850 LH2 complex of *Rb. sphaeroides*, Shreve et al. [56] concluded that the RT energy transfer time is $0.6 \pm 0.1$ ps upon direct B800 excitation. Sphaeroidene excitation had earlier suggested a transfer time of about 2–3 ps [474], which was subsequently interpreted as sphaeroidene → B800 excitation transfer [56]. Direct sphaeroidene → B850 excitation transfer would still occur with sub-ps kinetics [56]. Visscher et al. [57] extended these measurements by using low-intensity one-color pump-probe spectroscopy and showed that the room temperature time-constant for B800 → B850 energy transfer is $0.7 \pm 0.1$ ps in intact membranes of *Rb. sphaeroides*. For LH2 of *Rps. acidophila* strain 7050 (B800–820) and for LH2 of *Rps. palustris* (low light B800–850), the room temperature excited state lifetime was about 0.3 ps (close to pulse limited) when measured in the red edge of the B800 band. A mutant of LH2 of *Rb. sphaeroides* in which the Tyr$\alpha$44-Tyr$\alpha$45 motif in the $\alpha$ polypeptide was replaced by PheLeu resulting in a blue-shift of the 850 absorption band to 828 nm [25], also showed a B800 → B850 transfer time in the sub-picosecond time range at room temperature, in agreement with the increased spectral overlap [57]. The time-resolved initial absorption anisotropy in these LH2 complexes was high (at least upon excitation in the red wing of the B800 band) and no significant decay occurred during the transfer process. This observation suggests that in the red wing of the B800 absorption profile B800 → B800 energy transfer does not occur. Upon cooling to $\leq 77$ K the B800 → B850 energy transfer time increases by about a factor of 3–4 [57,450]. In membranes of *Rb. sphaeroides* time-resolved absorption measurements gave a value $2.4 \pm 1$ ps at 77 K upon pumping and probing in the red wing of the B800 absorption band. For the LH2 complex in LDAO a slightly faster rate was measured at 77 K: 1.7 ps [57]. Spectral hole-burning experiments were consistent with a B800 → B850 transfer time of 2.3–2.5 ps between 1.2 K and 30 K in membranes of *Rb. sphaeroides* [58,409,412] and of 1.8 ps in membranes of *Rps. acidophila* [413].

In the original model of Kramer et al. [388], energy transfer among (at least two) B800 molecules was as-

sumed to take place on a timescale (1 ps) that competes with the B800 → B850 transfer to explain the observed polarization of the B800 emission upon selective $Q_x$-excitation. Subsequent room temperature and low-temperature absorption anisotropy measurements using single wavelength pump-probe spectroscopy resulted in different $r(0)$ values, somewhat dependent on the wavelength of excitation/probing, on the species and on temperature [146,450]. However, a decay of the anisotropy was never observed and with the 0.5 ps, $\lambda \geq 800$ nm pulses high initial values ($r(0) \geq 0.35$) were observed [57]. These results showed that at low-temperature energy transfer among different B800 molecules in the red wing of the inhomogeneous distribution did not occur, which was thought to be inconsistent with the Kramer model. However, recent time-resolved sub-picosecond absorption and spectral hole-burning measurements have strongly indicated that within the inhomogeneously broadened B800 band 'blue' to 'red' energy transfer occurs on a sub-picosecond time-scale. In the low-light LH2 complex of *Rps. palustris*, which shows strong spectroscopic features arising from excitonic coupling between different B800 molecules, it was shown by pump-probe spectroscopy at 77 K that the excited state decay in the blue wing of the B800 band is in the subpicosecond time-range, while in the red wing the 1.5 ps process due to energy transfer to B850 is observed [404]. Transient absorption measurements with a 0.5 ps time-resolution showed that in all examined LH2 complexes the lifetime of the excited state shortened by a factor of 1.5–2 upon scanning the pump/probe wavelength from 'red' to 'blue' [57]. As shown in Fig. 9, transient absorption measurements in LH2 of *Rb. sphaeroides* using a 60–70 fs laser pulse revealed a 0.15 ps component at room temperature and significant depolarization of the transient absorption within less than 1 ps. Fig. 10 shows that the isotropic deay kinetics at 77 K exhibits a 0.3 ps time-constant, probably reflecting B800 → B800 energy transfer, followed by the well known 2.4 ps phase for B800 → B850 energy transfer. Note that in these experiments the spectral width of the excitation pulse is sufficiently large (10 nm) to hide variations of these kinetics over the B800 band. Spectral hole-burning in the B800 band of *Rps. acidophila* 7750 (B800–850) showed that blue excitation produced a broad hole in the red wing of the B800 band indicative for energy transfer within the B800 band. An accurate analysis of the efficiency of spectral hole-burning vs. the burning wavelength and vs. laser power in LH2 of *Rb. sphaeroides* showed that narrow 2.4 ps holes were only present in the red wing of the B800 band [419]. Upon burning at shorter wavelength the holewidth gradually increased, indicative for faster energy transfer processes within the B800 band, probably between 'blue' and 'red' B800 molecules.

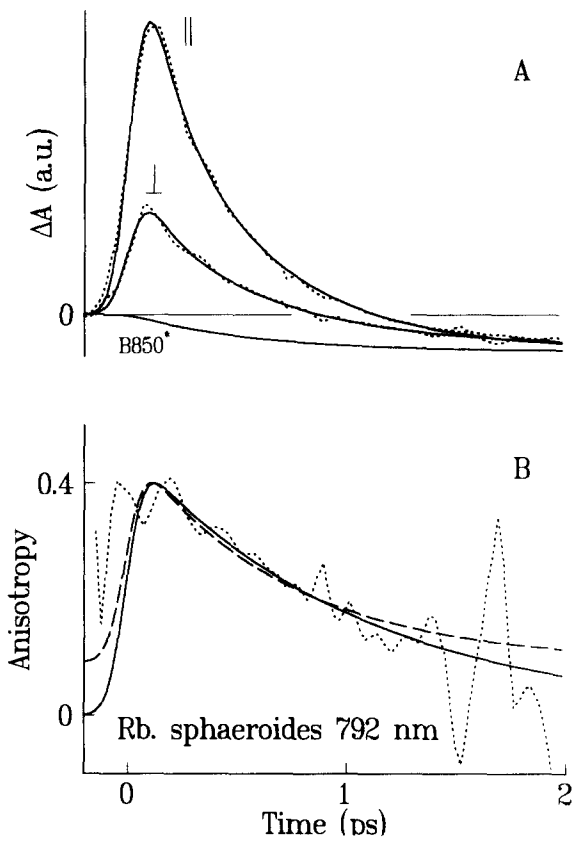


Fig. 9. (A) Measured absorption kinetics of *Rb. sphaeroides* at room temperature at 792 nm, with parallel and perpendicular polarizations. Bleaching is displayed as a positive signal. The slowly rising absorption curve (negative is the calculated signal due to excited state absorption from B850, used to obtain the time dependence of the anisotropy shown in 8B. The solid lines through the measurements represent the best fits to the experimental data (dashed) with a sum of exponentials with the following lifetimes and amplitudes: Parallel decay: $t_1 = 0.15$ ps (1), $t_2 = 0.52$ ps (1.9), $t_3 = 35$ ps (−0.2); perpendicular decay: $t_1 = 0.15$ ps (1), $t_2 = 0.63$ ps (2.7), $t_3 = 35$ ps (−0.7). (B) Anisotropy decay generated from the parallel and perpendicular kinetic curves shown in A. Dotted line represents the experimental data, the dashed line represent a fit assuming $r(\infty) = 0.1$ and the solid line a fit assuming $r(\infty) = 0.0$. The data were recorded by V. Sundström and co-workers.

Picosecond absorption and low-temperature fluorescence excitation experiments indicate the presence of at least two channels for carotenoid to B800/B850 energy transfer in LH2 of *Rb. sphaeroides* [56,387,388, 474]. Recent femtosecond pump-probe experiments have indicated that both the $^1B_u$-and the $^2A_g$-state are involved in the energy transfer [56,474]. Excitation transfer from the $^1B_u$-state to B800 or B850 occurred within 0.5 ps, whereas excitation transfer from the forbidden $^2A_g$-state took place on a much slower timescale (3–4 ps). Nevertheless, the latter is the dominant process. For a further discussion of carotenoid to (B)Chl excitation transfer we refer to Section 5 of this review.

### 4.2. Green photosynthetic bacteria

The green photosynthetic bacteria are composed of two families, the green gliding non-sulphur bacteria (*Chloroflexaceae*) and the green sulphur bacteria (*Chlorobiaceae*). The reaction center and core antenna of the *Chloroflexaceae* resemble those of the purple bacteria, while the reaction center and core antenna of the *Chlorobiaceae* is related to that of PS I of plants, green algae and cyanobacteria [475]. Both families of photosynthetic bacteria possess so-called chlorosomes, attached to the inner side of the cytoplasmic membrane. Chlorosomes are unique large pigment complexes, containing several thousands of BChl *c*, *d* or *e* molecules as light-harvesting pigments, among which very efficient energy transfer takes place. In the *Chloroflexaceae* the chlorosomes transfer their energy directly to the membrane associated reaction center core. The green sulphur bacteria contain an additional water soluble BChl *a*-containing pigment-protein complex that serves as an intermediate in the energy transfer process between the chlorosome and the reaction center core. The BChl *a* complex of the green sulphur bacterium *Prosthecochloris aestuarii* (further referred to as the Fenna-Matthews-Olson or FMO complex) was the first photosynthetic pigment-protein to be crystallized. Also from *Chromatium tepidum* a FMO complex was isolated with virtually identical spectroscopic properties [476]. In the following we shall first discuss the pigment organization and energy transfer properties of the FMO-complex from *Prosthecochloris aestuarii*, and then the properties of the chlorosomes and RC-core complexes of both families of green photosynthetic bacteria.

#### 4.2.1. The Fenna-Matthews-Olson complex of green sulfur bacteria

*4.2.1.1. Pigment organization and spectroscopy.* In the green sulfur bacteria, the FMO complex [477] connects the chlorosomes with the photosynthetic membrane. The FMO-complex was the first photosynthetic pigment-protein to be crystallized and today the structure is known with a resolution of less than 2 Å [478–480]. The FMO complex is organized as a trimer of identical subunits with $C_3$-symmetry; each subunit contains 7 BChl *a* molecules arranged in a rather non-symmetric fashion. It is the best-characterized photosynthetic antenna complex and ideally suited to analyze structure-spectroscopy relationships.

Several different models have been proposed for the ground- and excited-state electronic structures of the pigments within a monomer, in order to explain the observed spectroscopic properties (in particular ground state absorption and CD). It has since long been recognized that the BChl *a* molecules within a monomer (and possibly also within adjacent monomers) are excitonically coupled with interaction energies up to 200 $cm^{-1}$. A calculation based on the interaction among the seven BChl *a* molecules within a monomeric unit was presented by Pearlstein [481]; however, it was concluded that this model is not able to explain even the most obvious spectral properties of the complex. An extension of this model included the interaction between 14 BChl *a* molecules on two monomers located on two different trimers (reflecting a supposed interaction between individual trimers in solution) and resulted in a somewhat improved description [482]. In a third model the interaction between all 21 BChl *a* molecules in a trimer was calculated [76]; the distances

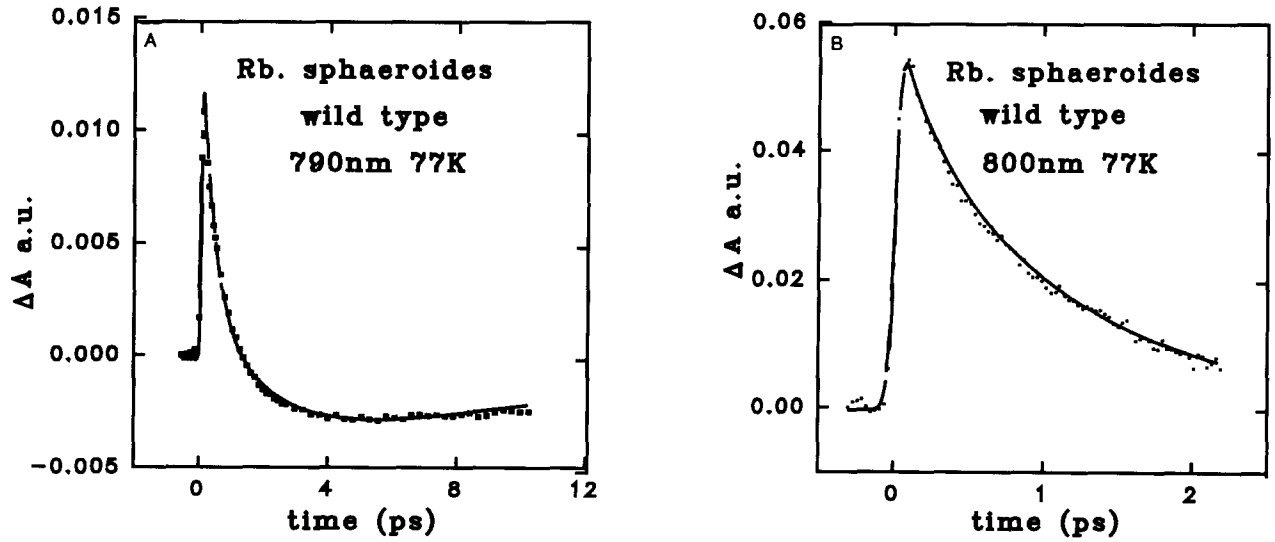


Fig. 10. Magic angle kinetics measured in the B800 band of *Rb. sphaeroides* at 77 K at 790 nm and 800 nm. The solid curve through the experimental trace is a fit to a sum of exponentials, with the following parameters: 800 nm: $t_1 = 0.3$ ps (0.45), $t_2 = 2.4$ ps (0.34), $t_3 = 10$ ps (−0.21); 790 nm: $t_1 = 0.3$ ps (0.47), $t_2 = 2.4$ ps (0.31), $t_3 = 10$ ps (−0.22). Note the different time-scale in both figures. The data were recorded by V. Sundström and co-workers.

between BChl *a* molecules in adjacent subunits are short enough to give rise to exciton interactions of the order of 20 $cm^{-1}$, i.e., of the same order of magnitude as the weaker interactions within a monomeric subunit.

So far, all spectroscopic properties were ascribed to more or less extensive exciton interactions between degenerate energy levels of the participating pigments. However, structural data for porphybhrins and (bacterio)chlorophylls have indicated that their light-absorption properties may be modulated strongly by conformational variations in their structure, for instance the nearby positioning of (partial) charges [432] and ring-puckering [483]. Applying this concept to the FMO-complex, Gudowska-Nowak et al. [433] calculated that the unperturbed energies of the 7 BChl *a* molecules in a monomer may easily show the experimentally observed variation (790–825 nm at low-temperatures in a glass). Recently, Pearlstein combined both views and obtained a satisfactory fit of the steady-state spectra. This 'final' model resulted in two sets of states, 7 of which are polarized parallel to the $C_3$-symmetry axis of the trimer and 7 pairs of states, which are doubly degenerate and polarized perpendicular to the $C_3$-axis [82]. Thus, from this model the absorption spectrum of the trimeric FMO-complex is predicted to consist of 14 bands. It is noteworthy to mention that the lowest monomer state (the 825 nm band) is far separated from the other electronic states and therefore reflects an excitation energy trap. Thus, the 825 nm band reflects a state that is almost fully localized on pigment No. 7 (in the numbering of Matthews and Fenna - Ref. [484]). Interestingly, pigment 7 is also special in another sense, since it is the pigment with the largest intersubunit interaction within the trimer [76].

Hole-burning spectra by Johnson and Small [80,417] showed that burning in one of the absorption bands affected all other bands in the spectrum. Similarly, the low-temperature triplet-minus-singlet spectrum contained contributions from most of the ground state absorption bands [81]. Eight exciton components were identified in the hole-burning experiments [80], consistent with an interaction model extending over more than one monomer; the resolution of two spectral components hidden in the 825 nm band which are separated by only 40 $cm^{-1}$ may favor the model of interaction between different monomers in one trimer. Recently, van Mourik et al. [81,485] showed that the photoselected polarized BChl *a* triplet state reversed in polarization if the excitation wavelength was scanned over the 825 nm band, which is consistent with the view that two degenerate states of the trimer absorb at the blue part of the main 825 nm band and carry $> 90\%$ of the oscillator strength, and that a single transition parallel to the $C_3$-axis absorbs slightly to the red and carries $< 10\%$ of the oscillator strength. The polarized singlet-triplet spectrum was surprisingly well fitted by the latest version of the Pearlstein Hamiltonian discussed above [70,81,82,485].

*4.2.1.2. Excitation energy transfer.* The hole-burning spectra of Johnson and Small [80,417] described above suggested the involvement of truly delocalized exciton states in the excitation energy transfer process. The 50 $cm^{-1}$ width of the holes burnt anywhere in the $Q_y$ absorption band (except the 825 nm band) is consistent with an inter-exciton state relaxation time of 100 fs. The two excitonic states contributing to the 825 nm band each show a narrow zero-phonon hole of $< 0.5$ $cm^{-1}$, corresponding to a $> 20$ ps relaxation time (at 4.2 K). This is roughly of the same order of magnitude as the excited state lifetime of about 80 ps obtained from time-resolved measurements at 77 K within the 825 nm band [486]. Johnson and Small [417,80] reasoned that the higher excited states of the FMO-complex are highly delocalized, while the two lowest states (824 nm and 827 nm) represent localized states. The inter-exciton state relaxation is in their view excitation energy transfer from those BChl *a*'s involved in the delocalized states to the BChl *a*'s with occupation density in the localized 825 nm state(s). According to this analysis the relaxation between exciton states having occupation density on different molecules may form an efficient mechanism for fast excitation energy transfer in such a strongly coupled system. In time-resolved measurements by Lyle and Struve [487] an ultrafast ($\ll 1$ ps) spectral shift was observed, which was proposed to be related to the 100 fs inter-exciton state relaxation process suggested by Johnson and Small. However, from a calculation of the experimentally observed picosecond-absorption difference spectrum by Van Amerongen and Struve [488], it could not be concluded that the excitations were either localized or delocalized after a few picoseconds. Direct time- and wavelength-resolved experiments with a high time-resolution using the FMO-complex from *Chlorobium tepidum* showed that much of the excitation equilibration occurs with 400 fs kinetics [489]. It is of interest to note that all anisotropies $r(t)$ decayed to values $\leq 0.4$ within 100 fs, indicatingthat the initial coherence is lost within 100 fs. The anisotropy decay function exhibited two major lifetimes: 100–130 fs and 1.7–2.0 ps. The short component may reflect single-step energy transfer kinetics in the FMO complex. The picosecond component corresponds to the 2.3 ps anisotropy decay resolved from earlier pump-probe experiments at room temperature by Lyle and Struve [487] in aggregates of the FMO-trimers, and may be ascribed to inter-monomer energy transfer within a trimer or between different trimers. The unresolved ($< 10$ ps) anisotropy decay observed by Gillbro et al. [486] in the blue and central part of the FMO-spectrum using pump-probe spectroscopy at 77 K may be of a similar origin. Low-tem-

perature (4 K and 77 K) singlet-triplet annihilation experiments indicated that Förster type of energy transfer may be the dominant process between monomers at these temperatures [81]. At 77 K perfect annihilation of singlets by triplets within a trimer was observed, but at 4 K the annihilation was strongly inhibited, suggesting that (at least at 4 K) the relatively slow energy transfer between different monomers in the FMO-trimer is the rate limiting factor.

*4.2.2. Chlorosomes*

*4.2.2.1. Pigment organization and spectroscopy.* The chlorosomes of the two families of green photosynthetic bacteria, green g(s)liding non-sulfur bacteria (Chloroflexaceae) and green sulfur bacteria (Chlorobiaceae) [477,491–495] are quite similar. They are ellipsoidally shaped vesicles of approximately 100–200 nm long and 30–70 nm in diameter (the exact dimensions depend on the species) and are attached to the inner side of the cytoplasmic membrane in which the reaction center and core antenna components are situated. They typically contain about 10000 BChl *c*, BChl *d* or BChl *e* molecules as major light-harvesting pigments together with a much smaller amount (1–5%) of BChl *a*.

Inside the chlorosome, the BChl *c*, BChl *d* or BChl *e* molecules are very densely packed and the transition dipoles interact strongly, which results in a spectral shift from 670 nm to about 740 nm (for BChl *c* containing chlorosomes of *Chloroflexus aurantiacus*). The BChl *c* chlorosomes of *Prosthecochloris aestuarii* show their major absorption at 750–760 nm, the BChl *d* chlorosomes of *Chlorobium (Cb.) vibrioforme* at 730 nm and the BChl *e* chlorosomes of *Cb. phaeovibrioides* at 710 nm. All polarized light experiments suggest a high degree of order among the BChl molecules in the chlorosome structure. In chlorosomes of *Cf. aurantiacus* the 740 nm $Q_y$ transition shows a highly polarized fluorescence and a strong linear dichroism [496–501]. A quantitative analysis of the polarized fluorescence and linear dichroism of chlorosomes of *Cf. aurantiacus* resulted in an average angle between the 740 nm transition moment and the chlorosome long axis of 15–20° [498,500]. The LD of chlorosomes of several other species of green bacteria suggests similar orientations for the major BChl *c*/*d*/*e* $Q_y$ transition moments [502–504]. For most chlorosomes, the polarization of the time-integrated [497,500,502] and time-resolved [77,505] fluorescence is high ($r > 0.3$). Polarized fluorescence measurements on oriented chlorosomes have further indicated that the chlorosomes show optical rotational symmetry [77,500].

Two opposing views exist for the role of proteins in the chlorosome. In the first view, specific BChl *c* binding proteins are proposed which coordinate BChl molecules to selected amino acid residues [293,506] and which form the rod-shaped pigment-protein structures that run along the long axis of the chlorosome [507]. For chlorosomes of *Cf. aurantiacus* a 5.6 kDa protein was identified [508]. The amino acid sequence was determined and a detailed model was suggested for the structural elements observed with EM [506]. The proteins that were proposed to bind BChl *c–e* in the chlorosomes of green sulfur bacteria, however, show little homology with the polypeptides of *Cf. aurantiacus* [509]. The latter have a mass of about 7.5 kDa in *Cb. limicola f. thiosulphatophilum* [510,511]) or of about 6.1 kDa in other green sulfur bacteria [509,512]).

These early models in which the formation of BChl *c* oligomers was correlated with a specific binding pattern on the 5.6 kDa proteins [506] now seem doubtful, since the 5.6 kDa could not be detected in the expected amounts [513]. Moreover, immunogold labelling has located the 5.6 kDa protein in the chlorosome envelope [514].

The alternative view proposes BChl *c* oligomers as main building blocks for the chlorosome architecture; the protein, if at all present, would only play a role in the outer matrix [515–517]. Support for this view was obtained from i) the observation that artificial aggregates of BChl *c* in organic solvents [518–521] or lipid mixtures [522,523] have spectroscopic properties that are close to identical (wavelength shift, hyperchromism, width, linear dichroism) to those of the chlorosomes, ii) the purification of protein- and BChl *a*-free chlorosomes from *Cf. aurantiacus* with 'native' spectroscopic properties [65,499,517,524–526] and iii) the finding that for intact chlorosomes the BChl *c* aggregation could be reversibly disrupted with hexanol (as judged by the disappearance of the 750 nm absorption band) [527]. Nevertheless, low concentrations of hexanol [521,528] and limited proteolysis of chlorosomes of *Cf. aurantiacus* [528,529] induce changes in the spectral properties of chlorosomes (for instance the intensity of the CD around 740 nm is about 10-fold increased) that make them (even) more similar to BChl *c* aggregates. These observations indicate a subtle interplay between BChl *c* aggregation and the 5.6 kDa (or another) protein in intact chlorosomes.

Many structural models exist for the aggregates that BChl *c* may form in the absence of proteins (see for a discussion the contributions in Ref. [530]). On the basis of biochemical data, Brune et al. [521] concluded that models in which the central Mg-atom of BChl *c* is 5-coordinated should be favored over earlier proposed 6-coordinate models [518–520]. Raman studies essentially confirmed this model [531,532] (but see also Ref. [526] for an alternative view). From $^{13}C$ NMR spectra of chlorosomes of *Cb. tepidum* (containing BChl *c*), a ring overlap model has been presented in which the BChl *c*'s are highly aggregated [528,522,533]. In this

model the BChl *c*'s form a linear array in which the C-2a hydroxyl-group is H-bonded to the Mg-ion of the next, the Mg-ion is 5-coordinated, the linear aggregates are stacked in such a way that the rings of adjacent BChl *c*'s directly overlap and the final aggregate forms a 5–6 nm diameter cylinder with the farnesyl tails pointing to the inside of the rod. In this model all $Q_y$'s are oriented along the long axis of the rod.

Recently, strong indications have been obtained that chlorosomes are spectroscopically heterogeneous. Widely varying CD-spectra have been reported for *Cf. aurantiacus* and *Cb. limicola* chlorosomes [499,534,535]. Brune et al. [535] suggested chlorosome instability as the reason for this variability. However, Van Mourik et al. [536] and Griebenow et al. [499] found that membrane-attached chlorosomes of *Cf. aurantiacus* prepared from different batches could give very different CD-spectra. From an analysis of the observed spectra it was concluded that the observed CD-spectrum could be described by a linear combination of two basic spectral types. These spectral types could relate to different chlorosome species or to different types of pigment aggregates. Other spectroscopic studies also suggested heterogeneity. The LD/A-value appeared not to be constant over the 740 nm absorption band [499,501,528], suggesting different spectral forms with different orientations, the shape of the emission spectrum varied as a function of temperature [65], pointing to at least two discrete emitting forms of BChl *c*, and resonance Raman spectra showed the presence of 5- and 6-coordinated Mg-ions of BChl *c* [526]. Otte et al. [504] observed a similar inhomogeneity in BChl *d* and BChl *e* containing chlorosomes from *Chlorobium vibrioforme* and *Chlorobium phaeovibrioides*, respectively, and suggested that in all species the BChl *c–e* pools consist of at least two spectral forms, with the long-wavelength fraction closest to the membrane.

Complicated excitonic interactions among many BChl *c* molecules may lead to multiple excitonic states, which in combination with a certain degree of disorder probably causes a large part of the observed heterogeneous spectral behavior. Assuming a helical arrangement of excitonically coupled BChl *c*'s not only explains the observed CD and the shape and polarization of the excited state spectra [77,500], but also reproduces the major features of the LD/A spectrum. Recent hole-burning experiments with intact cells of *Cf. aurantiacus* have further shown that the 740 nm transition is inhomogeneously broadened [537]. Narrow holes could only be burnt in the red wing of the band and these were always accompanied by a broad bleaching. The burning efficiency of the narrow feature peaked at 752 nm with fwhm of 90 $cm_{-1}$. The accompanying broad hole, which was the only hole observed for $\lambda_b < 743$ nm, had a shape closely similar to the chlorosome absorption spectrum. The 752 band was ascribed to the inhomogeneously broadened lowest exciton state of a BChl *c* oligomer and the broad hole to the bleaching of higher exciton states. The lack of finestructure on the broad hole was ascribed to disorder. Very similar results were obtained by the same authors for chlorosomes in intact cells of *Cb. limicola* [538]

The small amount of BChl *a* (1–5%) in the chlorosome (e.g., Refs. [496,497,502,539,540]) absorbs maximally at 790–795 nm and is organized in a separate BChl *a* protein in the chlorosome envelope at the attachment site to the cytoplasmic membrane (the so-called baseplate [508,514,539]). Linear dichroism spectra of BChl *a* containing chlorosomes have shown that the orientation of the BChl *a* transition moments is rather different from those of BChl *c* [496,497]. Time-resolved polarized fluorescence experiments at various temperatures have suggested heterogeneity in the baseplate BChl *a* pool [501,528,541].

*4.2.2.2. Excitation energy transfer.* In isolated chlorosomes, the chlorosomal BChl *a* is the final energy acceptor. In time-resolved measurements at low redox potential (anaerobic conditions), the BChl *a* fluorescence from *Cb. vibrioforme* chlorosomes was observed to decay in a biphasic manner with relatively long time-constants of 335 ps (18%) and 905 ps (75%) [542], which is about what one expects for a terminal BChl emitter. The BChl *d* to BChl *a* energy transfer is characterized by a time-constant of about 65 ps [542, 543], i.e., unchanged as compared to whole cells of *Cb. vibrioforme*. Under aerobic conditions, a BChl *d* lifetime of 10 ps was observed (again as in whole cells), along with a multiphasic decay of BChl *a* characterized by the time-constants ranging from 17 ps to 250 ps [542]. A similar redox state dependence of the BChl *a* excited state lifetime was observed with transient absorption measurements of chlorosomes from *Cb. limicola* [486]; also here, the BChl *c* to BChl *a* transfer times ($\tau = 20$ ps) were found to be identical in isolated chlorosomes and in whole cells (see 4.2.4 for more details on the redox state dependencies).

For chlorosomes of *Cf. aurantiacus*, which do not exhibit the redox state dependence of fluorescence yields, the lifetime of BChl *c* is short ($\sim$ 10–20 ps) [65,528,542,544] and has been ascribed to excitation energy transfer to BChl *a*-792. Also in this case relatively short ($< 200$ ps) BChl *a* lifetimes have been reported [65,545]. The observation that the fluorescence DAS of *Cf. aurantiacus* chlorosomes were very similar as those of intact cells led Causgrove et al. [542] to propose that the low fluorescence yield in *Cf. aurantiacus* chlorosomes was due to trapping of BChl *c*/BChl *a*-792 excitations by a small number of residual membrane-associated complexes. This suggestion is consistent with the results of Gillbro et al. [486] and shows that a chlorosome preparation that is not totally devoid

of membrane-bound pigments displays kinetics that is very similar to that of intact cells. These findings may possibly be understood as a result of the ultrafast energy transfer through the BChl *c* pigment pool and the fact that in vivo each chlorosome serves as the excitation energy donor to several reaction centers. Thus, only a small residual fraction of the original membrane bound complexes may be sufficient to quench a significant fraction of the excitation energy efficiently and to produce excited state decay kinetics that for a large part resemble those of the intact system. In addition, the isolation of the chlorosomes may also introduce new processes for quenching of the fluorescence from BChl *c*/BChl *a*-792 [545]. In chlorosomes of *Cf. aurantiacus* lacking the chlorosomal BChl *a* [65] the BChl *c* fluorescence remains strongly quenched and decays with a 14 ps time-constant.

Time-resolved polarized absorption and fluorescence experiments have documented the energy transfer within a chlorosome. Fetisova et al. [505,546] detected a close to maximum initial polarization of the fluorescence of chlorosomes in cells of *Cb. limicola* and *Cf. aurantiacus*. In both samples, little depolarization of the chlorosome fluorescence was observed during 200 ps. In picosecond pump-probe experiments by Gillbro et al. [486] with chlorosomes of *Cb. limicola*, the initial polarization of the absorption changes was not maximal ($r(0) = 0.2$–$0.25$), but also here no further depolarization occurred on a timescale of 100 ps. The relatively low $r(0)$ may partly be due to a fast energy transfer process among not perfectly parallel BChl *c* molecules.

The kinetics of intra-chlorosome energy transfer have been shown to take place on a picosecond timescale from the efficiency of singlet-singlet annihilation [547]. Intra-chlorosome energy transfer between different spectral species was resolved by Holzwarth et al. [65], who observed a 5 ps component in the fluorescence DAS of *Cf. aurantiacus* chlorosomes. Pump-probe experiments in *Cf. aurantiacus* chlorosomes by Lin et al. [77] essentially confirmed the existence of an energy transfer process on the time-scale of a few picoseconds. It was observed that the single wavelength pump-probe absorption difference spectrum was bipolar (bleaching for $\lambda > 735$ nm, excited state absorption for $\lambda < 725$ nm). Around the isosbestic point the transient absorption signal showed an initial bleaching followed by recovery on a timescale of a few picoseconds to a strongly absorbing state. As shown in Fig. 11, the absorption difference spectrum exhibited a dynamic blueshift of about 4 nm with a characteristic time of 7 ps. In addition, the time-resolved polarized absorption anisotropy showed a characteristic depolarization time of some 4 ps at 740 nm and 7 ps at 720 nm. At 740 nm the residual anisotropy was about 0.32, while in the blue wing of the BChl *c* absorption the depolarization

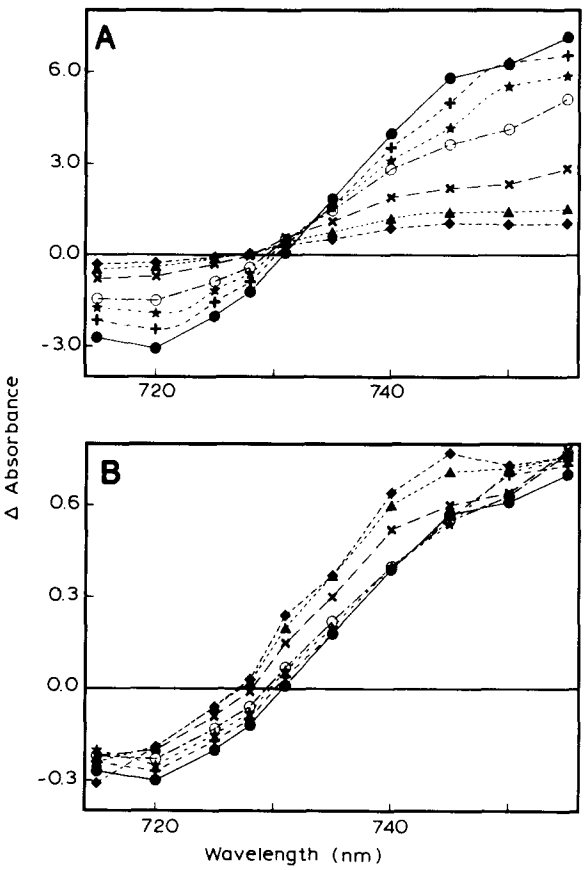


Fig. 11. Difference absorption spectra for fixed time delays for chlorosomes of *Cf. aurantiacus*. The spectra were constructed from isotropic single-wavelength pump-probe profiles recorded at ten wavelengths from 715–755 nm. (A) Spectra with actual relative magnitudes at different time delays; the latter are (from top to bottom at the right-hand side) 2, 3, 4, 5, 10, 20 and 50 ps. (B) The same spectra normalized to the respective lock-in amplifier signal ranges. Note that the zero-crossing in these difference spectra shows a dynamic blue-shift over about 4 nm with a rime constant of approx. 7 ps. (Figure taken from Ref. [77].)

was more pronounced. Recently, Gillbro and coworkers observed in chlorosomes of *Cf. aurantiacus* a 0.5 ps phase in the absorption anisotropy decay using 100 fs pump and probe pulses (T. Gillbro et al., unpublished observations). Using a $< 40$ fs Ti-sapphire laser, Savikhin et al. [62] observed 100 fs and 1 ps equilibration phases in the chlorosomes of *Cf. aurantiacus* preceding the slower 5–10 ps process.

The experiments of Lin et al. [77] were rationalized in terms of an exciton model that is essentially identical to that used for J-aggregates, with the modification that the structure of the BChl *c*-aggregate may show some helicity and that excited state absorption is now explicitly included in the calculations. In this model the dynamic blueshift is due to a picosecond relaxation process between various exciton levels. The authors claim that the experiments cannot be explained by assuming that the excitations are rapidly ($< 1$ ps) localized on single BChl *c* molecules. The observed residual

anisotropies were shown to be in quantitative agreement with earlier steady-state polarized fluorescence and linear dichroism experiments [497,498,500]. Alternatively, the dynamic blue-shift may be described to spectral diffusion due to ultrafast energy transfer in the chlorosome. Note that the model of Lin et al. explains the variation of the LD over the 740 nm band without invoking the existence of different spectral species of BChl *c* within the chlorosome [501,528] (see also section 4.2.2.1).

*4.2.3. Green gliding non-sulfur bacteria (Chloroflexus aurantiacus)*

*4.2.3.1. Pigment organization and spectroscopy.* The only well-known member of the family of green gliding non-sulfur bacteria (Chloroflexaceae) is *Chloroflexus (Cf.) aurantiacus*. This organism contains chlorosomes that are quite similar to those of the green sulfur bacteria (Chlorobiaceae). However, the intramembrane light-harvesting and reaction center pigment-proteins are not of the PS I type as in green sulfur bacteria, but of the purple bacterial type [548]. Typically there are about 30–35 antenna BChl *a* molecules per RC [549], most of which are organized in the LH1/2-like B806–866 complex. Linear dichroism and steady-state polarized fluorescence spectra have shown that the B866 molecules are organized in a very similar manner as the major LH2 and LH1 BChl molecules in *Rb. sphaeroides*, with $Q_y$-transitions in the plane of the membrane (without a preferred orientation within this plane) and $Q_x$-transitions perpendicular to this plane [549]. The BChl 808 $Q_y$-transitions make an average angle of about 44° with the membrane plane, suggesting a structural difference with the B800–850 complex of *Rb. sphaeroides*. The carotenoid:BChl *a* ratio is about 1:2 and carotenoid → BChl *a* energy transfer occurs with an efficiency of 40%. The reaction center contains 3 BChl *a* and 3 BPheo *a* molecules, in which probably one of the BPheo molecules is located at the position of the monomeric BChl *a* molecule in the M-branch of the purple bacterial reaction center [548]. The organization of the pigments in the *Chloroflexus* RC is probably quite similar to that in *Rps. viridis* or *Rb. sphaeroides*, but the rate of initial charge separation, however, may be somewhat slower (7 ps at 300 K [550,551]). The composition of the remaining part of the electron transport chain appears to be very similar to that of purple bacteria.

*4.2.3.2. Excitation energy transfer and trapping.* Already from the first experiments it became clear that energy transfer from BChl *c* in chlorosomes to BChl *a* in membranes occurs efficiently and fast (in about 10–30 ps) [545, 505]. Nevertheless, the detailed kinetics of energy transfer between BChl *c*, BChl *a*-792 and B808–866 remained obscure until quite recently. One particularly confusing point was the difficulty to recover a rise-time of the BChl *a*-792 fluorescence, corresponding to the BChl *c* decay time [541]. By using time-resolved fluorescence detection and global analysis deconvolution methods, Holzwarth and co-workers were the first to resolve this step in whole cells of *Cf. aurantiacus* and to demonstrate the matching between BChl *c* and BChl *a* 792 fluorescence kinetics [552]. In these experiments DAS-spectra were obtained in the wavelength interval 730–930 nm demonstrating a 16–19 ps transfer time for BChl *c* to BChl *a* 792, a 35 ps time-constant for energy transfer from chlorosomal BChl *a* 792 to B808–866 and a 106 ps time-constant reflecting the trapping by open reaction centers. A very low amplitude, 500 ps component was also observed, possibly corresponding to charge stabilization in the reaction center. Similar time-resolved fluorescence measurements on whole cells of *Cf. aurantiacus* were performed by Causgrove et al. [542], and by Miller et al. [544] on chlorosome preparations with membrane fractions attached and both studies confirmed the results of Müller et al. on all essential points. In Ref. [542] the trapping time was reported to be about 40–50 ps, which seems more reasonable in comparison to trapping times observed in LH1-containing purple bacteria. Thus, the energy transfer path in *Cf. aurantiacus* is summarized as follows:

$$\overset{\text{chlorosome}}{\left[\text{BChl } c \xrightarrow[16-19\text{ ps}]{} \text{BChl } a\ 792\right]} \xrightarrow[35-45\text{ ps}]{} \overset{\text{membrane}}{\left[\text{BChl } a\ 808-866 \xrightarrow[40-50\text{ ps}]{} \text{P870}\right]}$$

It should be noted that Mimuro et al. [541] in their earlier experiments could not distinguish the BChl *a*-792 risetime and consequently concluded that the majority of the BChl *c* → BChl *a*-792 energy transfer occurred within a ps or less. A more recent analysis by the same authors [528] showed that at a temperature of 55° the decay of BChl *c* and the rise of BChl *a*-792 matched. It was claimed that both the chlorosome emission (decay) and the BChl *a* 792 emission (rise and decay) were spectrally and kinetically heterogeneous. From the foregoing discussion there appears a general match between the BChl *c* decay and BChl *a*-792 rise. Nevertheless, the possibility cannot be excluded that faster processes, too, play a role in the BChl *c* → BChl *a* 792 energy transfer [541]. In this respect it is important to mention that the BChl *c* lifetime is essentially independent of the presence of BChl *a*-792 [65,535, 544].

The B808–866 antenna protein complex of *Cf. aurantiacus* was studied in the intact membrane and in its isolated form. From the observed BChl fluorescence yield Vasmel et al. [549] estimated that the BChl 808 → BChl 866 energy transfer occurs in about 6 ps at 200

K. Picosecond fluorescence experiments on intact systems confirmed that this energy transfer process is 'fast', but a time constant could not be established [541,542,552]. Picosecond fluorescence measurements on the isolated B808–866 complex yielded an equilibration time-constant of $5 \pm 1$ ps at room temperature [553]. Recent subpicosecond transient absorption measurements on *Cf. aurantiacus* membranes at 810 nm indicate an additional 1–2 ps phase preceding the 5 ps decay (T. Gillbro et al., unpublished observations). The time constant for excitation decay in BChl *a* 808–866 in the presence of closed reaction centers was estimated to be about 200 ps [545,546,554], which probably reflects decreased quenching by the closed RC, consistent with similar observations in purple bacteria.

*4.2.4. Green sulfur bacteria (Chlorobiaceae)*

*4.2.4.1. Pigment organization and spectroscopy.* The intramembrane antenna pigments of the green sulfur bacteria are organized in a core complex, in which amongst others the primary electron donor P840, a BChl *a* dimer, is situated [555,556]. Membrane fractions of these bacteria contain BChl *a* with a typical absorption at 810–820 nm and a pronounced shoulder at 830–840 nm and, in addition, a BChl *a*-complex with spectral properties rather similar to those of the FMO BChl *a* protein with absorption maxima at 813 nm and 826 nm [557]. More purified core complexes from *P. aestuarii* [6,558], *Cb. limicola* [559] and *Cb. tepidum* [560] contain about 20 BChl *a* per P840 and a few molecules of a pigment (BChl 663) absorbing near 670 nm, at least one of which is the primary electron acceptor. This pigment has been shown to be an isomer of Chl *a* [561]. The primary structure of the RC-core of *Cb. limicola* has recently been determined [562] and this pigment-protein most likely occurs as a homodimer [556,563]. The amino acid sequences of the corresponding proteins in *Cb. limicola, Heliobacillus mobilis* [564] and PS I are probably evolutionarily related, and detailed comparisons show many common features, in particular with respect to the putative binding sites of electron donor and acceptor residues [562,563,565,566], suggesting a common evolutionary origin of the reaction centers of PS I, heliobacteria and green sulfur bacteria.

Measurements of fluorescence excitation spectra and energy transfer efficiencies [494,502,540] have shown that the overall energy transfer scheme is for *Chlorobium limicola*:

chlorosome baseplate
[BChl *c* → BChl *a* 795] → [BChl *a* 809] →
FMO/membrane
[BChl *a* 813–836 → P840]

In *Cb. phaeovibrioides* energy is transferred from BChl *e* to chlorosomal BChl *a* with an efficiency of 25% at 6 K, whereas the efficiency from BChl *e* to BChl *a* in the membrane is about 10%. These numbers are compatible with the idea that also in this species chlorosomal BChl *a* is an energy transfer intermediate [504].

From steady-state measurements on *Cb. limicola* membranes and chlorosomes, the fluorescence emission was found to be strongly quenched (> 90%) under aerobic conditions and greatly increased in intensity under reducing conditions [476,495,502,547,567]. Previously, this effect was attributed to quenching by (oxidized) impurities, introduced in the chlorosome during the isolation procedure [547,568] or generated by the measuring light [568]. However, a recent systematic study of this fluorescence quenching effect revealed that, at low redox potentials (anaerobic conditions), a close to 100% efficiency of energy transfer from BChl *c* to the membrane occurred, which decreased to 10–20% under aerobic conditions [476,567]. It was proposed that the chlorosomes contain an efficient quencher at high redox potential, and that the effect may be the result of a control mechanism that prevents damage of pigments and protein (which could occur if photo-reduced Fe-S electron acceptors in the RC are re-oxidized by oxygen due to which highly reactive superoxide radicals will be generated [476]). Note that in *Cf. aurantiacus* with a purple bacterial type RC, lacking the ability to reduce oxygen to superoxide, the light-harvesting antenna fluorescence is seen to be independent of the redox conditions [547]. Finally, the chromosome fluorescence from both BChl *c* and BChl *a* is observed to depend strongly on temperature, even under anaerobic conditions [502,569,570]: an effect that is also observed in artificial aggregates of BChl *c*/*d* [570].

*4.2.4.2. Excitation energy transfer and trapping.* Time-resolved spectroscopy has basically confirmed the schemes described above and has provided information about the timescales of the individual steps in the energy transfer process. Note, however, that the experiments require a high time-resolution and precision, because many of the relevant processes occur on the picosecond timescale (1–50 ps) and because most of the absorption and fluorescence spectra are rather broad and strongly overlapping.

Early experiments have indicated that the energy transfer time from the chlorosome to the membrane is of the order of several tens of picoseconds in green sulfur bacteria [571]. Nevertheless, the results of time-resolved measurements (reported for *Cb. limicola* and *Cb. vibrioforme*) display a large amount of scatter in the lifetimes and to some extent a rather pronounced variation with the redox state of the RC [505,546,571, 572]. In this respect we note that, due to the very large BChl *c*/BChl *a* ratio and the relatively small energy difference, a significant part of the BChl *c* fluores-

cence will reflect the decay of the fully equilibrated state, which is (as described above) highly sensitive to the specific redox conditions. A detailed time-resolved fluorescence study has shown that under anaerobic conditions, energy transfer in *Cb. vibrioforme* from BChl *d* (the main chlorosomal pigment) to BChl *a* is relatively slow and takes about 66 ps, while the BChl *a* excitations decay with a 195 ps time constant [542]. Due to the strongly overlapping fluorescence spectra, the different energy transfer processes in the membrane could not be distinguished [542,546]. Closing the reaction centers resulted in a quenching time of about 300 ps [546], typical of what has been observed for *Cf. aurantiacus* and several species of purple bacteria. Under aerobic conditions, only a single lifetime of 11 ps was observed for the BChl *d* and BChl *a* fluorescence. No risetime for the BChl *a* fluorescence could be resolved from the global analysis fits. These results are fully consistent with the observations that steady-state fluorescence from BChl *c / d* and BChl *a* of *Cb. limicola / Cb. vibrioforme* is strongly quenched under aerobic conditions [542,567].

Recently, the energy transfer times from the chlorosome via the baseplate BChl *a* 795 to the membrane were determined to be 65 ps in the BChl *d* containing *Cb. vibrioforme* and 115 ps in the BChl *e* containing *Pelodityon phaeochalthratiforme* [543]. Combined with the earlier obtained corresponding time-constant of 30 ps in the BChl *c* containing *Cb. limicola*, it was concluded that these lifetimes correlate with the variation in overlap between the BChl *c / d / e* emission and the BChl *a*-795 absorption. The BChl *e* emission was found to be heterogeneous, consisting of a 'blue' and a 'red' fraction. Such a spectral heterogeneity of the chlorosomal BChl *c / d / e* pigments was also suggested on the basis of fluorescence lifetime and pump-probe absorption measurements on isolated chlorosomes and low-temperature fluorescence excitation spectra on cells of green sulfur bacteria [504,570]. At 77 K the BChl *c / d / e* energy transfer to chlorosomal BChl *a* was dominated by a 150–200 ps component with a fluorescence DAS showing a maximum around 770–780 nm, which may indicate the presence of a small quantity of a pigment absorbing between 720–750 nm (major form of BChl *c / d / e*) and 795 nm (chlorosomal BChl *a*), which then would act as an energy transfer intermediate to enhance the transfer efficiency.

Time-resolved absorbance measurements on purified, photoactive complexes from *P. aestuarii* containing either 80–100 BChl *a* per RC or 35 BChl *a* per RC have shown that trapping takes place within the duration of the laser pulse (30 ps). Even at 20 K the oxidation of the primary electron donor P-840 is complete within 40 ps. Energy transfer from FMO-BChl *a*-complexes, which presumably were present in some of the earlier preparations, to the reaction center core complex seemed slow and rather inefficient [554,573]. For these green sulphur bacterial RC-core systems it is unknown which process (energy migration, trapping or charge separation) dominates the fast excitation decay times that have been observed.

### 4.3. Heliobacteria

#### 4.3.1. Pigment organization and spectroscopy

Heliobacteria (*Heliobacterium chlorum, Heliobacillus mobilus*, etc.) represent a recently discovered class of photosynthetic organisms. In contrast to other photosynthetic prokaryotes, heliobacteria contain neither chlorosomes (as observed in green bacteria) nor invaginations of the intracytoplasmic membrane (as observed in the purple bacteria) [574–576]. The antenna and reaction center is situated in the cytoplasmic membrane and consists mainly of BChl *g* (BChl *g* resembles BChl *b* with the characteristic ethylidene group at ring II [577]).

The absorption properties of the two most extensively studied species (*H. chlorum* and *H. mobilis*) are closely related. At low temperature, the near-infrared region shows three characteristic peaks, at 778, 793 and 808 nm, which are associated with three distinct forms of BChl *g* [578]. The BChl *g* $Q_y$ transition moments are, on the average, oriented more or less parallel to the membrane plane [578].

It is generally thought that the structures of the reaction center is of the PS I type [563,565,566]. A pigment-protein complex with MW ~ 300 kDa was isolated from *H. chlorum* and *H. mobilis* [8,9], and contains the photochemical reaction center together about 30–40 associated BChl *g* molecules. The purified complex shows the same absorption characteristics as the original cells, indicating that all reaction center and antenna pigments occur within the same particle.

At room temperature the major bleaching due to the oxidation of the primary electron donor is found at 798 nm (P798); at 4 K the maximum is blue-shifted to 793 nm [579,580]. P798 is supposed to be a dimer of BChl *g'* [581]. The first electron acceptor is a species absorbing at about 670 nm, which was proposed to be $8^1$-hydroxychlorophyll *a* [582], while later electron acceptors may include a quinone [583] and a number of iron-sulfur centers [584].

#### 4.3.2. Energy transfer and trapping

Early picosecond transient absorption measurements on membranes at room temperature showed that the excitation energy is equilibrated over the various BChl-species within the 35 ps time-resolution of the experiment and that trapping and primary charge separation also occurred within less than 35 ps [585]. More recently, experiments with improved time-resolution indicated spectral equilibration among the various

pigment pools with a lifetime of 1–2 ps at RT [586, 587] and trapping from the equilibrated state with a time-constant of about 20–30 ps [8,586,588].

Picosecond transient absorption measurements at 15 K on *H. chlorum* membranes demonstrated efficient energy transfer to BChl-808 within 20 ps [589] and it was proposed that this pigment has the function of a low-energy antenna focussing the excitation energy in the vicinity of the RC, similar to what has been suggested for 'BChl-896' in LH1 of purple bacteria and specific red pigments in PS I. Since P-798 is at a higher energy than BChl-808, the probability of charge separation should be strongly temperature-dependent. Recently, Kleinherenbrink et al. [459] reported that the efficiency of charge separation is only 30% at 6 K and that, surprisingly, the efficiency is independent of the excitation wavelength. The authors argued that the low quantum efficiency would be consistent with an energy transfer rate from BChl-808 to P-798 of about (440 ps)$^{-1}$, and concluded that such a rate could be explained by the Förster mechanism. Low temperature time-resolved fluorescence [460] and pump-probe [589] measurements revealed strongly multiphasic BChl-808 decay kinetics with fast decays on the high-energy side (< 10 ps, 30–40 ps) and slow decays in the low-energy wing of the transient fluorescence/absorption spectrum. No rise-times could be observed. It was unclear whether the fast components were due to energy transfer to low-energy antenna states or reflected transfer to the P-798 trap. A comparison with the situation in photosynthetic purple bacteria (see the discussion on *Rps. viridis*) suggests that the latter will certainly be a major contribution, which might explain the absence of risetimes in the experiments of Van Noort et al. [589]. Lin et al. [587] observed that the bleaching of the 670 nm transition occurred with a time constant of 10 ps. The bleaching was accompanied by changes in absorption around 785 nm due to BChl *g*. The kinetic discrepancy between the 10 ps 670 nm bleaching and the 20–30 ps trapping process was proposed to reflect a picosecond equilibration between two states involved in the initial charge separaton.

Further charge stabilization was observed to proceed with a time-constant of 800 ps at room temperature and about 300 ps below 100 K [573,590]. In intact cells oxidized P-798 is reduced by cytochrome *c*-553 through a biphasic process characterized by characteristic times of 0.11 and 0.7 ms [591]. Much lower rates have been reported for intact membranes [580], but these low rates appear to be a consequence of modified electron transport in the membrane fragments.

The following scheme summarizes the time-constants and directionality of the primary energy and electron transport processes in *H. chlorum* at room temperature:

$$\text{BChl } g\text{-}778/793 \xrightarrow{<1\text{ ps}} \text{BChl } g\ 808 \xrightarrow{20\text{–}30\text{ ps}} \text{P-798}^{+}\text{I}^{-}\text{X}_1\text{X}_2 \xrightarrow{800\text{ ps}} \text{P-798}^{+}\text{IX}_1^{-}\text{X}_2 \xrightarrow{?} \text{P-798}^{+}\text{IX}_1\text{X}_2^{-} \xrightarrow{0.11;\,0.7\text{ ms}} \text{P-798}$$

in which $I = 8^1$-hydroxychlorophyll *a*, $X_1$ = quinone and $X_2$ = one/more FeS centers.

## 5. Carotenoids as light-harvesting pigments in photosynthesis

Carotenoids have at least two functions in photosynthetic systems. The first is to protect the organism from harmful (bacterio)chlorophyll triplet states that may give rise to the poisonous singlet oxygen [592–594]. The second function, which is the one that will be discussed in this review, is to absorb light and transfer it to other pigments (chlorophylls in plants, algae and cyanobacteria and bacteriochlorophylls in photosynthetic bacteria), which then deliver the energy to the photochemical reaction center [593,594]. This section of the review is divided into two parts. In the first we shall describe the photophysical properties of the carotenoid electronic states, in particular their location on the energy scale, since that is one of the important factors determining their energy transfer characteristics. The second part deals with time-resolved studies of energy transfer from carotenoids to (bacterio-)chlorophylls and an evaluation of our present understanding of the energy transfer mechanism.

### 5.1. Carotenoid photophysics

Carotenoids are polyenes. Therefore, if one wishes to understand the photophysics of the carotenoids it is natural to start with other polyenes, since their properties have been studied intensively over the past decades [595]. An important landmark in this field was the discovery that in short polyenes the observed fluorescence came from a low-lying, optically forbidden state,

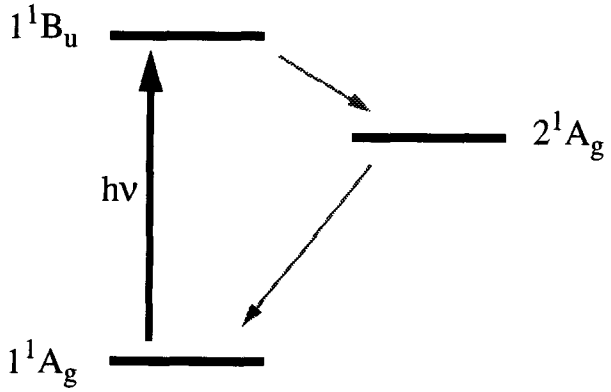


Fig. 12. General energy level scheme of carotenoids.

$2^1A_g$ in the notation of the $C_{2h}$-symmetry group [596] (see Fig. 12 for an energy diagram of the several energetic states). Shortly later, Schulten and Karplus showed that inclusion of electron correlation effects in the Pariser-Parr-Pope hamiltonian could explain the lowering of the $2^1A_g$-state below the strongly allowed $1^1B_u$-state [597]. These conclusions are now widely accepted and additional recent experimental and theoretical work on polyenes has verified the earlier models [595]. Due to the similarities between the structures of the polyenes in general and carotenoids one would expect the electronic structures and photophysical properties to be the same or at least closely related. However, there have been great obstacles to verify this statement, for the following reasons. Only spurious evidence for the presence of the forbidden $2^1A_g$-state has been found in carotenoids. It has proven to be difficult to record the emission from both states ($1^1B_u$ and $2^1A_g$) and, due to the ultrafast non-radiative relaxation rates, only a very few time-resolved studies have been reported. In addition, quantum mechanical calculations with sufficient accuracy are still very demanding to perform on carotenoids. We will discuss some of the recent developments concerning these points below.

*5.1.1. Carotenoid fluorescence*

So far only a limited number of studies of the carotenoid fluorescence has been reported, that include the recording of emission and excitation spectra and a determination of the fluorescence quantum yield. In the earlier literature some evidence can be found that carotenoids fluoresce weakly upon laser excitation [598,599]. Estimates of the quantum yield gave values of $< 10$–6. More recently, it was reported by two groups that the carotenoid fluorescence was detectable with sensitive instruments and that the fluorescence quantum yield was $> 10^{-5}$ [600,601]. The most important result of these papers is that it was shown that the $1^1B_u$-state is the emitting state. The low quantum yield, together with the calculated radiative lifetime of about 1 ns, resulted in a rate constant for non-radiative decay of about $10^{13}$ $s^{-1}$ or a lifetime of the order of 100 fs. The estimated rate constant for β-carotene was based on a measured fluorescence quantum yield of $6 \cdot 10^{-5}$; for sphaeroidene the fluorescence quantum yield was $2 \cdot 10^{-4}$. More recently [602,603] the quantum yield of β-carotene was found to be $2 \cdot 10^{-4}$, which yields a lifetime of 200 fs for the $1^1B_u$-state. For β-carotene, Shreve et al. [603] detected a transient signal in femtosecond absorption measurements with a lifetime of 200 fs. This experiment is the first direct verification of a 200 fs excited state decay process in the $1^1B_u$-state of β-carotene. As an example, Fig. 13 shows the excited state decay kinetics of okenone in $CS_2$ excited and probed at 580 nm. The risetime of about 250 fs represents the formation of $S_1$ through relaxation of $S_2$. For

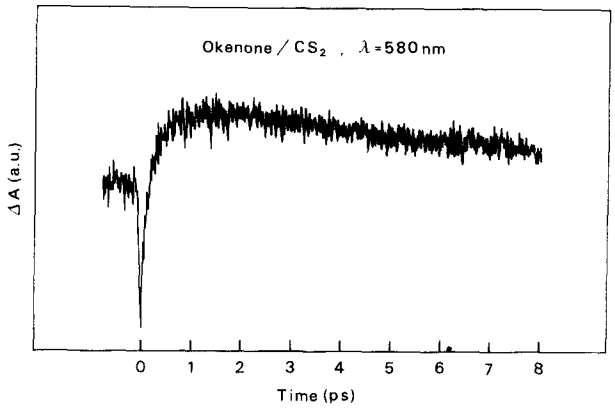


Fig. 13. Excited state decay kinetics of okenone in $CS_2$ excited and probed at 580 nm. The excitation pulsewidth was 70 fs. The risetime following the immediate bleaching represents the formation of $S_1$ through relaxation of $S_2$, the state that was originally excited. The slow approx. 8 ps decay of the $S_1$ state reflects the recovery to the ground state (from Cogdell, R.J. et al., Proc. 'Carotenoids', Trondheim 1993, in press).

a variety of other natural carotenoids (sphaeroidene, neurosporene, violaxanthin, etc.) fluorescence quantum yields [601,602,603,604] and/or $1^1B_u$ lifetimes [603, 605,474,606] have been measured and these are all consistent with a $1^1B_u \rightarrow 2^1A_g$ lifetime of a few hundred fs. One other property of the $1^1B_u$-state that should be pointed out is the high anisotropy of the emission (about 0.35) [601]. Since the anisotropy relaxation due to rotaton of the β-carotene molecule is supposed to take place on a time-scale of 100 ps in low viscosity solvents (e.g., hexane or $CS_2$), the lifetime of the emitting $1^1B_u$-state should be less than 10 ps to explain the close to maximum anisotropy. Measurements by Andersson et al. [607] have in fact shown that the anisotropy is constant as a function of solvent viscosity, suggesting that the value is a property inherent to the carotenoid chromophore.

Two-photon fluorescence experiments with fucoxanthin [608] and third harmonic generation (THG) experiments with β-carotene [609–611] have shown that the $1^1B_u$ is strongly dipole coupled to a nearly degenerate $n^1A_g$-state. This strong dipole coupling makes the $1^1B_u$-state highly polarizable and allows for a large induced dipole moment when the carotenoid is bound in an electrically asymmetric environment such as a protein (see for a further discussion [612,613]). Stark-spectroscopy has indeed shown that a large $S_2$-$S_0$ difference (permanent) dipole exists for sphaeroidene in the B800–850 light-harvesting complex (15 $D/f$, where $f$ is the local field correction factor) and in *Rb. sphaeroides* reaction centers (3–8 $D/f$) in comparison to sphaeroidene in solution ($< 5$ $D/f$) [613]. Finally, the large and linear electrochromic shift observed in membranes of *Rb. sphaeroides* upon formation of a transmembrane electrical field has similarly been at-

tributed to carotenoids in an electrically asymmetric environment [614,615]. Interestingly, it is the B800 carotenoid that seems to respond most strongly to the transmembrane electrical field [616].

Recently, experimental evidence has been presented that demonstrated the emission from the $2^1A_g$-state in fucoxanthin, a carotenoid containing the rare allene group [603,617]. The quantum yield was found to be $8 \cdot 10^{-4}$ and the emission maximum was shifted by about 3500 $cm^{-1}$ to lower energies in comparison to the $1^1B_u$-state. These interesting results suggested that there may be some hope for the detection of $2^1A_g$ fluorescence also in 'normal' polyene-type carotenoids in the near future. We will return to the problem of the $2^1A_g$ fluorescence when we discuss the spectroscopic properties of 'short' carotenoids.

*5.1.2. Location of the 2Ag-state*

As mentioned above there is ample evidence for a $2^1A_g$-state below the $1^1B_u$-state in moderately long polyenes [596]. So far, however, the direct experimental evidence of the $2^1A_g$-state in natural carotenoids has been very scanty indeed. Most of the discussion is based on the Raman excitation spectra of Trash et al. [618,619], in which peaks observed in the red-edge of the β-carotene absorption spectrum were interpreted as originating from the $2^1A_g$-state, with a 0–0 energy 3900 $cm^{-1}$ below that of the strong $1^1B_u$-transition. Other experiments, like for instance two-photon absorption studies, have demonstrated in the case of fucoxanthin that the $2^1A_g$-state is at 620 nm, about 100 nm to lower energy than the major $1^1B_u$-state at 525 nm [612]. There have appeared two reports about the absorption due to the $1^1A_g \rightarrow 2^1A_g$ transition. Fucoxanthin shows some oscillator strength at 620 nm (about 10% of the major transition at 525 nm [612]) and neurosporene for which an absorption located at about 623 nm with an extinction coefficient of 60 $M^{-1}$ $cm^{-1}$ was directly observed [620].

One approach to overcome this problem is to study the location of the $2^1A_g$-state in a series of carotenoids with different lengths of the polyene chain and by comparing the obtained result with theoretical predictions for the location of $2^1A_g$ [621,622]. De Coster et al. [623] recently investigated a series of carotenoids with 7 to 11 double bonds and found that with more than 8 double bonds the emission is mainly from $1^1B_u \rightarrow 1^1A_g$, while for the shorter polyene chains the $2^1A_g \rightarrow 1^1A_g$ emission dominates. Although for the longer carotenoids the $2^1A_g \rightarrow 1^1A_g$ emission is not directly observed, it was concluded by extrapolation that in β-carotene the $2^1A_g$-state should be 6500–7700 $cm^{-1}$ below $1^1B_u$, which is in contrast with the energy difference of ca. 3500 $cm^{-1}$ given by Thrash et al., and locates the $1^1A_g \rightarrow 2^1A_g$ well below the Chl *a* $Q_y$ at 15000 $cm^{-1}$ [623]. Andersson et al. [624] have studied a series of synthetic β-carotenes with 3–11 double bonds. Also in this case emission from the $2^1A_g$-state was observed for β-carotenes with less than 8 double bonds and only emission from the $1^1B_u$-state for 9 or more double bonds. The location of the $2^1A_g$-state, when detectable, closely followed the prediction from theory. When those results are extrapolated to β-carotene the $2^1A_g$-state is found at about 6000 $cm^{-1}$ below $1^1B_u$, at somewhat higher energy than proposed by De Coster et al. [623]. This implies that for β-carotene the $2^1A_g$ spectral origin is at about 14500 $cm^{-1}$. Similar experiments for a series of natural occurring polyenes (phytoene, phytofluene, ξ-carotene and neurosporene) yielded a $2^1A_g$ spectral origin of ca. 16000 $cm^{-1}$ for neurosporene, of 14500 $cm^{-1}$ for β-carotene and 13200 $cm^{-1}$ for lycopene [625]. Owens et al. [612] predict the $2^1A_g$ spectral origin of β-carotene also at 14500 $cm^{-1}$. Therefore, it seems fully justified to locate $2^1A_g$ at lower energy than previously assumed, although the precise location relative to the Chl *a* $Q_y$ remains a matter of debate. This will have important implications for the mechanism of energy ransfer between β-carotene and chlorophyll as will be discussed below (see section 5.2).

*5.1.3. Carotenoid ground state recovery times*

In comparison with the rather unclear picture that we have about the location of the electronic states and the other spectral properties of the forbidden $2^1A_g$-state, much more is known about its lifetime, due to several (sub-)picosecond experiments with a variety of carotenoids [56,626–628]. In these experiments the carotenoid was excited to the $1^1B_u$-state with a short laser pulse and the subsequent recovery of the ground state absorption was recorded (note that apart from the ground state bleaching the excited state difference spectra are characterized by the appearance of a broad absorption at longer wavelengths (Refs. [56,626] and Andersson, P.-O and Gillbro, T., unpublished data). Alternatively, the temporal development of the Raman spectrum of the $2^1A_g$-state was followed [629–631]. The data show that there is little variation in ground state recovery time over the various natural carotenoids used for these experiments. The lifetimes all range between 4 and 25 ps, with the exception of fucoxanthin, which has a relatively long lifetime of about 40 ps. This might be due to its rather different electronic structure. For the short synthetic mini-carotenes with 5 or 7 –C=C– double bonds the $2^1A_g$ lifetime was 2 ns and 350 ps, respectively [625]. This strong decrease in lifetime upon increasing number of –C=C– double bonds, or decreasing the $S_1$-$S_0$ energy difference, has been explained by the so-called energy gap law, which states that the relaxation rate between two energy levels is related to the logarithm of the energy difference between the levels [632]. The Raman spectra

show that the vibrational frequencies of the $-C \approx C-$ double bonds change dramatically upon excitation from the ground electronic state into the lowest excited $2^1A_g$-state. The frequency of the double bond is increased from 1521 to 1777 $cm^{-1}$ in $\beta$-carotene [633,634]. It is thought that this change of normal mode frequency may be the essential factor for the efficient non-radiative decay in carotenoids, at least from the $2^1A_g$-state [634,635].

### 5.2. Carotenoids and their role as light-harvesting pigments

At the time of the previous review [1] it was generally accepted that carotenoids were present in most light-harvesting antenna complexes and that they could transfer their excitation energy more or less efficiently to chlorophyll or bacteriochlorophyll. It is of course reasonable to expect that nature has chosen these abundant and strongly absorbing molecules ($\epsilon_{max} = 1.5 \cdot 10^5$ $cm^{-1}mol^{-1}$) for the efficient capture of solar energy, since their main absorption lies in the gap between Soret and $Q_x$-bands of chlorophyll and bacteriochlorophyll, i.e., at 400–550 nm. It is maybe worthwhile to mention that green light shows the maximum penetration depth in natural waters, which are inhabited by many photosynthetic organisms containing carotenoids [593,594]. Although the transfer of excitation energy from carotenoid to (bacterio)chlorophyll was discovered almost 40 years ago [636], it has only recently become possible to study directly the energy transfer between carotenoid and (bacterio-)chlorophyll using time-resolved laser spectroscopy. The main concern of this section is thus to review recent (sub-)picosecond work on carotenoid containing photosynthetic antennae.

#### 5.2.1. (Sub)picosecond studies of carotenoid → (bacterio)chlorophyll energy transfer

The first experiments in this area were performed by Wasielewski et al. [626] on the carotenoid to BChl energy transfer in the B800–850 light-harvesting complex of *Rps. acidophila*. The carotenoid was excited at 515 nm with 4 ps light pulses and the ground state recovery was found to take place with a time-constant of $5.6 \pm 0.9$ ps. Since the bleaching of the 850 band was observed to occur with a similar time-constant ($6.1 \pm 0.9$ ps), it was concluded that in the energy transfer from carotenoid to the B850 bacteriochlorophyll a pool occurs in about 6 ps. Notably, no transient bleaching in the B800 band was observed. A probable explanation for this is that the rate of transfer of excitation energy from B800 to B850 ($\ll 1$ ps at RT [56]) exceeds the carotenoid to B800 energy transfer rate and consequently in a linear scheme the amount of excited B800 at any moment is very small. In later experiments, Gillbro et al. [627] studied the rate of energy transfer in the related B800–820 complex of *Rps. acidophila* strain 7050. The carotenoid is of the spirilloxanthin family and has a red-shifted absorption, which allowed excitation with laser pulses from a cavity-dumped dye laser. At 543 nm a fast, pulse-limited signal was observed due to the bleaching of the carotenoid ground-state absorption, followed by the formation of a long-lived absorption due to BChl *a* excited-state absorption. Deconvolution with the 7 ps laser excitation pulse resulted in a transfer time of $3 \pm 1$ ps. It was not possible to assign the accepting species as either B800 or B820. In addition, a rather complex anisotropy kinetics was observed, possibly due to the involvement of excited-state absorption with a different polarization relative to the excitation pulse. Similar experiments with the B880 complex of *Rs. rubrum* yielded a 1–3 ps transfer time from the carotenoid excited at 548 nm to the B880 acceptor [602]. In a combined picosecond absorption and time-resolved resonance Raman work Hayashi et al. [637] observed a 6 ps transient and assigned this to the decay of the $S_1$ of carotenoids in B800–850 of *Chromatium vinosum* (rhodopin, spirilloxanthin).

More recent work by the group of Albrecht and co-workers has extended these experiments into the sub-picosecond time domain [56,474,612]. A detailed study of the B800–850 complex of *Rb. sphaeroides* [56,612] indicated that energy transfer from carotenoid to B800 occurs from both $S_2$ and $S_1$ with time-constants of 1.7 ps and 3.8 ps, respectively. Assuming radiationless decay times for $S_2$ and $S_1$ of 0.34 ps and 9.1 ps, respectively, and taking the B800 to B850 transfer time 0.7 ps these authors could successfully explain their transient kinetic data observed in the 800 nm region upon carotenoid excitation. We note that this interpretation of the data is markedly different from that originally given [474], in which the carotenoid-to-B800 transfer was assumed to be ultrafast (0.3–0.4 ps) and the B800-to-B850 transfer slow (2.2 ps). The more recent experiments [56] in addition show subpicosecond (0.2 ps) energy transfer from carotenoid $S_2$ to B850 as judged from the B850 excited state rise kinetics. This latter process would give an efficiency of 60% for energy transfer from $S_2$. How these results fit into the model originally proposed by Kramer et al. [387,388] in which B800 and B850 each have their own carotenoids is unclear. If a major part of the excitation transfer takes place via the very short-lived $1^1B_u$-state the observed branching ratio (3/4 direct to B850, 1/4 direct to B800 [387]) may also be due to kinetic competition. In fact, recent experiments with several site-directed mutants of LH2 of *Rb. sphaeroides* in which the binding site of B800 was destabilized indicated a $>$ 90% transfer efficiency from all the carotenoids to B850, supporting this latter idea [638]. The earlier

kinetic measurements at 520 nm [474] also showed a 1.4 ps component in the carotenoid ground state recovery, which was interpreted as a vibrational cooling time, since the amplitude of this signal was too large to be explained by for instance decoupled carotenoids.

Trautman et al. [605] and Shreve et al. [603] also studied the carotenoid excited state dynamics in thylakoid membrane fractions of two chlorophyll *a* containing species, i.e., the diatom *Phaedactylum tricornutum* and the eustigmatophyte *Nannochloropsis sp.* using sub-ps pump-probe spectroscopy with a time-resolution of 240 fs. The photon flux in those experiments was very high (about $10^{15}$ photons/cm$^2$), which should be compared with the threshold for singlet-singlet annihilation in the chlorophyll *a* pigment pool in thylakoids of $< 10^{13}$ photons/cm$^2$ [1]. The main result was the observation of a subpicosecond (0.24 ps) energy transfer time from carotenoid to chlorophyll *a* in *Nannochloropsis sp.* thylakoids, consistent with an energy transfer efficiency of more than 95%. In *P. tricornutum* thylakoids the transfer time was apparently much longer (0.9 ps). The latter signal was fitted to a two-exponential rise of 0.5 ps and 2.0 ps with relative amplitude ratio of 1.7:1. The wavelength dependence of the excitation transfer efficiency and the transfer times suggests an inhomogeneous distribution of carotenoid $S_0$-$S_2$ transition energies, with the red-most more strongly (exclusively) coupled to Chl *a*. It was suggested that the 'coupled' carotenoid fraction (with the 0.5 ps transfer time) occurs in a special binding site that also induces the red-shift. In fact the authors calculate from the two-photon absorption spectrum (representing $2^1A_g$) that a coupling of 60–120 cm$^{-1}$ is sufficient for a 0.25–1 ps excitation energy transfer rate. For fucoxanthin, both exchange coupling and Förster coupling may yield such an interaction matrix element, assuming the Car-Chl *a* distance $< 1$ nm.

### 5.2.2. Models for carotenoid to (bacterio)chlorophyll energy transfer in vivo

The mechanism of energy transfer between carotenoids and (bacterio-)chlorophylls has been a controversial subject for a long period of time. It is by now generally accepted that the energy transfer in other systems, e.g. the transfer of excitation energy in phycobilisomes and between chlorophylls or bacteriochlorophylls occurs predominantly by the dipole-dipole resonance mechanism proposed by Förster [36]. However, the energy transfer between carotenoids and (bacterio-)chlorophylls has been difficult to understand by the Förster resonance mechanism because (i) the spectral overlap between the carotenoid emission and the strong $Q_y$-transition of (bacterio-)chlorophyll is small, (ii) the lifetime of the $1^1B_u$-state is very short (about 200 fs, see above), which would diminish the quantum yield of energy transfer, unless the transfer rate is exceedingly high (100 fs), and (iii) the low-lying $2^1A_g$-state, which seems to be the longest-lived state, is optically forbidden and thus has a vanishingly small transition dipole moment. Razi Naqvi [639] has pointed out that the Dexter electron exchange mechanism [38] would be the preferred one, since in this case it is irrelevant whether or not the states involved are optically allowed. The Dexter mechanism, on the other hand requires that the molecules participating in the energy transfer are almost at Van der Waals distance to allow for a large overlap of the relevant molecular orbitals. If the $2^1A_g$-state is responsible for the energy transfer process, it should be possible to correlate experimentally obtained transfer efficiencies with the measured rate constants for the energy transfer process ($k_{ET}$) and the expected/experimentally measured lifetimes of the $2^1A_g$-state of the isolated carotenoid molecules. So far, a strict correlation remains to be demonstrated. The efficiency of energy transfer by the Dexter mechanism may be high. For instance, for the B800–850 light-harvesting complex of *Rb. sphaeroides* the transfer could be $> 90\%$ efficient, assuming an intrinsic 9.1 ps lifetime of $2^1A_g$, which is in good agreement with the observed efficiency [387,388,594].

The Dexter mechanism involving the forbidden $2^1A_g$-state has obtained experimental support. Recently, the B850-complex of *Rb. sphaeroides* R-26.1 was reconstituted with a series of carotenoids for which $n$, the number of $-C \approx C-$ double bonds increased from $n = 7$ to $n = 10$ (note that sphaeroidene, the carotenoid of WT *Rb. sphaeroides* contains 10 $-C \approx C-$ double bonds) [640]. The observed increase in energy transfer efficiency for the larger values of $n$ ($n = 7$–9) could be nicely explained by the increase in spectral overlap of the $2^1A_g$-emission and the major B850 $Q_y$-absorption. For sphaeroidene a slightly lower energy transfer efficiency was observed (in comparison with $n = 9$), probably because for that species the overlap integral did not improve much further, while the rate of internal conversion $2^1A_g \rightarrow 1^1A_g$ increased by more than a factor two due to the decreased energy gap (see 5.1.3).

Finally, also the work on model compounds has given support for the Dexter exchange mechanism as responsible for excitation energy transfer between carotenoids and chlorophylls (or chlorophyll-like molecules) [641,642]. For these model compounds it was observed that energy transfer occurred only with a measurable efficiency if the edge-to-edge distance between the chromophores was less than 0.5 nm. Note that in the Dexter model two factors are important for the transfer rate [643]: (i) the Franck Condon factor for the transition expressed as the overlap between the normalized donor emission spectrum and the acceptor absorption spectrum and (ii) the distance, which is usually expressed as a function of the type $\exp[-\beta(r -$

$r_0$)], where $r_0$ is the Van der Waals contact distance, $r$ the actual distance between the molecular centers and $\beta$ is a characteristic constant with a typical value of 1.3 $Å^{-1}$. The total Dexter equation is than given by: $k_{ET} = \nu_1 \exp[-\beta(r - r_0)]$, with $\nu_1$ having a maximum value of $10^{13}$ $s^{-1}$ at optimal overlap. For B800–820 of *Rps. acidophila* [627] $r$ was calculated to be $4.5 \pm 2.7$ Å, which indicates close contact between the carotenoid and the BChl in this case. The most unclear factor in this calculation may be the determination of the spectral overlap factor, since the location of the $2A_g$-state and its emission spectrum are highly speculative (see above). One might be able to obtain a better estimate for $r$ in the fucoxanthin containing species, for which the $2A_g$ emission has been observed [612].

If the $1A_g \rightarrow 2A_g$ is indeed close to or even below the $Q_y$ of Chl *a*, which maybe the case for $\beta$-carotene and zeaxanthin, energy transfer may also occur from the $1^1B_u$-state. Also for the other carotenoids it has been suggested that the strongly allowed dipole of the $1^1A_g \rightarrow 1^1B_u$ transition is involved in Förster-type energy transfer [56,612,640]. Nevertheless, the efficiency of this energy transfer process is expected to be small. For instance, in the B800–850 complex of *Rb. sphaeroides* the $1^1B_u$ lifetime was measured to be 0.2–0.34 ps, while the lifetime of $1^1B_u$ of sphaeroidene in $CS_2$ is a few hundred fs from the fluorescence quantum yield studies. This will make the efficiency of transfer from this state low (at most 50% and probably less), while the observed efficiency exceeds 90%. For $\beta$-carotene in higher plant light-harvesting systems the situation will be similarly critical and will again require a close distance. In specific cases, for instance for fucoxanthin, there may be sufficient dipole strength in the $2A_g \rightarrow 1A_g$ transition to allow for a Förster type of energy transfer. Moreover, accepting that the distance is short requires that higher order Coulombic (e.g. quadrupole) interactions play a role in the transfer of energy from the $2^1A_g$-state.

Clearly, our understanding of the energy transfer mechanism involving carotenoids would benefit enormously from high-resolution crystallographic studies of carotenoid containing light-harvesting proteins, in the same way as for instance the detailed structural information of phycobiliproteins has contributed to our understanding of the energy transfer between phycobilins.

## Acknowledgments

The completion of this manuscript in the present form would not have been possible without the numerous efforts of the co-workers in our groups and without the many discussions with the research groups with whom we are happy to collaborate. We are also very grateful to Drs. R.E. Blankenship and W.S. Struve for their critical comments on the manuscript. Research in our laboratories is supported by the Netherlands Organization for Scientific Research (NWO) and the Swedish Natural Science Research Council (NFR). J.P.D. is supported by a fellowship from the Royal Netherlands Academy of Arts and Sciences (KNAW).

## References

[1] Van Grondelle, R. (1985) Biochim. Biophys. Acta 811, 147–195.
[2] Nanba, O. and Satoh, K. (1987) Proc. Natl. Acad. Sci. USA 84, 109–112.
[3] Golbeck, J.H. (1987) Biochim. Biophys. Acta 895, 167–204.
[4] Bassi, R., Rigoni, F. and Giacometti, G.M. (1990) Photochem. Photobiol. 52, 1187–1206.
[5] Miller, J.F., Hinchigeri, S.B., Parkes-Loach, P.S., Callahan, P.M., Sprinkle, J.R. and Loach, P.A. (1987) Biochemistry 26, 5055–5062.
[6] Vasmel, H., Swarthoff, T., Kramer, H.J.M. and Amesz, J. (1983) Biochim. Biophys. Acta 725, 361–367.
[7] Hurt, E.C. and Hauska, G. (1984) FEBS Lett. 168, 149–154.
[8] Trost, J.T. and Blankenship, R.E. (1989) Biochemistry 28, 9898–9904.
[9] Van de Meent, E.J., Kleinherenbrink, F.A.M. and Amesz, J. (1990) Biochim. Biophys. Acta 1015, 223–230.
[10] Holzwarth, A.R. (1987) in The Light Reactions. Topics in Photosynthesis (Barber, J., ed.), Vol. 8, pp. 95–157, Elsevier, Amsterdam, The Netherlands.
[11] Geacintov, N.E. and Breton, J. (1987) CRC Crit. Rev. Plant Sci. 5, Issue 1, 1–44.
[12] Van Grondelle, R. and Sundström, V. (1988) in Photosynthetic Light-Harvesting Systems (Scheer, H. and Schneider, S., eds.), pp. 403–438, Walter de Gruyter, Berlin.
[13] Hunter, C.N., Van Grondelle, R. and Olsen, J.D. (1989) Trends Biochem. Sci. 14, 72–78.
[14] Holzwarth, A.R. (1991) in Chlorophylls (Scheer, H., ed.), pp. 1125–1151, CRC Press, Boca Raton.
[15] Sundström, V. and Van Grondelle, R. (1991) in Chlorophylls (Scheer, H., ed.), pp. 1097–1124, CRC Press, Boca Raton.
[16] Deisenhofer, J., Epp, O., Miki, K., Huber, R. and Michel, H. (1985) Nature 318, 618–624.
[17] Allen, J.P., Feher, G., Yeates, T.O., Komiya, H. and Rees, D.C. (1987) Proc. Natl. Acad. Sci. USA 84, 5730–5734.
[18] Kühlbrandt, W. and Wang, D.N. (1991) Nature 350, 130–134.
[19] Kühlbrandt, W., Wang, D.N. and Fujiyoshi, Y. (1994) Nature 367, 614–621.
[20] Krauss, N., Hinrichs, W., Witt, I., Fromme, P., Pritzkow, W., Dauter, Z., Betzel, C., Wilson, K.S., Witt, H.T. and Saenger, W. (1993) Nature 361, 326–331.
[21] Schirmer, T., Bode, W. and Huber, R. (1987) J. Mol. Biol. 196, 677–695.
[22] Duerring, M., Schmidt, G.B. and Huber, R. (1991) J. Mol. Biol. 217, 577–592.
[23] Robles, S.J., Breton, J. and Youvan, D.C. (1990) Science 248, 1402–1405.
[24] Gray, K.A., Farchaus, J.W., Wachtveitl, J., Breton, J. and Oesterhelt, D. (1990) EMBO J. 9, 2061–2070.
[25] Fowler, G.J.S., Visschers, R.W., Grief, G.G., Van Grondelle, R. and Hunter, C.N. (1992) Nature 355, 848–850.
[26] Duysens, L.N.M. (1964) Progr. Biophys. 14, 1–104.
[27] Knox, R.S. (1975) in Bioenergetics of Photosynthesis (Govindjee, ed.), pp. 183–221, Academic Press, New York.
[28] Knox, R.S. (1977) in Primary Processes of Photosynthesis

(Barber, J., ed.), pp. 55–97, Elsevier/North-Holland Biomedical Press, Amsterdam.
[29] Pearlstein, R.M. (1982) in Photosynthesis (Govindjee, ed.), pp. 293–330, Academic Press, New York.
[30] Ghanotakis, D.F. and Yocum, C.F. (1990) Annu. Rev. Plant Physiol. Plant Mol. Biol. 41, 255–276.
[31] Boekema, E.J., Boonstra, A.F., Dekker, J.P. and Rögner, M. (1994) J. Bioenerg. Biomembr. 26, 17–29.
[32] Zuber, H. and Brunisholz, R.A. (1991) in Chlorophylls (Scheer, H., ed.), pp. 627–704, CRC Press, Boca Raton, Florida.
[33] Brunisholz, R.A. and Zuber, H. (1992) J. Photochem. Photobiol. B 15, 113–140.
[34] Reddy, N.R.S., Lyle, P.A. and Small, G.J. (1992) Photosynth. Res. 31, 167–194.
[35] Renger, G. (1992) in The Photosystems: Structure, Function and Molecular Biology (Barber, J., ed.), pp. 45–99, Elsevier Science Publishers, Amsterdam.
[36] Förster, Th. (1948) Ann. Phys. (Leipzig) 2, 55–75.
[37] Förster, Th. (1965) in Modern Quantum Chemistry, Part III (Sinanoglu, O., ed.), pp. 93–137, Academic Press, New York.
[38] Dexter, D.L. (1953) J. Chem. Phys. 21, 836–850.
[39] Pearlstein, R.M. (1991) in Chlorophylls (Scheer, H., ed.), pp. 1047–1078, CRC Press, Boca Raton.
[40] Montroll, E.W. (1969) J. Math. Phys. 10, 753–765.
[41] Knox, R.S. (1968) J. Theor. Biol. 21, 244–259.
[42] Den Hollander, W.T.F., Bakker, J.G.C. and Van Grondelle, R. (1983) Biochim. Biophys. Acta 725, 492–507.
[43] Pearlstein, R.M. (1982) Photochem. Photobiol. 35, 835–844.
[44] Paillotin, G., Swenberg, C.E., Breton, J. and Geacintov, N.E. (1979) Biophys. J. 25, 513–533.
[45] Bakker, J.G.C., Van Grondelle, R. and den Hollander, W.T.F. (1983) Biochim. Biophys. Acta 725, 508–518.
[46] Owens, T.G., Webb, S.P., Mets, L., Alberte, R.S. and Fleming, G.R. (1987) Proc. Natl. Acad. Sci. USA 84, 1532–1536.
[47] Breton, J., Martin, J.-L., Fleming, G.R. and Lambry, J.-C. (1988) Biochemistry 27, 8276–8284.
[48] Durrant, J.R., Hastings, G., Joseph, D.M., Barber, J., Porter, G. and Klug, D.R. (1992) Proc. Natl. Acad. Sci. USA 89, 11632–11636.
[49] Eads, D.D., Castner Jr., E.W., Alberte, R.S., Mets, L. and Fleming, G.R. (1989) J. Phys. Chem. 93, 8271–8275.
[50] Kwa, S.L.S., Van Amerongen, H., Lin, S., Dekker, J.P., Van Grondelle, R. and Struve, W.S. (1992) Biochim. Biophys. Acta 1102, 202–212.
[51] Du, M., Xie, X., Mets, L. and Fleming, G.R. (1994) J. Phys. Chem. 98, 4736–4741.
[52] Du, M., Xie, X., Jia, Y., Mets, L. and Fleming, G.R. (1993) Chem. Phys. Lett. 201, 535–542.
[53] Sharkov, A.V., Kryukov, I.V., Khoroshilov, E.V., Kryukov, P.G., Fischer, R., Scheer, H. and Gillbro, T. (1992) Chem. Phys. Lett. 1991, 633–638.
[54] Gillbro, T., Sharkov, A.V., Kryukov, I.V., Khoroshilov, E.V., Kryukov, P.G., Fischer, R. and Scheer, H. (1993) Biochim. Biophys. Acta 1140, 321–326.
[55] Xie, X., Du, M., Mets, L. and Fleming, G.R. (1992) in Time-Resolved Laser Spectroscopy in Biochemistry III, S.P.I.E., Vol. 1640, pp. 690–706.
[56] Shreve, A.P., Trautmann, J.K., Frank, H.A., Owens, T.G. and Albrecht, A.C. (1991) Biochim. Biophys. Acta 1058, 280–288.
[57] Hess, S., Visscher, K.J., Feldshtein, F., Babin, A., Gulbinas, V., Pullerits, T., Van Grondelle, R., Åkeson, E. and Sundström, V. (1994) in Ultrafast Phenomena in Spectroscopy, in press.
[58] Van der Laan, H., Schmidt, Th., Visschers, R.W., Visscher, K.J., Van Grondelle, R. and Völker, S. (1990) Chem. Phys. Lett. 170, 231–238.
[59] Jean, J.M., Friesner, R.A. and Fleming, G.R. (1992) J. Chem. Phys. 96, 5827–5842.
[60] Vos, M.H., Rappaport, F., Lambry, J.-C., Breton, J. and Martin, J.-L. (1993) Nature 363, 320–325.
[61] Chachisvilis, M., Pullerits, T., Jones, M.R., Hunter, C.N. and Sundström, V. (1994) in Abstracts of the Ultrafast Phenomena Meeting, Dana Point, CA.
[62] Savikhin, S., Zhu, Y., Lin, S., Blankenship, R.E. and Struve, W.S. (1994) in Abstracts for the Ultrafast Meeting, Dana Point, CA, in press.
[63] Knox, R.S. and Gülen, D. (1993) Photochem. Photobiol. 57, 40–43.
[64] Van Amerongen, H. and Struve, W.S. (1994) Meth. Enzymol., in press.
[65] Holzwarth, A.R., Müller, M.G. and Griebenow, K.J. (1990) J. Photochem. Photobiol. B 5, 457–465.
[66] Causgrove, T.P., Brune, D.C., Blankenship, R.E. and Olson, J.M. (1990) Photosynth. Res. 25, 1–10.
[67] McCauley, S.W., Bittersman, E. and Holzwarth, A.R. (1989) FEBS Lett. 249, 285–288.
[68] Lin, S., Van Amerongen, H. and Struve, W.S. (1992) Biochim. Biophys. Acta 1140, 6–14.
[69] Schatz, G.H., Brock, H. and Holzwarth, A.R. (1988) Biophys. J. 54, 397–405.
[70] Van Mourik, F. (1993) Doctoral Thesis, Vrije Universiteit, Amsterdam, The Netherlands.
[71] Koolhaas, M.H.C., Van Mourik, F., Van der Zwan, G. and Van Grondelle, R. (1994) J. Luminescence, in press.
[72] Van Mourik, F., Van der Oord, C.J.R., Visscher, K.J., Parkes-Loach, P.S., Loach, P.A., Visschers, R.W. and Van Grondelle, R. (1991) Biochim. Biophys. Acta 1059, 111–119.
[73] Visschers, R.W., Van Mourik, F., Monshouwer, R. and Van Grondelle, R. (1993) Biochim. Biophys. Acta 1141, 238–244.
[74] Chang, M.C., Callahan, P.M., Parkes-Loach, P.S., Cotton, T.M. and Loach, P.A. (1990) Biochemistry 29, 421–429.
[75] Visschers, R.W., Van Grondelle, R. and Robert, B. (1993) Biochim. Biophys. Acta 1183, 369–373.
[76] Pearlstein, R.M. (1992) Photosynth. Res. 31, 213–226.
[77] Lin, S., Van Amerongen, H. and Struve, W.S. (1991) Biochim. Biophys. Acta 1060, 13–24.
[78] Scherer, P.O.J. and Fisher, S.F. (1991) in Chlorophylls (Scheer, H., ed.), pp. 1079–1096, CRC Press, Boca Raton, Florida.
[79] Sauer, K. and Scheer, H. (1988) Biochim. Biophys. Acta 936, 157–170.
[80] Johnson, S.G. and Small, G.J. (1991) J. Phys. Chem. 95, 471–479.
[81] Van Mourik, F., Verwijst, R.R., Mulder, J.M. and Van Grondelle, R. (1992) J. Luminesc. 53, 499–502.
[82] Lu, X. and Pearlstein, R.M. (1993) Photochem. Photobiol. 57, 86–91.
[83] Deinum, G., Aartsma, T.J., Van Grondelle, R. and Amesz, J. (1989) Biochim. Biophys. Acta 976, 63–69.
[84] Pullerits, T. and Freiberg, A. (1992) Biophys. J. 63, 879–896.
[85] Somsen, O.J.G., Van Mourik, F., Van Grondelle, R. and Valkunas, L. (1994) Biophys. J. 66, 1580–1596.
[86] Jia, Y., Jean, J.M., Werst, M.M., Chan, C.-K. and Fleming, G.R. (1992) Biophys. J. 63, 259–273.
[87] Pullerits, T., Van Mourik, F., Visschers, R.W., Monshouwer, R. and Van Grondelle, R. (1994) J. Luminesc. 58, 168–171.
[88] Jean, J.M., Chan, C.-K., Fleming, G.R. and Owens, T.G. (1989) Biophys. J. 56, 1203–1251.
[89] Kudzmauskas, S., Valkunas, L. and Borisov, A.Yu. (1983) J. Theor. Biol. 105, 13–23.
[90] Valkunas, L. (1986) Laser Chem. 6, 253–267.
[91] Valkunas, L. (1989) in Proc. 5th School on Quantum Electronics: Lasers-Physics and Applications (Spasov, A.Y., ed.), pp. 541–560, World Scientific Co., Singapore.
[92] Pullerits, T., Visscher, K.J., Hess, S., Sundström, V., Freiberg, A. and Van Grondelle, R. (1994) Biophys. J. 66, 236–248.

[93] Timpmann, K., Freiberg, A. and Godik, V.I. (1991) Chem. Phys. Lett. 182, 617–622.
[94] Wang, R.T. and Clayton, R.K. (1971) Photochem. Photobiol. 13, 215–224.
[95] Otte, S.C.M., Kleinherenbrink, F.A.M. and Amesz, J. (1993) Biochim. Biophys. Acta 1143, 84–90.
[96] Timpmann, K., Zhang, F.G., Freiberg, A. and Sundström, V. (1993) Biochim. Biophys. Acta 1183, 185–193.
[97] Beekman, L.M.P., Van Mourik, F., Jones, M.R., Visser, H.M., Hunter, C.N. and Van Grondelle, R. (1994) Biochemistry 33, 3143–3147.
[98] Owens, T.G., Webb, S.P., Alberte, R.S., Mets, L. and Fleming, G.R. (1988) Biophys. J. 53, 733–745.
[99] Holzwarth, A.R., Haehnel, W., Ratajczak, R., Bittersman, E. and Schatz, G.H. (1990) in Current Research in Photosynthesis (Baltscheffsky, M., ed.), Vol. II, pp. 611–614, Kluwer Academic Publishers, Dordrecht.
[100] Holzwarth, A.R., Schatz, G., Brock, H. and Bittersman, E. (1993) Biophys. J. 64, 1813–1826.
[101] Schatz, G.H., Brock, H. and Holzwarth, A.R. (1987) Proc. Natl. Acad. Sci. USA 84, 8414–8418.
[102] Roelofs, T.A., Lee, C.-H. and Holzwarth, A.R. (1992) Biophys. J. 61, 1147–1163.
[103] Dau, H. and Sauer, K. (1992) Biochim. Biophys. Acta 1102, 91–106.
[104] Sonoike, K. and Katoh, S. (1988) Biochim. Biophys. Acta 935, 61–71.
[105] Sonoike, K. and Katoh, S. (1989) Biochim. Biophys. Acta 976, 210–213.
[106] Ikegami, I. and Ke, B. (1984) Biochim. Biophys. Acta 764, 70–79.
[107] Ikegami, I. and Katoh, S. (1989) Plant Cell Physiol. 30, 175–182.
[108] Malkin, R., Ortiz, W., Lam, E. and Bonnerjea, J. (1985) Physiol. Veg. 23, 619–625.
[109] Ford, R.C., Picot, D. and Garavito, R.M. (1987) EMBO J. 6, 1581–1586.
[110] Witt, I., Witt, H.T., Gerken, S., Saenger, W., Dekker, J.P. and Rögner, M. (1987) FEBS Lett. 221, 260–264.
[111] Almog, O., Shoham, G., Michaeli, D. and Nechustai, R. (1991) Proc. Natl. Acad. Sci. USA 88, 5312–5316.
[112] Boekema, E.J., Dekker, J.P., Van Heel, M., Rögner, M., Saenger, W., Witt, I. and Witt, H.T. (1987) FEBS Lett. 217, 283–286.
[113] Ford, R.C. and Holzenburg, A. (1988) EMBO J. 7, 2287–2293.
[114] Rögner, M., Mühlenhoff, U., Boekema, E.J. and Witt, H.T. (1990) Biochim. Biophys. Acta 1015, 415–424.
[115] Boekema, E.J., Wynn, R.M. and Malkin, R. (1990) Biochim. Biophys. Acta 1017, 49–56.
[116] Van der Staay, G.W.M., Boekema, E.J., Dekker, J.P. and Matthijs, H.C.P. (1993) Biochim. Biophys. Acta 1142, 189–193.
[117] Ford, R.C., Hefti, A. and Engel, A. (1990) EMBO J. 9, 3067–3075.
[118] Böttcher, B., Gräber, P. and Boekema, E.J. (1992) Biochim. Biophys. Acta 1100, 125–136.
[119] Van Haeringen, B., Dekker, J.P., Bloemendal, M., Rögner, M., Van Grondelle, R. and Van Amerongen, H. (1994) Biophys. J., in press.
[120] Kruip, J., Boekema, E.J., Bald, D., Boonstra, A.F. and Rögner, M. (1993) J. Biol. Chem. 268, 23353–23360.
[121] Hladík, J. and Sofrová, D. (1991) Photosynth. Res. 29, 171–175.
[122] Chitnis, V.P. and Chitnis, P.R. (1993) FEBS Lett. 336, 330–334.
[123] Kruip, J., Bald, D., Boekema, E.J. and Rögner, M. (1994) Photosynth. Res., in press.
[124] Hefti, A., Ford, R.C., Miller, M., Cox, R.P. and Engel, A. (1992) FEBS Lett. 296, 29–32.
[125] Witt, H.T., Krauss, N., Hinrichs, W., Witt, I., Fromme, P. and Saenger, W. (1992) in Research in Photosynthesis (Murata, N., ed.), Vol. I, pp. 521–528, Kluwer, Dordrecht.
[126] Van der Lee, J., Bald, D., Kwa, S.L.S., Van Grondelle, R., Rögner, M. and Dekker, J.P. (1993) Photosynth. Res. 35, 311–321.
[127] Gobets, B., Van Amerongen, H., Monshouwer, R., Kruip. J., Rögner, M., Van Grondelle, R. and Dekker, J.P. (1994) Biochim. Biophys. Acta, in press.
[128] Holzwarth, A.R. (1992) in Research in Photosynthesis (Murata, N., ed.), Vol. I, pp. 187–194, Kluwer Academic Publishers, Dordrecht.
[129] Shubin, V.V., Bezsmertnaya, I.N. and Karapetyan, N.V. (1992) FEBS Lett. 309, 340–342.
[130] Tapie, P., Choquet, Y., Breton, J., Delepelaire, P. and Wollman, F.-A. (1984) Biochim. Biophys. Acta 767, 57–69.
[131] Breton, J. and Ikegami, I. (1989) Photosynth. Res. 21, 27–36.
[132] Nechustai, R., Nourizadeh, S.D. and Thornber, J.P. (1986) Biochim. Biophys. Acta 848, 193–200.
[133] Holzwarth, A.R., Wendler, J. and Haehnel, W. (1985) Biochim. Biophys. Acta 807, 155–167.
[134] Gulotty, R.J., Mets, L., Alberte, R.S. and Fleming, G.R. (1985) Photochem. Photobiol. 41, 487–496.
[135] Nuijs, A.M., Shuvalov, V.A., Van Gorkom, H.J., Plijter, J.J. and Duysens, L.N.M. (1986) Biochim. Biophys. Acta 850, 310–318.
[136] Wittmershaus, B.P., Berns, D.S. and Huang, C. (1987) Biophys. J. 52, 829–836.
[137] Searle, G.F.W., Tamkivi, R., Van Hoek, A. and Schaafsma, T.J. (1988) J. Chem. Soc. Faraday Trans. II 84, 315–327.
[138] Causgrove, T.P., Yang, S. and Struve, W.S. (1988) J. Phys. Chem. 92, 6121–6124.
[139] Klug, D.R., Giorgi, L.B., Crystall, B., Barber, J. and Porter, G. (1989) Photosynth. Res. 22, 277–284.
[140] Sparrow, R., Brown, R.G., Evans, E.H. and Shaw, D. (1990) J. Photochem. Photobiol. 5, 445–455.
[141] Werst, M., Jia, Y., Mets, L. and Fleming, G.R. (1992) Biophys. J. 61, 868–878.
[142] Turconi, S., Schweitzer, G. and Holzwarth, A.R. (1993) Photochem. Photobiol. 57, 113–119.
[143] Pålsson, L.O., Tjus, S.E., Andersson, B. and Gillbro, T., Photochem. Photobiol., submitted.
[144] Hastings, G., Kleinherenbrink, F.A.M., Lin, S. and Blankenship, R.E. (1994) Biochemistry 33, 3185–3192.
[145] Sundström, V., Van Grondelle, R., Bergström, H., Åkesson, E. and Gillbro, T. (1986) Biochim. Biophys. Acta 851, 431–446.
[146] Bergström, H., Sundström, V., Van Grondelle, R., Åkesson, E. and Gillbro, T. (1986) Biochim. Biophys. Acta 852, 279–287.
[147] Zinth, W., Nuss, M.C., Franz, M.A. and Kaiser, W. (1985) in Antennas and Reaction Centers of Photosynthetic Bacteria (Michel-Beyerle, M.E., ed.), pp. 286–291, Springer, Berlin.
[148] Breton, J., Martin, J.-L., Migus, A., Antonetti, A. and Orszag, A. (1986) Proc. Natl. Acad. Sci. USA 83, 5121–5125.
[149] Owens, T.G., Webb, S.P., Mets, L., Alberte, R.S. and Fleming, G.R. (1989) Biophys. J. 56, 95–106.
[150] Trissl, H.-W., Hecks, B. and Wolf, K. (1993) Photochem. Photobiol. 57, 108–112.
[151] Mukerji, I. and Sauer, K. (1989) in Photosynthesis (Briggs, W.H., ed.), pp. 105–122, AR Liss, New York.
[152] Causgrove, T.P., Yang, S. and Struve, W.S. (1989) J. Phys. Chem. 93, 6844–6850.
[153] Trissl, H.-W., Gao, Y. and Wulf, K. (1993) Biophys. J. 64, 974–988.
[154] Beauregard, M., Martin, I. and Holzwarth, A.R. (1991) Biochim. Biophys. Acta 1060, 271–283.
[155] Lyle, P.A. and Struve, W.S. (1991) Photochem. Photobiol. 53, 359–365.

[156] Wittmershaus, B.P., Nordlund, T.M., Knox, W.H., Knox, R.S., Geacintov, N.E. and Breton, J. (1985) Biochim. Biophys. Acta 806, 93–106.
[157] Wittmershaus, B.P. (1987) in Progress in Photosynthesis Research (Biggins, J., ed.), Vol. I, pp. 75–82, Martinus Nijhoff Publishers, Dordrecht.
[158] Mukerji, I. and Sauer, K. (1990) in Current Research in Photosynthesis (Baltscheffsky, M., ed.), Vol. II, pp. 321–324, Kluwer, Dordrecht.
[159] Mukerji, I. and Sauer, K. (1993) Biochim. Biophys. Acta 1142, 311–320.
[160] Trinkunas, G. and Holzwarth, A.R. (1994) Biophys. J. 66, 415–429.
[161] Wittmershaus, B.P., Woolf, V.M. and Vermaas, W.F.J. (1992) Photosynth. Res. 31, 75–87.
[162] Gillie, J.K., Lyle, P.A., Small, G.J. and Golbeck, J.H. (1989) Photosynth. Res. 22, 233–246.
[163] Gillie, J.K., Small, G.J. and Golbeck, J.H. (1989) J. Phys. Chem. 93, 1620–1627.
[164] Hemelrijk, P.W., Kwa, S.L.S., Van Grondelle, R. and Dekker, J.P. (1992) Biochim. Biophys. Acta 1098, 159–166.
[165] Haworth, P., Tapie, P., Arntzen, C.J. and Breton, J. (1982) Biochim. Biophys. Acta 682, 152–159.
[166] Kwa, S.L.S., Groeneveld, F.G., Dekker, J.P., Van Grondelle, R., Van Amerongen, H., Lin, S. and Struve, W.S. (1992) Biochim. Biophys. Acta 1101, 143–146.
[167] Van der Vos, R., Carbonera, D. and Hoff, A.J. (1991) Appl. Magn. Res. 2, 179–202.
[168] Van Amerongen, H., Van Bolhuis, B.M., Kwa, S.L.S. and Van Grondelle, R. (1994) Biophys. J., in press.
[169] Nußberger, S., Dekker, J.P., Kühlbrandt, W., Van Bolhuis, B.M., Van Grondelle, R. and Van Amerongen, H. Biochemistry, submitted.
[170] Kwa, S.L.S., Völker, S., Tilly, N.T., Van Grondelle, R. and Dekker, J.P. (1994) Photochem. Photobiol. 59, 219–228.
[171] Reddy, N.R.S., Van Amerongen, H., Kwa, S.L.S., Van Grondelle, R. and Small, G.J. (1994). J. Phys. Chem. 98, 4729–4735.
[172] Van Metter, R.L. (1977) Biochim. Biophys. Acta 462, 642–658.
[173] Shepansky, J.F. and Knox, R.S. (1981) Isr. J. Chem. 21, 325–331.
[174] Gülen, D. and Knox, R.S. (1984) Photobiochem. Photobiophys. 7, 277–286.
[175] Mullet, J.E. and Arntzen, C.J. (1980) Biochim. Biophys. Acta 589, 100–117.
[176] Horton, P., Ruban, A.V., Rees, D., Pascal, A., Noctor, G.D. and Young, A. (1991) FEBS Lett. 292, 1–4.
[177] Ruban, A.V. and Horton, P. (1992) Biochim. Biophys. Acta 1102, 30–38.
[178] Weis, E. and Berry, J.A. (1987) Biochim. Biophys. Acta 894, 198–208.
[179] Demmig-Adams, B. and Adams, W.W. (1992) Annu. Rev. Plant Physiol. Plant. Mol. Biol. 43, 599–626.
[180] Krieger, A., Moya, I. and Weis, E. (1992) Biochim. Biophys. Acta 1102, 167–176.
[181] Ruban, A.V. and Horton, P. (1993) Biochim. Biophys. Acta 1142, 203–206.
[182] Ide, J.P., Klug, D.R., Kühlbrandt, W., Giorgi, L.B. and Porter, G. (1987) Biochim. Biophys. Acta 893, 349–364.
[183] Gillbro, T., Sandström, Å., Spangfort, M., Sundström, V. and Van Grondelle, R. (1988) Biochim. Biophys. Acta 934, 369–374.
[184] Mullineaux, C.W., Pascal, A.A., Horton, P. and Holzwarth, A.R. (1993) Biochim. Biophys. Acta 1141, 23–28.
[185] Gillbro, T., Sundström, V., Sandström, Å., Spangfort, M. and Andersson, B. (1985) FEBS Lett. 193, 267–270.
[186] Savikhin, S., Van Amerongen, H., Kwa, S.L.S., Van Grondelle, R. and Struve, W.S. (1994) Biophys. J. 66, 1597–1603.
[187] Pålsson, L.O., Spangfort, M.D., Golbings, V. and Gillbro, T. (1994) FEBS Lett. 339, 134–138.
[188] Michel, H. and Deisenhofer, J. (1988) Biochemistry 27, 1–7.
[189] Okamura, M.Y., Satoh, K., Isaacson, R.A. and Feher, G. (1987) in Progress in Photosynthesis Research (Biggins, J., ed.), Vol. I, pp. 379–382, Martinus Nijhoff Publishers, Dordrecht.
[190] Tang, X.-S., Fushimi, K. and Satoh, K. (1990) FEBS Lett. 273, 257–260.
[191] Durrant, J.R., Giorgi, L.B., Barber, J., Klug, D.R. and Porter, G. (1990) Biochim. Biophys. Acta 1017, 167–175.
[192] Seibert, M., Picorel, R., Rubin, A.B. and Connolly, J.S. (1988) Plant Physiol. 87, 303–306.
[193] Chapman, D.J., Gounaris, K. and Barber, J. (1988) Biochim. Biophys. Acta 933, 423–431.
[194] Satoh, K. and Nakane, H. (1990) in Current Research in Photosynthesis (Baltscheffsky, M., ed.), Vol. I, pp. 271–274, Kluwer, Dordrecht.
[195] Van Leeuwen, P.J., Nieveen, M.C., Van de Meent, E.J., Dekker, J.P. and Van Gorkom, H.J. (1991) Photosynth. Res. 28, 149–153.
[196] Ghanotakis, D.F., De Paula, J.C., Demetriou, D.M., Bowlby, N.R., Petersen, J., Babcock, G.T. and Yocum, C.F. (1989) Biochim. Biophys. Acta 974, 44–53.
[197] Kobayashi, M., Maeda, H., Watanabe, T., Nakane, H. and Satoh, K. (1990) FEBS Lett. 260, 138–140.
[198] Gounaris, K., Chapman, D.J., Booth, P., Crystall, B., Giorgi, L.B., Klug, D.R., Porter, G. and Barber, J. (1990) FEBS Lett. 265, 88–92.
[199] Montoya, G., Iruela, I. and Picorel, R. (1991) FEBS Lett. 283, 255–258.
[200] Van Kan, P.J.M., Otte, S.C.M., Kleinherenbrink, F.A.M., Nieveen, M.C., Aartsma, T.J. and Van Gorkom, H.J. (1990) Biochim. Biophys. Acta 1020, 146–152.
[201] Van Leeuwen, P.J. (1993) Doctoral Thesis, University of Leiden, The Netherlands.
[202] Jankowiak, R. and Small, G.J. (1993) in Photosynthetic Reaction Centers (Deisenhofer, J. and Norris, J., eds), Academic Press, New York, in press.
[203] Groot, M.L., Peterman, E.J.G., Van Stokkum, I.H.M., Van Kan, P.J.M., Dekker, J.P. and Van Grondelle, R. (1994) Biophys. J., in press.
[204] Tang, D., Jankowiak, R., Seibert, M., Yocum, C.F. and Small, G.J. (1990) J. Phys. Chem. 94, 6519–6522.
[205] Van der Vos, R., Van Leeuwen, P.J., Braun, P. and Hoff, A.J. (1992) Biochim. Biophys. Acta 1140, 184–198.
[206] Van Dorssen, R.J., Breton, J., Plijter, J.J., Satoh, K., Van Gorkom, H.J. and Amesz, J. (1987) Biochim. Biophys. Acta 893, 267–274.
[207] Breton, J. (1990) in Perspectives in Photosynthesis (Jortner, J. and Pullman, B., eds.), pp. 23–28, Kluwer, Dordrecht.
[208] Kwa, S.L.S., Newell, W.R., Van Grondelle, R. and Dekker, J.P. (1992) Biochim. Biophys. Acta 1099, 193–202.
[209] Otte, S.C.M., Van der Vos, R. and Van Gorkom, H.J. (1990) J. Photochem. Photobiol. B 15, 5–14.
[210] Moënne-Loccoz, P., Robert, B. and Lutz, M. (1989) Biochemistry 28, 3641–3645.
[211] Lubitz, W., Isaacson, R.A., Okamura, M.Y., Abresch, E.C., Plato, M. and Feher, G. (1989) Biochim. Biophys. Acta 977, 227–232.
[212] Nabedryk, E., Andrianambinintsoa, S., Berger, G., Leonhard, M., Mantele, W. and Breton, J. (1990) Biochim. Biophys. Acta 1016, 49–54.
[213] Van Mieghem, F.J.E., Satoh, K. and Rutherford, A.W. (1991) Biochim. Biophys. Acta 1058, 379–385.
[214] Kwa, S.L.S. (1993) Doctoral Thesis, Vrije Universiteit, Amsterdam, The Netherlands.

[215] Schelvis, J.P.M., Van Noort, P.I., Aartsma, T.J. and Van Gorkom, H.J. (1994) Biochim. Biophys. Acta 1184, 242–250.
[216] Kwa, S.L.S., Eijckelhoff, C., Van Grondelle, R. and Dekker, J.P. (1994) J. Phys. Chem., in press.
[217] Noguchi, T., Inoue, Y. and Satoh, K. (1993) Biochemistry 32, 7186–7195.
[218] Van Gorkom, H.J. and Schelvis, J.P.M. (1993) Photosynth. Res. 38, 297–301.
[219] Van Mieghem, F.J.E. (1994) Doctoral Thesis, University of Wageningen, The Netherlands.
[220] Kwa, S.L.S., Tilly, N.T., Eijckelhoff, C., Van Grondelle, R. and Dekker, J.P. (1994) J. Phys. Chem., in press.
[221] Danielius, R.V., Satoh, K., Van Kan, P.J.M., Plijter, J.J., Nuijs, A.M. and Van Gorkom, H.J. (1987) FEBS Lett. 213, 241–244.
[222] Takahashi, Y., Hansson, Ö., Mathis, P. and Satoh, K. (1987) Biochim. Biophys. Acta 893, 49–59.
[223] Mimuro, M., Yamazaki, I., Itoh, S., Tamai, N. and Satoh, K. (1988) Biochim. Biophys. Acta 933, 478–486.
[224] Crystall, B., Booth, P.J., Klug, D.R., Barber, J. and Porter, G. (1989) FEBS Lett. 249, 75–78.
[225] Volk, M., Gilbert, M., Rousseau, G., Richter, M., Ogrodnik, A. and Michel-Beyerle, M.-E. (1993) FEBS Lett. 336, 357–362.
[226] Govindjee, Van de Ven, M., Preston, C., Seibert, M. and Gratton, E. (1990) Biochim. Biophys. Acta 1015, 173–179.
[227] Booth, P.J., Crystall, B., Ahmad, I., Barber, J., Porter, G. and Klug, D.R. (1991) Biochemistry 30, 7573–7586.
[228] Roelofs, T.A., Kwa, S.L.S., Van Grondelle, R., Dekker, J.P. and Holzwarth, A.R. (1993) Biochim. Biophys. Acta 1143, 147–157.
[229] Durrant, J.R., Hastings, G., Hong, Q., Barber, J., Porter, G. and Klug, D.R. (1992) Chem. Phys. Lett. 188, 54–60.
[230] Durrant, J.R., Hastings, G., Joseph, D.M., Barber, J., Porter, G. and Klug, D.R. (1993) Biochemistry 32, 8259–8267.
[231] Wasielewski, M.R., Johnson, D.G., Seibert, M. and Govindjee (1989) Proc. Natl. Acad. Sci. USA 86, 524–528.
[232] Roelofs, T.A., Gilbert, M., Shuvalov, V.A. and Holzwarth, A.R. (1991) Biochim. Biophys. Acta 1060, 237–244.
[233] Hastings, G., Durrant, J.R., Barber, J., Porter, G. and Klug, D.R. (1992) Biochemistry 31, 7638–7647.
[234] Wasielewski, M.R., Johnson, D.G., Govindjee, Preston, C. and Seibert, M. (1989) Photosynth. Res. 22, 89–99.
[235] Jankowiak, R., Tang, D., Small, G.J. and Seibert, M. (1989) J. Phys. Chem. 93, 1649–1654.
[236] Tang, D.M., Jankowiak, R., Seibert, M. and Small, G.J. (1991) Photosynth. Res. 27, 19–29.
[237] Freiberg, A., Timpmann, K., Moskalenko, A.A. and Kuznetsova, N.Yu. (1994) Biochim. Biophys. Acta 1184, 45–53.
[238] Bricker, T.M. (1990) Photosynth. Res. 24, 1–13.
[239] Mörschel, E. and Schatz, G.H. (1987) Planta 172, 145–154.
[240] Rögner, M., Dekker, J.P., Boekema, E.J. and Witt, H.T. (1987) FEBS Lett. 219, 207–211.
[241] Dekker, J.P., Boekema, E.J., Witt, H.T. and Rögner, M. (1988) Biochim. Biophys. Acta 936, 307–318.
[242] Peter, G.F. and Thornber, J.P. (1991) Plant Cell Physiol. 32, 1237–1250.
[243] Bassi, R., Magaldi, A.G., Tognon, G., Giacometti, G.M. and Miller, K.R. (1989) Eur. J. Cell. Biol. 50, 84–93.
[244] Holzenburg, A., Bewley, M.C., Wilson, F.H., Nicholson, W.V. and Ford, R.C. (1993) Nature 363, 470–472.
[245] Boekema, E.J., Hankamer, B., Bald, D., Kruip, J., Nield, J., Boonstra, A.F., Barber, J. and Rögner, M., submitted.
[246] Dekker, J.P., Bowlby, N.R. and Yocum, C.F. (1989) FEBS Lett. 254, 150–154.
[247] Petersen, J., Dekker, J.P., Bowlby, N.R., Ghanotakis, D.F., Yocum, C.F. and Babcock, G.T. (1990) Biochemistry 29, 3226–3231.
[248] Rögner, M., Chisholm, D.A. and Diner, B.A. (1991) Biochemistry 30, 5387–5395.
[249] De las Rivas, J., Crystall, B., Booth, P.J., Durrant, J.R., Özer, S., Porter, G., Klug, D.R. and Barber, J. (1992) Photosynth. Res. 34, 419–431.
[250] Barbato, R., Race, H.L., Friso, G. and Barber, J. (1991) FEBS Lett. 286, 86–90.
[251] Kwa, S.L.S., Van Kan, P.J.M., Groot, M.L., Van Grondelle, R., Yocum, C.F. and Dekker, J.P. (1992) in Research in Photosynthesis (Murata, N., ed.), Vol. I, pp. 263–266, Kluwer, Dordrecht.
[252] Breton, J. and Katoh, S. (1987) Biochim. Biophys. Acta 892, 99–107.
[253] Van Kan, P.J.M., Groot, M.L., Van Stokkum, I.H.M., Kwa, S.L.S., Van Grondelle, R. and Dekker, J.P. (1992) in Research in Photosynthesis (Murata, N., ed.), Vol. I, pp. 271–274, Kluwer Academic Publishers, Dordrecht.
[254] Van Dorssen, R.J., Plijter, J.J., Dekker, J.P., Den Ouden, A., Amesz, J. and Van Gorkom, H.J. (1987) Biochim. Biophys. Acta 890, 134–143.
[255] Kramer, H.J.M. and Amesz, J. (1982) Biochim. Biophys. Acta 682, 201–207.
[256] Tapie, P., Choquet, Y., Wollman, F., Diner, B. and Breton, J. (1986) Biochim. Biophys. Acta 850, 156–161.
[257] Carbonera, D., Giacometti, G., Agostini, G., Angerhofer, A. and Aust, V. (1992) Chem. Phys. Lett. 194, 275–281.
[258] Van Kan, P.J.M., Groot, M.L., Kwa, S.L.S., Dekker, J.P. and Van Grondelle, R. (1992) in The Photosynthetic Bacterial Reaction Centre II (Breton, J. and Verméglio, A., eds.), pp. 411–420, Plenum Press, New York.
[259] Nuijs, A.M., Van Gorkom, H.J., Plijter, J.J. and Duysens, L.N.M. (1986) Biochim. Biophys. Acta 848, 167–175.
[260] Eckert, H.-J., Wiese, N., Bernarding, J., Eichler, H.-J. and Renger, G. (1988) FEBS Lett. 240, 153–158.
[261] Hodges, M. and Moya, I. (1988) Biochim. Biophys. Acta 935, 41–52.
[262] Van Mieghem, F.J.E., Searle, G.F.W., Rutherford, A.W. and Schaafsma, T.J. (1992) Biochim. Biophys. Acta 1100, 198–206.
[263] Leibl, W., Breton. J., Deprez, J. and Trissl, H.-W. (1989) Photosynth. Res. 22, 257–275.
[264] Van Gorkom, H.J. (1985) Photosynth. Res. 6, 97–112.
[265] Schlodder, E. and Brettel, K. (1988) Biochim. Biophys. Acta 933, 22–34.
[266] Berens, S.J., Scheele, J., Butler, W.L. and Madge, D. (1985) Photochem. Photobiol. 42, 51–57.
[267] Berens, S.J., Scheele, J., Butler, W.L. and Madge, D. (1985) Photochem. Photobiol. 42, 59–68.
[268] Hodges, M. and Moya, I. (1986) Biochim. Biophys. Acta 849, 193–202.
[269] Moya, I., Hodges, M., Briantais, J.-M. and Hervo, G. (1986) Photosynth. Res. 10, 319–325.
[270] Hodges, M. and Moya, I. (1987) Biochim. Biophys. Acta 892, 42–47.
[271] Mimuro, M., Tamai, N., Yamazaki, T. and Yamazaki, I. (1987) FEBS Lett. 213, 119–122.
[272] Keuper, H.J.K. and Sauer, K. (1989) Photosynth. Res. 20, 85–103.
[273] Roelofs, T.A. and Holzwarth, A.R. (1990) Biophys. J. 57, 1141–1153.
[274] Vass, I., Gatzen, G. and Holzwarth, A.R. (1993) Biochim. Biophys. Acta 1183, 388–396.
[275] Butler, W.L., Madge, D. and Berens, S.J. (1983) Proc. Natl. Acad. Sci. USA 80, 7510–7514.
[276] Klimov, V.V., Klevanik, A.V., Shuvalov, V.A. and Krasnovsky, A.A. (1977) FEBS Lett. 82, 183–186.

[277] Karukstis, K.K. (1991) in Chlorophylls (Scheer, H., ed.), pp. 95–157, CRC Press, Boca Raton, USA.
[278] Berthold, D.A., Babcock, G.T. and Yocum. C.F. (1981) FEBS Lett. 134, 231–234.
[279] Kuwabara, T. and Murata, N. (1982) Plant Cell Physiol. 23, 533–539.
[280] Melis, A. (1991) Biochim. Biophys. Acta 1058, 87–106.
[281] Trissl, H.-W., Breton, J., Deprez, J. and Leibl, W. (1987) Biochim. Biophys. Acta 893, 305–319.
[282] Spangfort, M. and Andersson, B. (1989) Biochim. Biophys. Acta 977, 163–170.
[283] Du, M., Rosenthal, S.J., Xie, X., DiMagno, T.J., Schmidt, M., Hanson, D.K., Schiffer, M., Norris, J.R. and Fleming, G.R. (1992) Proc. Natl. Acad. Sci. USA 89, 8517–8521.
[284] Gantt, E. (1981) Annu. Rev. Physiol. 32, 327–347.
[285] Glazer, A.N. (1984) Biochim. Biophys. Acta 768, 29–51.
[286] MacColl, R. and Guard-Friar, D. (1987) Phycobiliproteins, CRC Press, Bora Raton, FL.
[287] Glazer, A.N., Lundell, D.J., Yamanaka, G. and Williams, R.E. (1983) Ann. Microbiol. (Inst. Pasteur) 134B, 159–180.
[288] Gantt, E. (1980) Int. Rev. Cytology 66, 45–80.
[289] Scheer, H. (1982) In: Light Reaction Path of Photosynthesis (Fong, F.K., ed.), pp. 7–45, Springer, Berlin.
[290] Grabowski, J. and Gantt E. (1978) Photochem. Photobiol. 28, 47–54.
[291] Holzwarth, A.R. (1987) in The Light Reactions; Topics in Photosynthesis (Barber, J., ed.), pp. 95–157, Elsevier, Amsterdam.
[292] Holzwarth, A.R., Lehner, H., Braslavsky, S.E. and Schaffner, K. (1978) Liebigs. Ann. Chem. 1978, 2002–2017.
[293] Zuber, H. (1985) Photochem. Photobiol. 42, 821–844.
[294] Berns, D.S. and MacColl, R. (1989) Chem. Rev. 89, 807–825.
[295] Porter, G., Tredwell, C.J., Searle, G.F.W. and Barber, J. (1978) Biochim. Biophys. Acta 501, 232–245.
[296] Searle, G.F.W., Barber, J., Porter, G. and Tredwell, C.J. (1978) Biochim. Biophys. Acta 501, 246–256.
[297] Brody, S.S., Porter, G., Tredwell, C.J. and Barber, J. (1981) Photobiochem. Photobiophys. 2, 11–14.
[298] Brody, S.S., Tredwell, C.J. and Barber, J. (1981) Biophys. J. 34, 439–449.
[299] Yamazaki, I., Mimuro, M., Murao, T., Yamazaki, T., Yoshihara, K. and Fujita, Y. (1984) Photochem. Photobiol. 39, 233–240.
[300] Yamanaka, G. and Glazer, A.N. (1981) Arch. Microbiol. 130, 23–30.
[301] Gillbro, T., Sandström, Å., Sundström, V. and Holzwarth, A.R. (1983) FEBS Lett. 162, 64–68.
[302] Gillbro, T., Sandström, Å., Sundström, V., Wendler, J. and Holzwarth, A.R. (1985) Biochim. Biophys. Acta 808, 52–65.
[303] Sandström, Å., Gillbro, T., Sundström, V., Wendler, J. and Holzwarth, A.R. (1988) Biochim. Biophys. Acta 933, 54–64.
[304] Suter, G.W., Mazzola, P., Wendler, J. and Holzwarth, A.R. (1984) Biochim. Biophys. Acta 766, 269–276.
[305] Suter, G.W. and Holzwarth, A.R. (1987) Biophys. J. 52, 673–683.
[306] Bhalevao, R.P., Gillbro, T. and Gustafsson, D. (1991) Biochim. Biophys. Acta 1060, 59–66.
[307] Demidov, A.A. and Borisov, A.Yu. (1993) Biophys. J. 64, 1375–1383.
[308] Lundell, D.J., Williams, R.C. and Glazer, A.N. (1981) J. Biol. Chem. 256, 3580–3592.
[309] Glazer, A.N. and Clark, J.H. (1986) Biophys. J. 49, 115–116.
[310] Glazer, A.N. Yeh, S.W., Webb, S.P. and Clark, J.H. (1985) Science 227, 419–423.
[311] Schirmer, T., Bode, W., Huber, R., Sidler, W. and Zuber, H. (1985) J. Mol. Biol. 184, 257–277.
[312] Schirmer, T., Huber, R., Schneider, M., Bode, W., Miller, M. and Hackert, M.L. (1986) J. Mol. Biol. 188, 651–676.
[313] Duerring, M., Huber, R., Bode, W., Ruembeli, R. and Zuber, H. (1990) J. Mol. Biol. 211, 633–644.
[314] Sidler, W., Gysi, J., Isker, E. and Zuber, H. (1981) Hoppe-Seyler's Z. Physiol. Chem. 362, 611–628.
[315] Frank, G., Sidler, W., Widmer, H. and Zuber, H. (1978) Hoppe-Seyler's Z. Physiol. Chem. 359, 491–507.
[316] Fuglistaller, P., Suter, F. and Zuber, H. (1983) Hoppe-Seyler's Z. Physiol. Chemie 364, 691–712.
[317] Wendler, J., John, W., Scheer, H. and Holzwarth, A.R. (1986) Photochem. Photobiol. 44, 79–85.
[318] Sandström, Å., Gillbro, T., Sundström, V., Fischer, R. and Scheer, H. (1988) Biochim. Biophys. Acta 939, 42–53.
[319] Holzwarth, A.R., Wendler, J. and Suter, G.W. (1987) Biophys. J. 51, 1–12.
[320] Schneider, S., Geiselhout, P., Siebzehnrübl, S., Fischer, R. and Scheer, H.(1988) Z. Naturforsch. 43C, 55–62.
[321] Dale, R.B. and Teale, F.W.J. (1970) Photochem. Photobiol. 12, 99–117.
[322] Sauer, K., Scheer, H. and Sauer, P. (1987) Photochem. Photobiol. 46, 427–440.
[323] Debreczeny, M.P., Sauer, K., Zhou, J. and Bryant, D.A. (1993) J. Phys. Chem. 97, 9852–9862.
[324] Khoroshilov, E.V., Kryukov, I.U., Kryukov, P.G., Sharkov, A.V and Gillbro, T. (1990) Proc. SPIE, Vol. 1403, Laser Applications in Life Sciences, pp. 431–433.
[325] Beck, W.F. and Sauer, K. (1992) J. Phys. Chem. 96, 4658–4666.
[326] Sharkov, A.V., Kryukov, I.V., Khoroshilov, E.V., Kryukov, P.G., Fischer, R., Scheer, H. and Gillbro, T. (1994) Biochim. Biophys. Acta, in press.
[327] Hucke, M., Schweitzer, G., Holzwarth, A.R., Sidler, W. and Zuber, H. (1993) Photochem. Photobiol. 57, 76–80.
[328] Pålsson, L.O., Gillbro, T., Sharkov, A.V., Fischer, R. and Scheer, H. (1993) In: Ultrafast Phenomena III, Springer Series in Chemical Physics 55 (Martin, J.-L., Migus, A., Mourou, G.A. and Zewail, A.H., eds.), pp. 555–556, Springer, Berlin.
[329] Kenkre, V.M. and Knox, R.S.(1974) Phys. Rev. Lett. 93, 803–806.
[330] Knox, R.S. (1977) In: The Intact Chloroplast Vol. 2 (Barber, J. ed.), pp. 55–97, Elsevier Scientific Publ. Comp., Amsterdam.
[331] Csatorday, K., MacColl, R., Csizmadia, V., Grabowski, J. and Bagyinka, C. (1984) Biochemistry 23, 6466–6470.
[332] Canaani, O.D. and Gantt, E. (1980) Biochemistry 19, 2950–2956.
[333] Holzwarth, A.R., Bittersmann, E., Reuter, W. and Wehrmeyer, W. (1990) Biophys. J. 57, 133–145.
[334] Szalontai, B., Gombos, Z., Csizmadia, V. and Lutz, M. (1987) Biochim. Biophys. Acta 893, 296–304.
[335] Szalontai, B., Gombos, Z. and Czismadia, V. (1985) Biochem. Biophys. Res. Commun. 130, 358–363.
[336] Schneider, S., Baumann, F., Klüter, U. and Gege, P. (1988) Croat. Chem. Acta 61, 505–527.
[337] Schneider, S., Prenzel, C.-J., Brehm, G., Gedeck, P., Manthi Sai, P.S., Gottschalk, L. and Scheer, H. (1993) Photochem. Photobiol. 57, 56–62.
[338] Gillbro, T., Sandström, Å., Sundström, V., Fischer, R. and Scheer, H. (1988) In: Photosynthetic Light-Harvesting Systems (Scheer, H. and Schneider, S., eds.), pp. 457–467, Walter de Gruyter & Co., Berlin.
[339] Holzwarth, A.R., Wendler, J. and Wehrmeyer, W. (1983) Biochim. Biophys. Acta 724, 388–395.
[340] Malak, H. and MacColl, R. (1991) Biochim. Biophys. Acta 1059, 165–170.
[341] Malak, H. and MacColl, R. (1991) Photochem. Photobiol. 53, 367–370.

[342] Guard-Friar, D., Hanzlik, C. and MacColl, R. (1989) Biochim. Biophys. Acta 973, 118–123.
[343] Scharnagl, C. and Schneider, S. (1991) J. Photochem. Photobiol. B8, 129–157.
[344] Deisenhofer, J., Epp, O., Miki, K., Huber, R. and Michel, H. (1984) J. Mol. Biol. 180, 385–398.
[345] Allen, J.P., Feher, G., Yeates, T.O., Komiya, H. and Rees, D.C. (1987) Proc. Natl. Acad. Sci. USA 84, 6162–6166.
[346] Yeates, T.O., Komiya, H., Rees, D.C., Allen, J.P. and Feher, G. (1987) Proc. Natl. Acad. Sci. 84, 6438–6442.
[347] Robert, B. and Lutz, M. (1985) Biochim. Biophys. Acta 807, 10–23.
[348] Brunisholz, R.A., Jay, F.A., Suter, F. and Zuber, H. (1985) Biol. Chem. Hoppe-Seyler 366, 87–98.
[349] Aagard, J. and Sistrom, W.R. (1972) Photochem. Photobiol. 15, 209–225.
[350] Dawkins, D.J., Ferguson, L.A. and Cogdell, R.J. (1988) in Photosynthetic Light-Harvesting Systems (Scheer, H. and Schneider, S., eds.), pp. 115–127, Walter de Gruyter, Berlin.
[351] Beekman, L.M.P., Visschers, R.W., Visscher, K.J., Althuis, B., Barz, W., Oesterhelt, D., Sundström, V. and Van Grondelle, R. (1993) in Ultrafast Phenomena VIII. Springer Series in Chemical Physics Vol. 55 (Martin, J.L., Migus, A., Mourou, G. and Zewail, A.H., eds.), pp. 552–554, Springer, Berlin.
[352] Miller, K.R. (1982) Nature 300, 53–55.
[353] Engelhardt, H., Baumeister, W. and Saxton, W.O. (1983) Arch. Microbiol. 135, 169–175.
[354] Stark, W., Kühlbrandt, W., Wildhaber, I., Wehrli, E. and Muhlethaler, K. (1984) EMBO J. 3, 777–783.
[355] Stark, W., Jay, F.A. and Mühlethaler, K. (1986) Arch. Microbiol. 146, 130–133.
[356] Boonstra, A.F., Germeroth, L. and Boekema, E.J. (1994) Biochim. Biophys. Acta, in press.
[357] Meckenstock, R.M., Krusche, K., Brunisholz, R.A. and Zuber, H. (1992) FEBS Lett. 311, 135–138.
[358] Boonstra, A.F., Visschers, R.W., Calkoen, F., Van Grondelle, R., Van Bruggen, E.F.J. and Boekema, E.J. (1993) Biochim. Biophys. Acta 1142, 181–188.
[359] Breton, J. and Verméglio, A. (1982) in Photosynthesis: Energy Conversion by Plants and Bacteria (Govindjee, ed.), Vol. 1, pp. 153–194, Academic Press, New York.
[360] Vredenberg, W. and Duysens, L.N.M. (1963) Nature 197, 355–357.
[361] Clayton, R.K. (1966) Photochem. Photobiol. 5, 807–821.
[362] Kingma, H., Duysens, L.N.M. and Van Grondelle, R. (1983) Biochim. Biophys. Acta 725, 434–443.
[363] Vos, M., Van Grondelle, R., Van der Kooij, F.W., Van de Poll, D., Amesz, J. and Duysens, L.N.M. (1986) Biochim Biophys Acta 850, 501–512.
[364] Vos, M., Van Dorssen, R.J., Amesz, J., Van Grondelle, R. and Hunter, C.N. (1988) Biochim. Biophys. Acta 933, 132–140.
[365] Trissl, H.W., Breton, J., Deprez, J., Dobek, A. and Leibl, W. (1990) Biochim. Biophys. Acta 1015, 322–333.
[366] Deinum, G., Otte, S.C.M., Gardiner, A.T., Aartsma, T.J., Cogdell, R.J. and Amesz, J. (1991) Biochim Biophys Acta 1060, 125–131.
[367] Deinum, G., Aartsma, T.J. and Amesz, J. (1992) in Research in Photosynthesis (Murata, M., ed.), Vol. I, pp. 161–164, Kluwer, Dordrecht.
[368] Van Mourik, F., Visscher, K.J., Mulder, J.M. and Van Grondelle, R. (1993) Photochem. Photobiol. 57, 19–23.
[369] Theiler, R., Suter, F., Wiemken, V. and Zuber, H. (1984) Hoppe-Seyler's Z. Physiol. Chem. 365, 703–719.
[370] Theiler, R. and Zuber, H. (1984) Hoppe-Seyler's Z. Physiol. Chem. 365, 721–729.
[371] Theiler, R., Suter, F., Zuber, H. and Cogdell, R.J. (1984) FEBS Lett. 175, 231–237.
[372] Scherz, A. and Rosenbach-Belkin, V. (1989) Proc. Natl. Acad. Sci. USA 86, 1505–1509.
[373] Scherz, A., Rosenbach-Belkin, V. and Fisher, R.E. (1990) Proc. Natl. Acad. Sci. USA 87, 5430–5434.
[374] Braun, P. and Scherz, A. (1991) Biochemistry 30, 5177–5184.
[375] Loach, P.A., Parkes, P.S., Miller, J.F., Hinchigeri, S.B. and Callahan, P.M. (1985) in Cold Spring Harbor Symposium on Molecular Biology of the Photosynthetic Apparatus (Arntzen, C., Bogorad, L., Bonitz, S. and Steinback, K., eds.), pp. 197–209, Cold Spring Harbor Laboratory, Cold Spring Harbor, NY.
[376] Parkes-Loach, P.S., Sprinkle, J.R. and Loach, P.A. (1988) Biochemistry 27, 2718–2727.
[377] Ghosh, R., Hauser, H. and Bachofen, R. (1988) Biochemistry 27, 1004–1014.
[378] Chang, M.C., Meyer, L. and Loach, P.A. (1990) Photochem. Photobiol. 52, 873–881.
[379] Heller, B.A. and Loach, P.A. (1990) Photochem. Photobiol. 51, 621–627.
[380] Meckenstock, R.M., Brunisholz, R.A. and Zuber, H. (1992) FEBS Lett. 311, 128–134.
[381] Jirsakova, V., Agalidis, I. and Reiss-Husson, F. (1992) in Research in Photosynthesis (Murata, M., ed.), Vol. I, pp. 33–36, Kluwer, Dordrecht.
[382] Hawthornthwaite, A.M. and Cogdell, R.J. (1991) in Chlorophylls (Scheer, H., ed.), pp. 493–528, CRC Press, Boca Raton.
[383] Thornber, J.P., Cogdell, R.J., Pierson, B.K. and Seftor, R.E.B. (1983) J. Cell Biochem. 23, 159–169.
[384] Evans, M.B., Cogdell, R.J. and Britton, G. (1988) Biochim. Biophys. Acta 935, 292–298.
[385] Bolt, J.D. and Sauer, K. (1979) Biochim. Biophys. Acta 546, 54–63.
[386] Breton, J,, Verméglio, A., Garrigos, M. and Paillotin, G. (1981) in Photosynthesis (Akoyunoglou, G., ed.), Vol. 3, pp. 445–459, Balaban International Science Services, Philadelphia.
[387] Van Grondelle, R., Kramer, H.J.M. and Rijgersberg, C.P. (1982) Biochim. Biophys. Acta 682, 208–215.
[388] Kramer, H.J.M., Van Grondelle, R., Hunter, C.N., Westerhuis, W.H J. and Amesz, J. (1984) Biochim. Biophys. Acta 765, 156–165.
[389] Hess, S., Visscher, K., Ulander, J., Pullerits, T., Jones. M.R., Hunter, C.N. and Sundström, V. (1993) Biochemistry 32, 10314–10322.
[390] Hawthornthwaite, A.M., Cogdell, R.J., Woolley, K.J., Wightman, P.A., Ferguson, L.A. and Lindsay, J.G. (1989) J. Mol. Biol. 209, 833–835.
[391] Monger, T.G. and Parson, W.W. (1977) Biochim. Biophys. Acta 460, 393–407.
[392] Deinum, G., Kleinherenbrink, F.A.M., Aartsma, T.J. and Amesz, J. (1992) Biochim. Biophys. Acta 1099, 81–84.
[393] Trüper, H.G. (1968) J. Bacteriol. 95, 1910–1920.
[394] Leguijt, T., Visschers, R.W., Crielaard, W., Van Grondelle, R. and Hellingwerf, K.J. (1992) Biochim Biophys Acta 1102, 177–185.
[395] Garcia, D., Parot, P., Verméglio, A. and Madigan, M.T. (1986) Biochim. Biophys. Acta 850, 390–395.
[396] Bolt, J.D., Hunter, C.N., Niederman, R.A. and Sauer, K. (1981) Photochem. Photobiol. 34, 653–656.
[397] Bolt, J.D. and Sauer, K. (1981) Biochim. Biophys. Acta 637, 342–347.
[398] Kramer, H.J.M., Pennoyer, L., Van Grondelle, R., Westerhuis, W.H.J., Niederman, R.A. and Amesz, J. (1984) Biochim. Biophys. Acta 767, 335–344.
[399] Clayton, R.K. and Clayton, B.J. (1981) Proc. Natl. Acad. Sci. USA 78, 5583–5587.
[400] Chadwick, B.J., Zhang, C., Cogdell, R.J. and Frank, H.A. (1987) Biochim. Biophys. Acta 893, 444–451.

[401] Hayashi, H., Nakano, M. and Morita, S. (1982) J. Biochem. 92, 1805–1811.
[402] Hayashi, H., Nozawa, T., Hatano, M. and Morita, S. (1982) J. Biochem. 91, 1029–1038.
[403] Hayashi, H., Miyao, M. and Morita, S. (1982) J. Biochem. 91, 1016–1027.
[404] Van Mourik, F., Hawthornthwaite, A.M., Vonk, C., Evans, M.B., Cogdell, R.J., Sundström, V. and Van Grondelle, R. (1992) Biochim Biophys Acta 1140, 85–93.
[405] Borisov, A.Y., Gadonas, R.A., Danielius, R.V., Piskarskas, A.S. and Razjivin, A.P. (1982) FEBS Lett 138, 25–28.
[406] Bergström, H., Westerhuis, W.H.J., Sundström, V., Van Grondelle, R., Niederman, R.A. and Gillbro, T. (1988) FEBS Lett. 233, 12–16.
[407] Shimada, K., Mimuro, M., Tamai, N. and Yamazaki, I. (1989) Biochim. Biophys. Acta 975, 72–79.
[408] Hunter, C.N., Bergström, H., Van Grondelle, R. and Sundström, V. (1990) Biochemistry 29, 3203–3207.
[409] Reddy, N.R.S., Picorel, R. and Small, G.J. (1992) J. Phys. Chem. 96, 6458–6464.
[410] Van Dorssen, R.J., Hunter, C.N., Van Grondelle, R., Korenhof, A.H. and Amesz, J. (1988) Biochim. Biophys. Acta 932, 179–188.
[411] Van Mourik, F., Visschers, R.W. and Van Grondelle, R. (1992) Chem. Phys. Lett. 193, 1–7.
[412] Reddy, N.R.S., Small, G.J., Seibert, M. and Picorel, R. (1991) Chem. Phys. Lett. 181, 391–399.
[413] Reddy, N.R.S., Cogdell, R.J., Zhao, L. and Small, G.J. (1992) Photochem. Photobiol. 57, 35–39.
[414] Breton, J., Farkas, D.L. and Parson, W.W. (1985) Biochim. Biophys. Acta 808, 421–427.
[415] Deinum, G. (1991) Ph.D. Thesis, State University of Leiden.
[416] Monshouwer, R., Visschers, R.W., Van Mourik, F., Freiberg, A. and Van Grondelle, R., submitted.
[417] Johnson, S.G. and Small, G.J. (1989) Chem. Phys. Lett. 155, 371–375.
[418] Van der Laan, H., De Caro, C., Schmidt, Th., Visschers, R.W., Van Grondelle, R., Fowler, G.J.S., Hunter, C.N. and Völker, S. (1993) Chem. Phys. Lett. 212, 569–580.
[419] De Caro, C., Visschers, R.W., Van Grondelle, R. and Völker, S. (1994) J. Luminescence 58, 149–153.
[420] Gottfried, D.S., Stocker, J.W. and Boxer, S.G. (1991) Biochim. Biophys. Acta 1059, 63–75.
[421] Lockhart, D.J. and Boxer, S.G. (1988) Proc. Natl. Acad. Sci. USA 85, 107–111.
[422] Visschers, R.W., Nunn, R., Calkoen, F., Van Mourik, F., Hunter, C.N., Rice, D.W. and Van Grondelle, R. (1992) Biochim. Biophys. Acta 1100, 259–266.
[423] Visschers, R.W., Chang, M.C., Van Mourik, F., Parkes-Loach, P.S., Heller, B.A., Loach, P.A. and Van Grondelle, R. (1991) Biochemistry 27, 1004–1014.
[424] Van Mourik, F., Corten, E.P.M., Van Stokkum, I.H.M., Visschers, R.W., Loach, P.A., Kraayenhof, R. and Van Grondelle, R. (1992) in Research in Photosynthesis (Murata, M., ed.), Vol. I, pp. 101–104, Kluwer, Dordrecht.
[425] Scherz, A. and Parson, W.W. (1984) Biochim. Biophys. Acta 766, 666–678.
[426] Scherz, A. and Parson, W.W. (1986) Photosynth. Res. 9, 21–32.
[427] Breton, J. (1985) Biochim. Biophys. Acta 810, 235–245.
[428] Picorel, R., L'Ecuyer, A., Potier, M. and Gingras, G. (1986) J. Biol. Chem. 261, 3020–3024.
[429] Gingras, G. and Picorel, R. (1990) Proc. Natl. Acad. Sci. USA 87, 3405–3409.
[430] Fowler, G.J.S., Hunter, C.N. and Robert, B. (1993) Proc. Natl. Acad. Sci. USA, submitted.
[431] Davis, R.C., Ditson, S.L., Fentiman, A.F. and Pearlstein, R.M. (1981) J. Am. Chem. Soc. 103, 6823–6826.
[432] Eccles, J. and Honig, B. (1983) Proc. Natl. Acad. Sci. USA 80, 4959–4962.
[433] Gudowska-Nowak, E., Newton, M.D. and Fajer, J. (1991) J. Phys. Chem. 94, 5795–5801.
[434] Altmann, R.B., Renge, I., Kador, L. and Haarer, D. (1992) J. Chem. Phys. 97, 5316–5322.
[435] Van Grondelle, R., Hunter, C.N., Bakker, J.G.C. and Kramer, H.J.M. (1983) Biochim. Biophys. Acta 723, 30–36.
[436] Nuijs, A.M., Van Grondelle, R., Joppe, H.L.P., Van Bochove, A.C. and Duysens, L.N.M. (1985) Biochim. Biophys. Acta 810, 94–105.
[437] Nuijs, A.M., Van Grondelle, R., Joppe H.L.P., Van Bochove, A.C. and Duysens, L.N.M. (1986) Biochim. Biophys. Acta 850, 286–293.
[438] Freiberg, A., Godik, V.I. and Timpmann, K. (1984) in Progress in Photosynthesis Research (Sybesma, C., ed.), Vol. I, pp. 45–48, Martinus Nijhoff/ Dr W Junk Publishers, Dordrecht.
[439] Borisov, A.Y., Freiberg, A., Godik, V., Rebane, K.K. and Timpmann, K.E. (1985) Biochim Biophys Acta 807, 221–229.
[440] Freiberg, A., Godik, V.I. and Timpmann, K. (1987) in Progress in Photosynthesis Research (Biggins, J., ed.), Vol. I, pp. 45–48, Martinus Nijhoff Publishers, Dordrecht.
[441] Freiberg, A., Godik, V.I., Pullerits, T. and Timpmann, K. (1990) in Current Research in Photosynthesis (Baltscheffsky, M., ed.), Vol. II, pp. 157–160, Kluwer, Dordrecht.
[442] Valkunas, L., Liuolia, V. and Freiberg, A. (1991) Photosynth Res 27, 83–95.
[443] Bergström, H., Van Grondelle, R. and Sundström, V. (1989) FEBS Lett. 250, 503–508.
[444] Visscher, K.J., Sundström, V., Bergström, H. and Van Grondelle, R. (1989) Photosynth. Res. 22, 211–217.
[445] Rijgersberg, C.P., Van Grondelle, R. and Amesz, J. (1980) Biochim. Biophys. Acta 592, 53–64.
[446] Van Grondelle, R., Bergström, H., Sundström, V. and Gillbro, T. (1987) Biochim. Biophys. Acta 894, 313–326.
[447] Freiberg, A., Pullerits, T. and Timpmann, K. (1988) in Ultrafast Phenomena VI (Yayima, T., Yoshihara, K., Harris, C.B. and Shionoya, S., eds.), pp. 593–595, Springer, Berlin.
[448] Freiberg, A., Godik, V.I., Pullerits, T. and Timpmann, K (1988) Chem. Phys. 128, 227–235.
[449] Valkunas, L., Van Mourik, F. and Van Grondelle, R. (1992) J. Photochem. Photobiol. 15, 159–170.
[450] Bergström, H., Sundström, V., Van Grondelle, R., Gillbro, T. and Cogdell, R.J. (1988) Biochim. Biophys. Acta 936, 90–98.
[451] Bradforth, S., Jimenez, R., Fidler, V., Fleming, G., Nagarajan, S., Norris, J., Van Mourik, F. and Van Grondelle, R. (1994) in Abstracts for the Ultrafast Phenomena Meeting, Dana Point, CA.
[452] Duysens, L.N.M. (1979) in Chlorophyll Organization and Energy Transfer in Photosynthesis, CIBA Foundation Symposium 61 (new series), pp. 323–340, Elsevier, Amsterdam.
[453] Olson, J.M. and Clayton, R.K. (1966) Photochem. Photobiol. 5, 665–660.
[454] Finkele, U., Lauterwasser, C., Zinth, W., Gray, K.A. and Oesterhelt, D. (1990) Biochemistry 29, 8517–8521.
[455] Du, M., Rosenthal, S.J., Xie, X., DiMagno, T.J., Schmidt, M., Hanson, D.K., Schiffer, M., Norris, J.R. and Fleming, G.R. (1992). Proc. Natl. Acad. Sci. USA 89, 8517–8521.
[456] Deprez, J., Trissl, H.W. and Breton, J. (1986) Proc. Natl. Acad. Sci. USA 83, 1699–1703.
[457] Bittersmann, E., Blankenship, R.E. and Woodbury, N. (1990) in Current Research in Photosynthesis (Baltscheffsky, M., ed.), Vol. II, pp. 169–172, Kluwer, Dordrecht.
[458] Zhang, F.G., Gillbro, T., Van Grondelle, R. and Sundström, V. (1992) Biophys. J. 61, 694–703.
[459] Kleinherenbrink, F.A.M., Deinum, G., Otte, S.C.M., Hoff, A.J. and Amesz, J. (1992) Biochim. Biophys. Acta 1099, 175–181.

[460] Kleinherenbrink, F.A.M., Cheng, P., Amesz, J. and Blankenship, R.E. (1993) Photochem. Photobiol. 57, 13–16.
[461] Pearlstein, R.M. (1992) J. Luminescence 51, 139–147.
[462] Van Grondelle, R., Bergström, H., Sundström, V., Van Dorssen, R.J., Vos, M. and Hunter, C.N. (1988) in Photosynthetic Light-Harvesting Systems (Scheer, H. and Schneider, S., eds.), pp. 519–530, Walter de Gruyter, Berlin.
[463] Freiberg, A., Godik, V.I., Pullerits, T. and Timpmann, K.E. (1989) Biochim. Biophys. Acta 973, 93–104.
[464] Zhang, F.G., Van Grondelle, R. and Sundström, V. (1992) Biophys. J. 61, 911–920.
[465] Müller, M.G., Drews, G. and Holzwarth, A.R. (1993) Biochim. Biophys. Acta 1142, 49–58.
[466] Shimada, K., Yamazaki, I., Tamai, N. and Mimuro, M. (1990) Biochim. Biophys. Acta 1016, 266–271.
[467] Shimada, K., Hirota, M., Nishimura, Y., Yamazaki, I. and Mimuro, M. (1992) in Research in Photosynthesis (Murata, M., ed.), Vol. I, pp. 137–140, Kluwer, Dordrecht.
[468] Westerhuis, W.H.J., Vos, M., Van Dorssen, R.J., Van Grondelle, R., Amesz, J. and Niederman, R.A. (1987) in Progress in Photosynthesis Research (Biggins, J., ed.), Vol. I, pp. 29–32, Martinus Nijhoff Publishers, Dordrecht.
[469] Hunter, C.N., Pennoyer, J.D., Sturgis, J.N., Farrelly, D. and Niederman, R.A. (1988) Biochemistry 27, 3459–3467.
[470] Westerhuis, W.H.J., Xiao, Z. and Niederman, R.A. (1992) in Research in Photosynthesis (Murata, M., ed.), Vol. I, pp. 37–40, Kluwer, Dordrecht.
[471] Sebban, P., Robert, B. and Jolchine, G. (1985) Photochem. Photobiol. 42, 573–578.
[472] Hess, S., Feldshtein, F., Babin, A., Nurgaleev, I., Pullerits, T., Sergeev, A. and Sundström, V. (1994) Chem. Phys. Lett., in press.
[473] Freiberg, A. and Timpmann, K. (1992) J. Photochem. Photobiol. B 15, 156–172.
[474] Trautman, J.K., Shreve, A.P., Violette, C.A., Frank, H.A., Owens, T.G. and Albrecht, A.C. (1990) Proc. Natl. Acad. Sci. USA 87, 215–219.
[475] Amesz, J. (1991) in Variations in Autotrophic Life (Shively, J.M. and Barton, L.L., eds.), pp. 99–119, Academic Press, London.
[476] Blankenship, R.E., Cheng, P., Causgrove, T.P., Brune, D.C., Wang, S.H.H., Choh, J.U. and Wang, J. (1993) Photochem. Photobiol. 57, 103–107.
[477] Olson, J.M. (1980) Biochim. Biophys. Acta 594, 33–51.
[478] Fenna, R.E. and Matthews, B.W. (1975) Nature 258, 573–577.
[479] Matthews, B.W., Fenna, R.E., Bolognesi, M.C., Schmid, M.F. and Olson, J.M. (1979) J. Mol. Biol. 131, 259–285.
[480] Tronrud, D.E., Schmid, M.F. and Olson, J.M. (1986) J. Mol. Biol. 188, 443–454.
[481] Pearlstein, R.M. and Hemenger, R.P. (1978) Proc. Natl. Acad. Sci. USA 75, 4920–4924.
[482] Pearlstein, R.M. (1988) in Photosynthetic Light-Harvesting Systems (Scheer, H. and Schneider, S., eds.), pp. 555–566, Walter de Gruyter, Berlin.
[483] Barkigia, K.M., Chantranupong, L., Smith, K.M. and Fajer, J. (1988) J. Am. Chem. Soc. 110, 7566.
[484] Matthews, B.W. and Fenna, R.E. (1980) Acc. Chem. Res. 13, 390–403.
[485] Van Mourik, F., Verwijst, R.R., Mulder, J.M. and Van Grondelle, R. (1994) J. Phys. Chem., in press.
[486] Gillbro, T., Sandström, Å., Sundström, V. and Olson, J.M. (1988) in Green Photosynthetic Bacteria (Olson, J.M., Ormerod, J.G., Amesz, J., Stackebrandt, E. and Trüper, H.G., eds.), pp. 91–96, Plenum Press, New York.
[487] Lyle, P.A. and Struve, W.S. (1990) J. Phys. Chem. 94, 7338–7339.
[488] Van Amerongen, H. and Struve, W.S. (1991) J. Phys. Chem. 95, 9020–9023.
[489] Savikhin, S., Zhou, W., Blankenship, R.E. and Struve, W.S. (1994) Biophys. J. 66, 110–114.
[490] Causgrove, T., Yang, S. and Struve, W.S. (1988) J. Phys. Chem. 92, 6790–6795.
[491] Pierson, B.K. and Castenholz, R.W. (1978) in The Photosynthetic Bacteria (Clayton, R.K. and Sistrom, W.R., eds.), pp. 179–197, Plenum Press, New York.
[492] Staehelin, L.A., Golecki, J.R., Fuller, R.C. and Drews, G. (1978) Arch. Microbiol. 119, 269–277.
[493] Blankenship, R.E. and Fuller, R.C. (1986) in Encyclopedia of Plant Physiology (Staehelin, L.A. and Arntzen, C.J., eds.), pp. 390–399, Springer, Berlin.
[494] Amesz, J. (1990) in Current Research in Photosynthesis (Baltscheffsky, M., ed.), Vol. II, pp. 25–31, Kluwer, Dordrecht.
[495] Blankenship, R.E., Wang, J., Causgrove, T.P. and Brune, D.C. (1990) in Current Research in Photosynthesis (Baltscheffsky, M., ed.), Vol. II, pp. 17–24, Kluwer, Dordrecht.
[496] Betti, J.A., Blankenship, R.E., Natarajan, L.V., Dickinson, L.C. and Fuller, R.C. (1982) Biochim Biophys Acta 680, 194–201.
[497] Van Dorssen, R.J., Vasmel, H. and Amesz, J. (1986) Photosynth. Res. 9, 33–45.
[498] Van Amerongen, H., Vasmel, H. and Van Grondelle, R. (1988) Biophys. J. 54, 65–76.
[499] Griebenow, K., Holzwarth, A.R., Van Mourik, F. and Van Grondelle, R. (1991) Biochim. Biophys. Acta 1058, 194–202.
[500] Van Amerongen, H., Van Haeringen, B., Van Gurp, M. and Van Grondelle, R. (1991) Biophys. J. 59, 992–1001.
[501] Matsuura, K., Hirota, M., Shimada, K. and Mimuro, M. (1993) Photochem. Photobiol. 57, 92–98.
[502] Van Dorssen, R.J., Gerola, P.D., Olson, J.M. and Amesz, J. (1986) Biochim. Biophys. Acta 848, 77–82.
[503] Fetisova, Z.G., Khardenko, S.G. and Abdourakhmanov, I.A. (1986) FEBS Lett. 199, 234–236.
[504] Otte, S.C.M., Van der Heiden, J.C., Pfennig, N. and Amesz, J. (1991) Photosynth. Res 28, 77–87.
[505] Fetisova, Z.G., Freiberg, A.M. and Timpmann, K.E. (1988) Nature 334, 633–634.
[506] Wechsler, T., Suter, F., Fuller, R.C. and Zuber, H. (1985) FEBS Lett. 181, 173–178.
[507] Feick, R.G., Fitzpatrick, M. and Fuller, R.C. (1982) J. Bact. 150, 905–915.
[508] Feick, R.G. and Fuller, R.C. (1984) Biochemistry 23, 3693–3700.
[509] Wagner-Huber, R., Fischer, U., Brunisholz, R., Rümbeli, M., Frank, G. and Zuber, H. (1990) Z. Naturforsch. 45c, 818–822.
[510] Gerola, P., Højrup, P. and Olson, J.M. (1988) in Photosynthetic Light-Harvesting Systems (Scheer, H. and Schneider, S., eds.), pp. 129–139, Walter de Gruyter, Berlin.
[511] Gerola, P., Højrup, P., Knudsen, J., Roepstorff, P. and Olson, J.M. (1988) in Green Photosynthetic Bacteria (Olson, J.M., Ormerod, J.G., Amesz, J., Stackebrandt, E. and Trüper, H.G., eds.), pp. 43–52, Plenum, New York.
[512] Wagner-Huber, R., Fischer, U., Brunisholz, R., Frank, G. and Zuber, H. (1988) FEBS Lett 239, 8–12.
[513] Griebenow, K., Holzwarth, A.R. and Schaffner, K. (1990) Z. Naturforsch. 45c, 12–18.
[514] Wullink, W., Knudsen, J., Olson, J.M., Redlinger, T.E. and Van Bruggen, E.F.J. (1991) Biochim. Biophys. Acta 1060, 97–105.
[515] Blankenship, R.E., Brune, D.C. and Wittmershaus, B.P. (1988) in Light Energy Transduction in Photosynthesis: Higher Plant and Bacterial Models (Stevens, S.E. Jr. and Bryant, D.A., eds.), pp. 32–64, American Society of Plant Physiologists.

[516] Brune, D.C., King, G.H. and Blankenship, R.E. (1988) in Photosynthetic Light-Harvesting Systems (Scheer, H. and Schneider, S., eds.), pp. 141–151, Walter de Gruyter, Berlin.
[517] Holzwarth, A.R., Griebenow, K. and Schaffner, K. (1992) J. Photochem. Photobiol. A 65, 61–71.
[518] Bystrova, M.I., Mal'gosheva, I.N. and Krasnovsky, A.A. (1979) Mol. Biol. 13, 582–594.
[519] Krasnovsky, A.A. and Bystrova, M.I. (1980) BioSystems 12, 181–194.
[520] Smith, K.M., Kehres, L.A. and Fajer, J. (1983) J. Am. Chem. Soc. 105, 1387–1389.
[521] Brune, D.C., Nozawa, T. and Blankenship, R.E. (1987) Biochemistry 26, 8644–8652.
[522] Hirota, M., Tsuji, K., Shimada, K. and Matsuura, K. (1992) in Research in Photosynthesis (Murata, M., ed.), Vol. I, pp. 81–84, Kluwer, Dordrecht.
[523] Hirota, M., Moriyama, T., Shimada, K., Miller, M., Olson, J.M. and Matsuura, K. (1992) Biochim Biophys Acta 1099, 271–274.
[524] Griebenow, K. and Holzwarth, A.R. (1989) Biochim. Biophys. Acta 973, 235–240.
[525] Holzwarth, A.R., Griebenow, K. and Schaffner, K. (1990) Z. Naturforsch. 45c, 203–209.
[526] Hildebrandt, P., Griebenow, K., Holzwarth, A.R. and Schaffner, K. (1991) Z. Naturforsch. 46c, 228–232.
[527] Matsuura, K. and Olson, J.M. (1990) Biochim. Biophys. Acta 1019, 233–238.
[528] Mimuro, M., Hirota, H., Shimada, K., Nishimura, Y., Yamazaki, I. and Matsuura, K. (1992) in Research in Photosynthesis (Murata, M., ed.), Vol. I, pp. 17–24, Kluwer, Dordrecht.
[529] Niedermeier, G., Scheer, H. and Feick, R.G. (1992) Eur. J. Biochem. 204, 685–692.
[530] Olson, J.M., Ormerod,.J.G, Amesz, J., Stackebrandt, E. and Trüper, H.G. (eds.) Plenum Press, New York.
[531] Lutz, M. and Van Brakel, G. (1988) in Green Photosynthetic Bacteria (Olson, J.M., Ormerod, J.G., Amesz, J., Stackebrandt, E. and Trüper, H.G., eds.), pp. 23–34, Plenum, New York.
[532] Nozawa et al. (1990) J. Biochem. 108, 737–740.
[533] Worcester, D.L., Michalski, T.J. and Katz, J.J. (1986) Proc. Natl. Acad. Sci. USA 83, 3791–3795.
[534] Olson, J.M., Brune, D.C. and Gerola, P.D. (1990) in Molecular Biology of Membrane-Bound Complexes in Photosynthetic Bacteria (Drews, G. and Dawes, E.A., eds.), pp. 227–234, Plenum, New York.
[535] Brune, D.C., Gerola, P.D. and Olson, J.M. (1990) Photosynth. Res. 24, 253–263.
[536] Van Mourik, F., Griebenow, K., Van Haeringen, B., Holzwarth, A.R. and Van Grondelle, R. (1990) in Current Research in Photosynthesis (Baltscheffsky, M., ed.), Vol. II, pp. 141–144, Kluwer, Dordrecht.
[537] Fetisova, Z.G. and Mauring, K. (1992) FEBS Lett. 307, 371–374.
[538] Fetisova, Z.G. and Mauring, K. (1993) FEBS Lett. 323, 159–162.
[539] Gerola, P.D. and Olson, J.M. (1986) Biochim. Biophys. Acta 848, 69–76.
[540] Van Dorssen, R.J., Vos, M. and Amesz, J. (1988) in Photosynthetic Light-Harvesting Systems (Scheer, H. and Schneider, S., eds.), pp. 531–542, Walter de Gruyter, Berlin.
[541] Mimuro, M., Nozawa, T., Tamai, N., Shimada, K., Yamazaki, I., Lin, S., Knox, R.S., Wittmershaus, B.P., Brune, D.C. and Blankenship, R.E. (1989) J. Phys. Chem. 93, 7503–7509.
[542] Causgrove, T.P., Brune, D.C., Wang, J., Wittmershaus, B.P. and Blankenship, R.E. (1990) Photosynth. Res. 26, 39–48.
[543] Causgrove, T.P., Brune, D.C. and Blankenship, R.E. (1992) J. Photochem. Photobiol. B 15, 171–179.
[544] Miller, M., Cox, R.P. and Gillbro, T. (1991) Biochim. Biophys. Acta 1057, 187–194.
[545] Brune, D.C., King, G.H., Infosino, A., Steiner, T., Thewalt, M.L. and Blankenship, R.E. (1987) Biochemistry 26, 8652–8658.
[546] Freiberg, A.M., Timpmann, K.E. and Fetisova, Z.G. (1988) in Green Photosynthetic Bacteria (Olson, J.M., Ormerod, J.G., Amesz, J., Stackebrandt, E. and Trüper, H.G., eds.), pp. 81–90, Plenum, New York.
[547] Vos, M., Nuijs, A.M., Van Grondelle, R., Van Dorssen, R.J., Gerola, P.D. and Amesz, J. (1987) Biochim. Biophys. Acta 891, 275–285.
[548] Pierson, B.K. and Thornber, J.P. (1983) Proc. Natl. Acad. Sci. USA 80, 80–83.
[549] Vasmel, H., Van Dorssen, R.J., De Vos, G.J. and Amesz, J. (1986) Photosynth. Res. 7, 281–294.
[550] Becker, M., Nagarajan, V., Middendorf, D., Parson, W.W., Martin, J.E. and Blankenship, R.E. (1991) Biochim. Biophys. Acta 1057, 299–312.
[551] Müller, M.G., Griebenow, K. and Holzwarth, A.R. (1991) Biochim. Biophys. Acta 1098, 1–12.
[552] Müller, M.G., Griebenow, K. and Holzwarth, A.R. (1990) in Current Research in Photosynthesis (Baltscheffsky, M., ed.), Vol. II, pp. 177–180, Kluwer, Dordrecht.
[553] Griebenow, K., Müller, M.G. and Holzwarth, A.R. (1991) Biochim. Biophys. Acta 1059, 226–232.
[554] Nuijs, A.M., Vasmel, H., Duysens, L.N.M. and Amesz, J. (1986) Biochim. Biophys. Acta 849, 316–324.
[555] Nitschke, W., Feiler, U. and Rutherford, A.W. (1990) Biochemistry 29, 3834–3842.
[556] Buttner, M., Xie, D.L., Nelson, H., Pinther, W., Hauska, G. and Nelson, N. (1992) Biochim. Biophys. Acta 1101, 154–156.
[557] Swarthoff, T. and Amesz, J. (1979) Biochim. Biophys. Acta 548, 427–432.
[558] Vasmel, H., den Blanken, H.J., Dijkman, J.T., Hoff, A.J. and Amesz, J. (1984) Biochim. Biophys. Acta 767, 200–208.
[559] Oh-oka, H., Kakitani, S., Itoh, S., Matsubara, H. and Malkin, R. (1992) in Research in Photosynthesis (Murata, M., ed.), Vol. I, pp. 385–388, Kluwer, Dordrecht.
[560] Kusumoto, N., Inoue, K., Nasu, H., Takano, H. and Sakurai, H. (1992) in Research in Photosynthesis (Murata, M., ed.), Vol. I, pp. 389–392, Kluwer, Dordrecht.
[561] Van de Meent, E.J., Kobayashi, M., Erkelens, C., Van Veelen, P.A., Otte, S.C.M. and Amesz, J. (1992) Biochim Biophys Acta 1102, 371–378.
[562] Buttner, M., Xie, D.L., Nelson, H., Pinther, W., Hauska, G. and Nelson, N. (1992) Proc. Natl. Acad. Sci. USA 89, 8135–8139.
[563] Xie, D.L., Büttner, M., Nelson, H., Chitnis, P., Pinther, W., Hauska, G. and Nelson, N. (1992) in Research in Photosynthesis (Murata, M., ed.), Vol. I, pp. 513–520, Kluwer, Dordrecht.
[564] Trost, J.T., Brune, D.C. and Blankenship, R.E. (1992) Photosynth. Res. 32, 11–22.
[565] Nitschke, W. and Rutherford, A.W. (1991) Trends Biochem. Sci. 16, 241–245.
[566] Liebl, U., Mockensturm-Wilson, M., Trost, J.T., Brune, D.C., Blankenship, R.E. and Vermaas, W.F.J. (1993) Proc. Natl. Acad. Sci. USA 90, 7124–7128.
[567] Wang, J., Brune, D.C. and Blankenship, R.E. (1990) Biochim. Biophys. Acta 1015, 457–463.
[568] Wittmershaus, B.P., Brune, D.C. and Blankenship, R.E. (1988) in Photosynthetic Light-Harvesting Systems (Scheer, H. and Schneider, S., eds.), pp. 543–554, Walter de Gruyter, Berlin.
[569] Van Dorssen, R.J. and Amesz, J. (1988) Photosynth. Res. 15, 177–189.
[570] Cheng, P. and Blankenship, R.E. (1992) in Research in Photo-

synthesis (Murata, M., ed.), Vol. I, pp. 121–124, Kluwer, Dordrecht.
[571] Fetisova, Z.G. and Borisov, A.Y. (1980) FEBS Lett. 114, 323–326.
[572] Fetisova, Z.G., Freiberg, A.M. and Timpmann, K.E. (1987) FEBS Lett. 223, 161–164.
[573] Van Kan, P.J.M. (1991) Doctoral Thesis, State University of Leiden.
[574] Gest, H. and Favinger, J.L. (1983) Arch. Microbiol. 136, 11–16.
[575] Miller, K.R., Jacob, J.S., Smith, U., Kolaczkowski, S. and Bowman, M.K. (1986) Arch. Microbiol. 146, 111–114.
[576] Beer-Romero, P. and Gest, H. (1987) FEMS Microbiol. Lett. 41, 109–114.
[577] Brockmann, H. Jr. and Lipinski, A. (1983) Arch. Microbiol. 136, 17–19.
[578] Van Dorssen, R.J., Vasmel, H. and Amesz, J. (1985) Biochim. Biophys. Acta 809, 199–203.
[579] Van Kan, P.J.M., Aartsma. T.J. and Amesz, J. (1989) Photosynth. Res. 22, 61–68.
[580] Smit, H.W.J., Van Dorssen, R.J. and Amesz, J. (1989) Biochim. Biophys. Acta 973, 212–219.
[581] Kobayashi, M., Van de Meent, E.J., Erkelens, C., Amesz, J., Ikegami, I. and Watanabe, T. (1991) Biochim. Biophys. Acta 1057, 89–96.
[582] Van de Meent, E.J., Kobayashi, M., Erkelens, C., Van Veelen, P.A., Amesz, J. and Watanabe, T. (1991) Biochim. Biophys. Acta 1058, 356–362.
[583] Hiraishi, A. (1989) Arch. Microbiol. 151, 378–379.
[584] Nitschke, W., Sétif, P., Liebl, U., Feiler, U. and Rutherford, A.W. (1990) Biochemistry 29, 11079–11088.
[585] Nuijs, A.M., Van Dorssen, R.J., Duysens, L.N.M. and Amesz, J. (1985) Proc. Natl. Acad. Sci. USA 82, 6865–6868.
[586] Lin, S., Chiou, H.-C. and Blankenship, R.E. (1992) in Research in Photosynthesis (Murata, M., ed.), Vol. I, pp. 417–420, Kluwer, Dordrecht.
[587] Lin, S., Chiou, H.-C., Kleinherenbrink, F.A.M. and Blankenship, R.E. (1994) Biophys. J. 66, 437–445.
[588] Van Noort, P.I., Gormin, D.A., Aartsma, T.J. and Amesz, J. (1992) Biochim. Biophys. Acta 1140, 15–21.
[589] Van Noort, P.I., Aartsma, T.J. and Amesz, J. (1992) in Research in Photosynthesis (Murata, M., ed.), Vol. I, pp. 105–108, Kluwer, Dordrecht.
[590] Van Kan, P.J.M. and Amesz, J. (1993) in Ultrafast Processes in Spectroscopy (Laubereau, A. and Seilmeier, A., eds.), pp. 627–630, IOP Publishing, Bristol.
[591] Vos, M.H., Klaassen, H.E. and Van Gorkom, H.J. (1989) Biochim. Biophys. Acta 973, 163–169.
[592] Krinsky, N.I. (1979) Pure Appl. Chem. 51, 649–660.
[593] Siefermann-Harms, D. (1985) Biochim. Biophys. Acta 811, 325–355.
[594] Cogdell, R.J. and Frank, H.A. (1987) Biochim. Biophys. Acta 895, 63–79.
[595] Hudson, B.S., Kohler, B.E. and Schulten, K. (1982) in Excited States (Lim, E.C., ed.), Vol. 6, pp 22–95, Academic Press, New York.
[596] Hudson, B.S. and Kohler, B.E. (1972) Chem. Phys. Lett. 14, 299–304.
[597] Schulten, K. and Karplus, M. (1972) Chem. Phys. Lett 15, 305–309.
[598] Wylie, I.W. and Koningstein, J.A. (1984) J. Phys. Chem. 88, 2950–2953.
[599] Watanabe, J., Kinoshita, S. and Kushida, T. (1986) Chem. Phys. Lett. 126, 197–200.
[600] Bondarev, S.L., Bachilo, S.M., Dvornikov, S.S. and Tikhomirov, S.A. (1989) J. Photochem. Photobiol. A 46, 315–322.
[601] Gillbro, T. and Cogdell, R.J. (1989) Chem. Phys. Lett 158, 312–316.
[602] Cogdell, R.J., Andersson, P.-O. and Gillbro, T. (1992) J. Photochem. Photobiol. B 15, 105–112.
[603] Shreve, A.P., Trautman, J.K., Owens, T.G. and Albrecht, A.C. (1991) Chem. Phys. Lett 178, 89–96.
[604] Mimuro, M., Nishimura, Y., Yamazaki, I., Katoh, T. and Nagashima, U. (1991) J. Luminescence 50, 1–10.
[605] Trautman, J.K., Shreve, A.P., Owens, T.G. and Albrecht, A.C. (1990) Chem. Phys. Lett 166, 369–374.
[606] Gillbro, T., Andersson, P.-O., Lin, R.S.H., Asato, A.E. and Cogdell, R.J. (1993) in Frontiers of Photobiology (Shima, A., Ichahashi, M., Fujiwara, Y. and Takebe, H., eds.), pp. 25–30, Elsevier, Amsterdam.
[607] Andersson, P.-O., Gillbro, T., Ferguson, L. and Cogdell, R.J. (1991) Photochem. Photobiol. 54, 353–360.
[608] Shreve, A.P., Trautman, J.K., Owens, T.G. and Albrecht, A.C. (1990) Chem. Phys. Lett. 170, 51–56.
[609] Van Beek, J.B., Kajzar, F. and Albrecht, A.C. (1991) J. Chem. Phys. 95, 6400–6412.
[610] Van Beek, J.B., Kajzar, F. and Albrecht, A.C. (1992) Chem. Phys. 16, 299–311.
[611] Van Beek, J.B. and Albrecht, A.C. (1991) Chem. Phys. Lett. 187, 267–276.
[612] Owens, T.G., Shreve, A.P. and Albrecht, A.C. (1992) in Research in Photosynthesis (Murata, M., ed.), Vol. I, pp. 179–186, Kluwer, Dordrecht.
[613] Gottfried, D.S., Steffen, M.A. and Boxer, S.G. (1991) Biochim. Biophys. Acta. 1059, 76–90.
[614] De Grooth, B.G. and Amesz, J. (1977) Biochim. Biophys. Acta 462, 237–246.
[615] De Grooth, B.G. and Amesz, J. (1977) Biochim. Biophys. Acta 462, 247–258.
[616] Crielaard W., Van Mourik, F., Van Grondelle, R., Konings, W.N. and Hellingwerf, K.J. (1992) Biochim. Biophys. Acta 1100, 9–14.
[617] Katoh, T., Nagashima, U. and Mimuro, M. (1990) Photosynth. Res. 27, 221–226.
[618] Trash, R.J., Fang, H.L.-B. and Leroi, G.E. (1977) J. Chem. Phys. 67, 5930–5933.
[619] Trash, R.J., Fang, H.L.-B. and Leroi, G.E. (1979) Photochem. Photobiol 29, 1049–1050.
[620] Mimuro, M., Nagashima, U., Nagaoka, S.-T., Takaichi, S., Yamazaki, I., Nishimura, Y. and Katoh, T. (1993) Chem. Phys. Lett. 213, 576–580.
[621] Tavan, P. and Schulten, K. (1988) Mat. Res. Soc. Proc. 109, 163–169.
[622] Tavan, P. and Schulten, K. (1986) J. Chem. Phys. 85, 6602–6609.
[623] De Coster, B., Christensen, R.L., Gebhard, R., Lugtenburg, J., Farhoosh, R. and Frank, H.A. (1992) Biochim. Biophys. Acta 1102, 107–114.
[624] Andersson, P.-O., Gillbro, T., Asato, A.E. and Lin, R.S.H. (1992) J. Luminesc. 51, 11–20.
[625] Gillbro, T., Andersson, P.-O., Lin, R.S.H., Asato, A.E., Takaishi, S. and Cogdell, R.J. (1993) Photochem. Photobiol. 57, 44–48.
[626] Wasielewski, M.R., Tiede, D.M. and Frank, H.A. (1986) in Ultrafast Phenomena V. Springer Series in Chemical Physics Vol. 46 (Fleming, G.R. and Siegmann, A.E., eds.), pp. 388–392, Springer, Berlin.
[627] Gillbro, T., Cogdell, R.J. and Sundström, V. (1988) FEBS Lett. 235, 169–172.
[628] Wasielewski, M.R. and Kispert, L.D. (1986) Chem. Phys. Lett 128, 238–243.
[629] Noguchi, T., Kolaczkowski, S.V., Arbour, C., Aramaki, S., Atkinson, G.H., Hayashi, H. and Tasumi, M. (1989) Photochem. Photobiol. 50, 603–609.
[630] Carroll, P.J. and Brus, L.E. (1987) J. Chem. Phys. 86, 6584–6590.

[631] Hashimoto, H. and Koyama, Y. (1989) Chem. Phys. Lett. 154, 321–325.
[632] Freed, K.F. (1978) Acc. Chem. Res. 11, 74–80.
[633] Aoyagi, M., Ohmine, I. and Kohler, B.E. (1990) J. Phys. Chem 94, 3922–3926.
[634] Noguchi, T., Hayashi, H., Tasumi, M. and Atkinson, G.H. (1990) Chem. Phys. Lett 175, 163–169.
[635] Dinu, U., Hemley, R.J. and Karplus, M. (1983) J. Phys. Chem. 87, 924–932.
[636] Duysens, L.N.M. (1952) Doctoral Thesis, University of Utrecht.
[637] Hayashi, H., Kolaczkowski, S.V., Nuguchi, T., Blanchard, D. and Atkinson, G.H. (1990) J. Am. Chem. Soc. 112, 4664–4670.
[638] Visschers, R.W., Crielaard, W., Fowler, G.J.S., Hunter, C.N. and Van Grondelle, R. (1994) Biochim. Biohys. Acta 1183, 483–490.
[639] Razi Naqvi, K. (1980) Photochem. Photobiol. 31, 523–524.
[640] Frank, H.A., Farhoosh, R., Aldema, M.L., De Coster, B., Christensen, R.L., Gebhard, R. and Lugtenburg, J. (1993) Photochem Photobiol 57, 49–55.
[641] Dirks, G., Moore, A.L., Moore, T.A. and Gust, D. (1980) Photochem. Photobiol. 32, 277–280.
[642] Wasielewski, M.R., Liddell, P.A., Barrett, P., Moore, T.A. and Gust, D. (1986) Nature 322, 570–574.
[643] Davidovitch, M.A. and Knox, R.S. (1979) Chem. Phys. Lett. 68, 391–394.